SEISMIC MARGIN REVIEW

VOLUME V

DIESEL GENERATOR BUILDING

by

D. A. Wesley
R. P. Kennedy
R. H. Kincaid
P. S. Hashimoto
R. D. Thrasher
W. H. Tong

Approved: D A Wesley for
R. P. Kennedy
President

Approved: Thomas R. Kipp
T. R. Kipp
Manager of
Quality Assurance

prepared for

CONSUMERS POWER COMPANY
Jackson, Michigan

July, 1983

STRUCTURAL
MECHANICS
ASSOCIATES
A Calif. Corp.

5160 Birch Street, Newport Beach, Calif. 92660 (714) 833-7552

REVISIONS

Document Number SMA 13701.05R003(VOLUME V)

Title SEISMIC MARGIN REVIEW
VOLUME V
DIESEL GENERATOR BUILDING

Rev.	Description	QA	Project Manager
3/1983	Draft for Review	Thomas R. Kipp 3/2/83	D A Wesley 3/2/83
4/1983	Initial Issue	Thomas R. Kipp 4-22-83	D A Wesley 4/22/83
7/1983	Revised to incorporate corrected seismic loads	Thomas R. Kipp 7/25/83	Raymond B. Ofstead for D. A. Wesley 7/25/83

SEISMIC MARGIN REVIEW
MIDLAND ENERGY CENTER PROJECT

TABLE OF CONTENTS

TABLE OF CONTENTS

1. INTRODUCTION

A seismic margin evaluation of the Midland Energy Center has been conducted. The purpose of this assessment was to provide confidence in the safety and structural integrity of critical structures and equipment required to remain operational during an earthquake in order to achieve safe shutdown. This volume presents the results of the seismic analysis conducted for the diesel generator building.

The plant was designed in accordance with criteria and codes described in the FSAR (Reference 1). Recently, the expected seismic input at the Midland site has been reevaluated using current methodology (Reference 3, 4 and 5). Seismic inputs applicable for the diesel generator building were determined in terms of site specific response spectra at the top-of-fill location. These site specific response spectra as well as the overall methodology used to develop the seismic models and in-structure response spectra for equipment evaluation are contained in Volume I of this report.

1.1 DESCRIPTION OF THE STRUCTURE

The diesel generator building is located to the south of, and adjacent to the turbine building. It is a two-story rectangular, reinforced concrete structure that houses four emergency diesel generators for Units 1 and 2. Overall plan dimensions of the structure are approximately 155 feet by 70 feet with a total internal height of approximately 44 feet. A sectional view of this structure is presented in Figure V-1-1.

The diesel generator building is of reinforced concrete shear wall and slab construction with steel beams provided for vertical load support. The foundation for the exterior and interior walls consist of continuous reinforced concrete footings, 10'-0" wide and 2'-6" thick,

with a bottom of footing elevation at 628 feet. The diesel generators rest on 6'-6" thick concrete pedestals. The diesel generation units are isolated by expansion joints from the rest of the structure. A slab on grade supports light, miscellaneous equipment located on the ground floor.

1.2 GROUND MOTION

The diesel generator building is founded on approximately 30 feet of fill material underlaid by thick glacial till at the Midland site. The Seismic Margin Earthquake (SME) top of fill response spectra appropriate for use with structures founded on the top of fill were presented in Volume I and are shown in Figure V-1-2 for reference.

1.3 SOIL PROPERTIES

The diesel generator building is founded on approximately 30 feet of fill material. The fill is underlain by deposits of very stiff to hard cohesive soils, predominantly grey, silty clay. Bedrock is at approximately Elevation 260'. The details of the site geology are discussed in the FSAR (Reference 1). The site characteristics for the Midland plant have been developed as discussed in Volume I of this report. Figures V-1-3 and V-1-4 show the soft site and stiff site profiles, respectively. The fill material properties used in both profiles from Elevation 596' to Elevation 628' are based on the Weston Geophysical (stiff site) soils data. The development of the low strain shear moduli, strain degradation effects, and other foundation characteristics used in the Seismic Margin Review (SMR) are discussed in Volume I of this report. Use of this wide range of soil properties in the seismic analysis of the diesel generator building ensures conservative response results for both the structure loads and in-structure response spectra.

1.4 STRAIN DEGRADATION EFFECTS

The soil profiles shown in Figures V-1-3 and V-1-4 were developed based on the low strain shear moduli, G_{max}, for the soil. The effect of earthquake induced shear strains on the soil material properties was estimated by determining the equivalent linear high strain soil shear moduli, G_{SME}, applicable at SME ground motion levels, by using shear modulus degradation relationships. The procedure for estimating peak soil shear strains was presented in Volume I. The development of strain degradation effects for the glacial till material below Elevation 596' was presented in Volume I and will not be repeated here.

The development of the degraded soil shear modulus, G_{SME}, for the fill material followed the same type of procedure outlined in Volume I. However, for the fill material close to the ground surface an additional correction must be applied which accounts for the effective increase in the low strain soil modulus due to the surcharge of the soil from the structure weight.

Based upon the Hardin and Drnevich approach (Reference 7), the building surcharge effect on the low strain shear modulus can be estimated from:

$$G_{ms} \approx G_{max} \sqrt{\sigma_s/\sigma_o} \qquad (1\text{-}1)$$

where G_{ms} is the low strain shear modulus corrected for surcharge, σ_s is the mean effective stress with surcharge and σ_o is the free-field mean effective stress. The following estimates of G_{ms}/G_{max} beneath the diesel generator building have been made:

Elevation 622':	$G_{ms}/G_{max} = 1.56$
Elevation 609':	$G_{ms}/G_{max} = 1.25$
Elevation 600':	$G_{ms}/G_{max} = 1.17$

Estimates of intermediate elevations can be obtained by interpolation.

Figure V-1-5 (from Reference 7) presents the relationship between the effective shear modulus at high seismic shear strains, G_{SME}, and the low strain shear modulus, G_{ms}. The following ranges of seismic shear strains, γ, and G_{SME}/G_{ms} have been estimated for the seismic margin earthquake. Results for the glacial till material are presented for reference.

SOFT SITE REPRESENTATION

Elevation (feet)	γ (%)	(G_{SME}/G_{ms})*
615 to 628	0.086	0.21
603 to 615	0.46	0.28
596 to 603	0.038	0.28
550 to 596	0.018 to 0.026	0.29
410 to 550	0.013 to 0.018	0.35
260 to 410	0.008	0.67

*Glacial till results from Volume I. For glacial till $G_{ms} = G_{max}$.

STIFF SITE REPRESENTATION

Elevation (feet)	γ (%)	(G_{SME}/G_{ms})*
615 to 628	0.057	0.40
596 to 615	0.029	0.51
463 to 596	0.009 to 0.011	0.60
363 to 463	0.007 to 0.008	0.66
263 to 363	0.007	0.82

*Glacial till results from Volume I. For glacial till $G_{ms} = G_{max}$.

Upper and lower bound soil profiles were developed for the diesel generator building based on the effective layer shear modulus, G_{SME}, presented above. The upper and lower bound soil profiles represent the range of soil properties which might be possible at the Midland site. This is considered to conservatively account for the variability from such factors as uncertainty in strain degradation effects, uncertainty in modeling soil-structure interaction, and the uncertainty in the knowledge of soil characteristics in the soil profiles studied. These uncertainties have already been incorporated into the development of the low strain shear modulus for the fill material as discussed in Section 1.4. Thus, for the fill material, G_{SME} (lower bound) = G_{SME} (soft site representation) and G_{SME} (upper bound) = G_{SME} (stiff site representation). However, the low strain shear modulus for the glacial till material below Elevation 596' does not account for possible variability due to these uncertainties. Therefore, in order to account for these possible uncertainties, it was determined for the glacial till that G_{SME} (lower bound) = 0.6 x G_{SME} (soft site representation) was a realistic lower bound profile for use in the SME. Similarly, G_{SME} (upper bound) = 1.3 x G_{SME} (stiff site representation) was considered to be a realistic upper bound soil profile for the glacial till material. The details of the procedure used in developing the upper and lower bound uncertainty factors of 1.3 and 0.6 are presented in Volume I. The effective soil shear moduli, G_{SME}, used in the CLASSI layered site analyses which account for these uncertainties are shown in Figures V-1-3 and V-1-4.

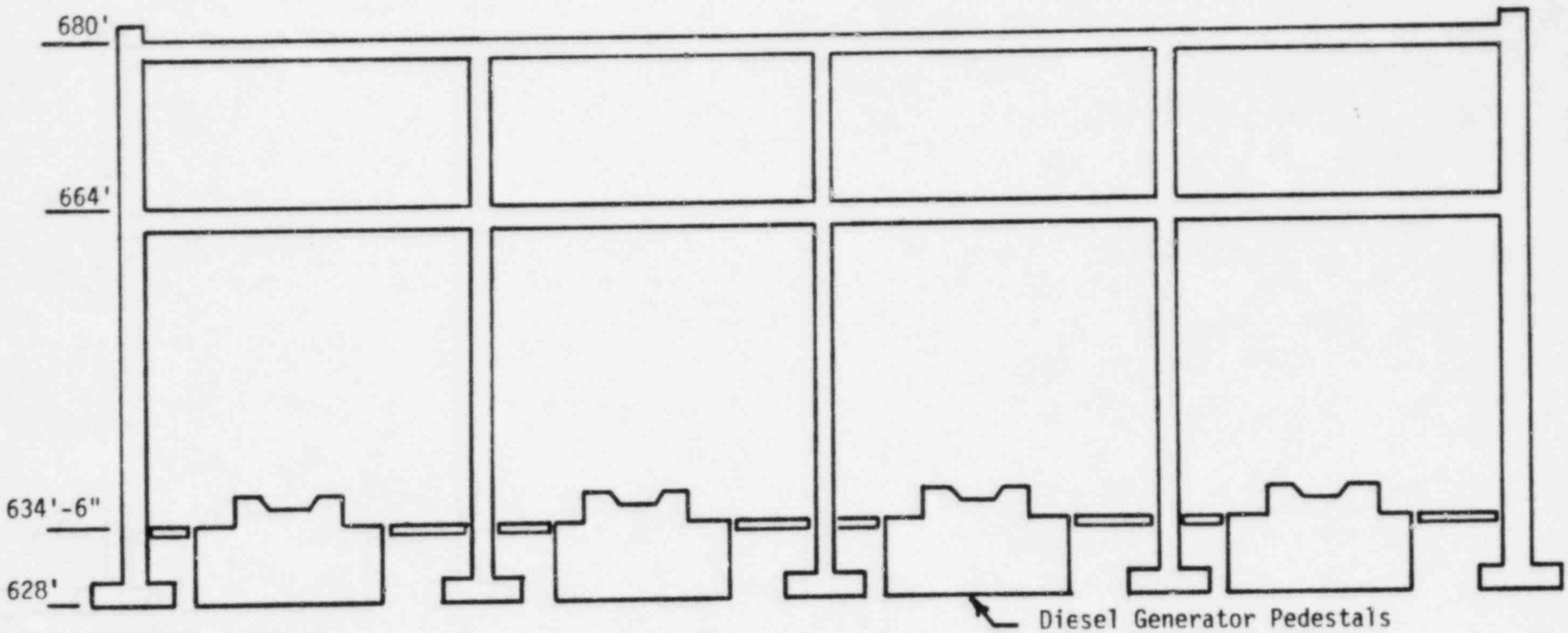

FIGURE V-1-1. SECTIONAL VIEW OF THE DIESEL GENERATOR BUILDING

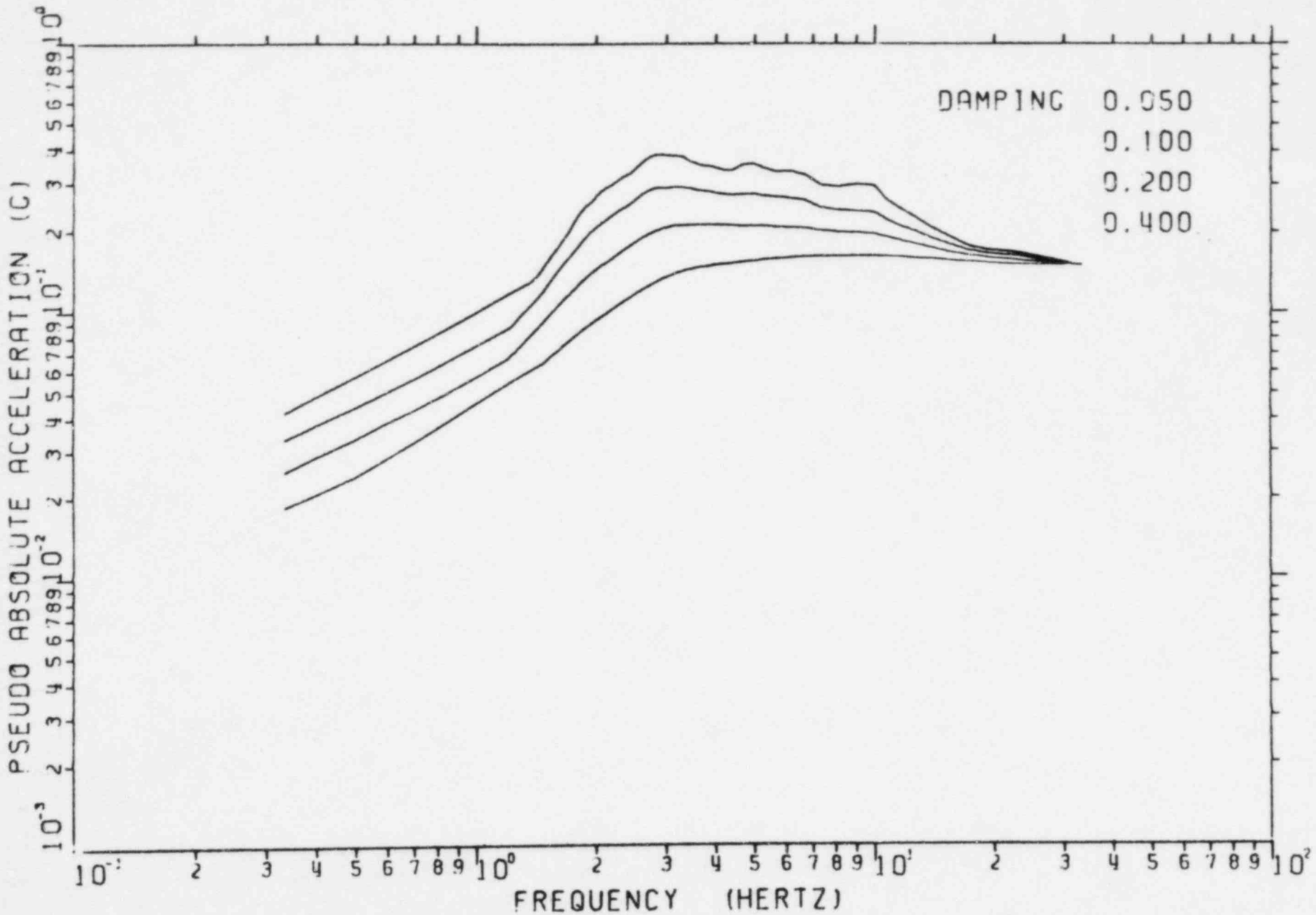

FIGURE V-1-2. SEISMIC MARGIN EARTHQUAKE TOP OF FILL ENVELOPE RESPONSE SPECTRA

Elevation				
634				
628				
Fill	W_s = 120 pcf		G_{max} = 0.9 x 10^6 psf	
	ν = 0.42		G_{ms} = 1.40 x 10^6 psf	
	V_s = 490 fps		G_{SME} = 0.30 x 10^6 psf	
615				
Fill	W_s = 120 pcf		G_{max} = 2.0 x 10^6 psf	
	ν = 0.42		G_{ms} = 2.50 x 10^6 psf	
	V_s = 730 fps		G_{SME} = 0.70 x 10^6 psf	
603				
Fill	W_s = 120 pcf		G_{max} = 2.7 x 10^6 psf	
	ν = 0.42		G_{ms} = 3.16 x 10^6 psf	
	V_s = 850 fps		G_{SME} = 0.85 x 10^6 psf	
596				
Glacial Till	W_s = 135		G_{max} = 7.0 x 10^6 psf	
	ν = 0.47			
	V_s = 1290 fps		G_{SME} = 1.2 x 10^6 psf	
550				
Glacial Till	W_s = 135 pcf		G_{max} = 12 x 10^6 psf	
	ν = 0.47			
	V_s = 1690 fps		G_{SME} = 2.5 x 10^6 psf	
410				
Dense Cohesionless Material	W_s = 135 pcf	V_s = 2540 fps	G_{max} = 27 x 10^6 psf	Elevation 410
	ν = 0.34		G_{SME} = 10.7 x 10^6 psf	
		V_s = 2970 fps	G_{max} = 37 x 10^6 psf	Elevation 260
			G_{SME} = 15.1 x 10^6 psf	
260				
Bedrock	W_s = 150 pcf	V_s = 500		
	ν = 0.33			

FIGURE V-1-3. LOWER BOUND LAYERED SOIL PROFILE BASED ON SOFT SITE DATA

Elevation		
634		
628		
Fill	W_s = 120 pcf	G_{max} = 1.2 x 10^6 psf
	ν = 0.42	G_{ms} = 1.87 x 10^6 psf
	V_s = 570 fps	G_{SME} = 0.75 x 10^6 psf
615		
Fill	W_s = 120 pcf	G_{max} = 2.7 x 10^6 psf
	ν = 0.42	G_{ms} = 3.28 x 10^6 psf
	V_s = 850 fps	G_{SME} = 1.7 x 10^6 psf
596		
Glacial Till	W_s = 135 pcf	G_{max} = 22.2 x 10^6 psf
	ν = 0.42	
	V_s = 2300 fps	G_{SME} = 17.3 x 10^6 psf
463		
Glacial Till	W_s = 135 pcf	G_{max} = 37.8 x 10^6 psf
	ν = 0.42	
	V_s = 3000 fps	G_{SME} = 32.5 x 10^6 psf
363		
Dense Cohesionless Material	W_s = 135 pcf	G_{max} = 37.8 x 10^6 psf
	ν = 0.34	
	V_s = 3000 fps	G_{SME} = 40.3 x 10^6 psf
263		
Bedrock	w_s = 150 pcf	V_s = 5000 fps
	ν = 0.33	

FIGURE V-1-4. UPPER BOUND LAYERED SOIL PROFILE BASED ON STIFF SITE DATA

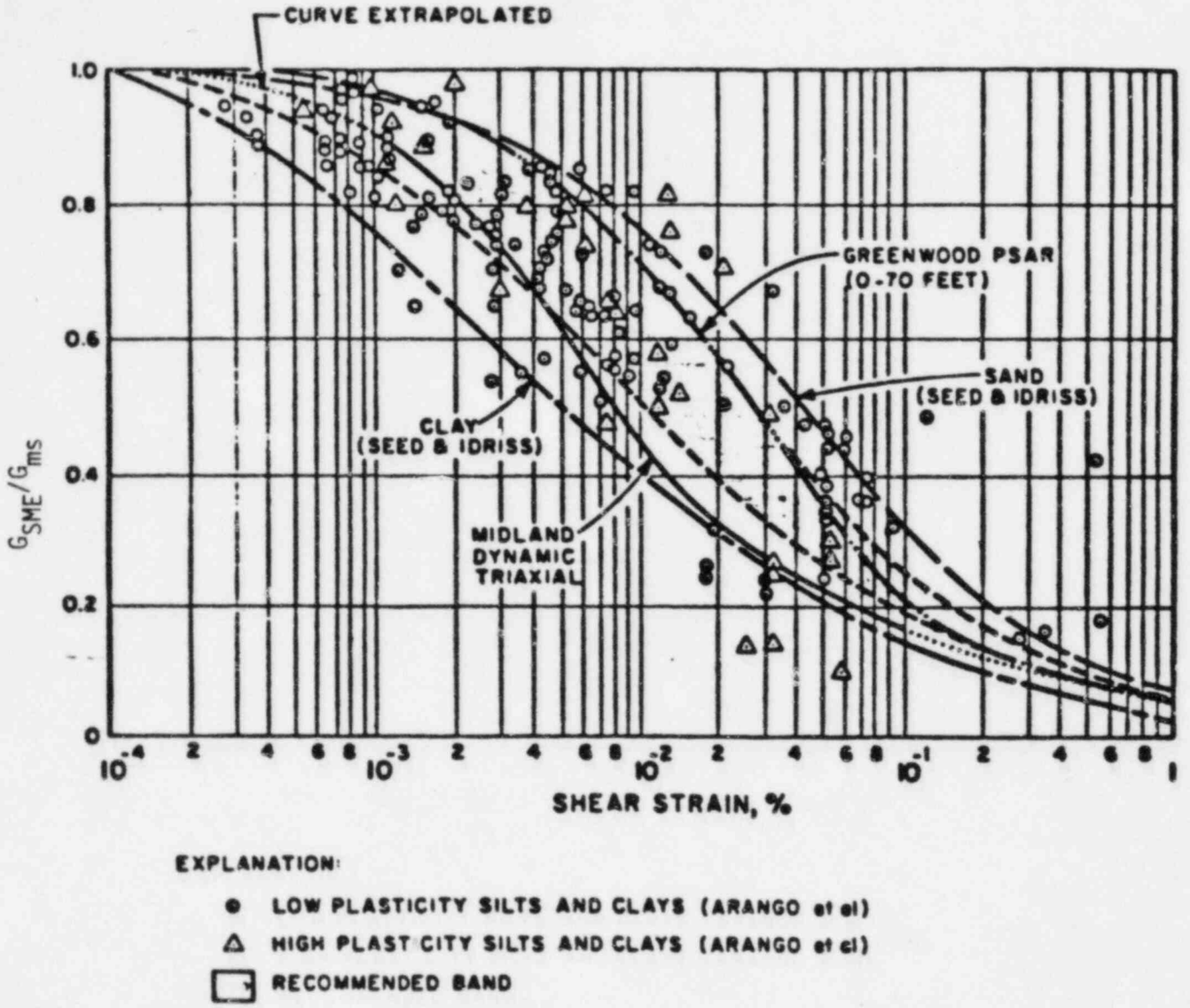

FIGURE V-1-5. STRAIN DEGRADATION RELATIONSHIPS FOR MIDLAND SITE (after Ref. 7)

2. SEISMIC ANALYSIS

2.1 STRUCTURE DYNAMIC MODEL

The two-dimensional dynamic lumped mass model for the diesel generator building is shown in Figure V-2-1. The diesel generator building mathematical model was developed by Bechtel (Reference 8). As part of the SMR, this model was reviewed to ensure that the overall dynamic characteristics of the structure have been adequately represented. The diesel generator building dynamic structure model described herein was used to evaluate overall building response to seismic loadings as well as to generate in-structure (floor) response spectra. The overall building dynamic responses developed from this dynamic structure model were also used to develop loads in the individual structural elements.

The diesel generator building dynamic model shown in Figure V-2-1 uses a single lumped mass, vertical beam element to represent the reinforced concrete shear wall building. The mass of the structure is lumped at the roof (Elevation 680'), at the partial floor (Elevation 664') and at about halfway between the ground (Elevation 634'-6") and the floor at Elevation 664'. The mass includes the concrete, steel, 25 percent of the design live load, and all major equipment items. Because the structure is considered to be symmetric, the center of mass for each floor coincides with geometric centroid of the structure.

Beam elements define the stiffness characteristics of the structural stiffnesses between floor levels. All structural stiffnesses were considered to be symmetric and coincide with the center of mass locations.

In order to conservatively bound dynamic structural response, soil impedances representing the stiffness and damping of the underlying soil were coupled with the structure dynamic model shown in Figure V-2-1

in determining seismic response loads in the structure. Two cases were studied. The first case studied considers the structure, entrapped soil, and diesel generators to be coupled and responding in-phase. The mass of the entrapped soil, diesel generators and diesel generator pedestals are included in this model. This lumped mass was located at Elevation 630'-6" in the dynamic model. Soil impedances for this model were developed consistent with the foundation base mat lumped mass considerations. Since the entire structure and entrapped soil are assumed to be responding in-phase, the soil impedances for all degrees-of-freedom were developed based on the gross exterior dimensions of the foundation footings as discussed in Section 2.2.4. The soil impedances are located at the bottom of the spread footings at Elevation 628' for this model. This dynamic structure model and corresponding soil impedances are defined as the upper bound relative soil stiffness case.

The second case studied considers the structure and diesel generators to be uncoupled. The foundation base mat mass and soil stiffnesses are located at ground level at Elevation 634'-6". Entrapped soil, spread footings, diesel generator pedestals, and diesel generator masses are not included in this model. The soil impedances for this model were based on foundation contact area only as discussed in Section 2.2.4. This dynamic structure model and corresponding soil impedances are defined as the lower bound relative soil stiffness case. Dynamic responses from both models were evaluated in determining peak loads and in-structure response spectra for the SMR.

2.2 SOIL-STRUCTURE INTERACTION

2.2.1 Layered Site Analyses

The effects of the layered site characteristics on the diesel generator building seismic response were evaluated by developing equivalent elastic half-space soil impedances based on layered site analyses. These equivalent elastic half-space impedance functions were then modified to account for non-standard foundation shapes. The layered site soil pro-

files presented in the previous section were used in conducting layered site analyses using the program CLASSI (Reference 9) which calculates the frequency dependent soil impedances for the structure. The diesel generator building exterior foundation geometry was idealized as a 77.5' by 162.5' rectangular foundation as shown in Figure V-2-2 in all CLASSI analyses. This idealized foundation is founded at Elevation 628 feet. The diesel generator building foundation was considered to be unembedded.

The layered site profiles presented in Figures V-1-3 and V-1-4 and used in the CLASSI analyses are considered to be conservative representations of the soil profiles at the Midland site. These profiles define a number of distinct soil layers with significant impedance mismatches occurring at some layer interfaces. These impedance mismatches reduce the soil geometric damping. This low damping tends to maximize seismic response loads in the structure. Actual site characteristics would be expected to show more gradual changes in soil properties in the fill material and upper glacial till layers than were used in the idealized soil profiles. Impedance mismatches would be minimized with corresponding higher geometric damping and lower seismic response loads determined for the structure. Thus, the use of the soil profiles presented in the previous section is judged to conservatively predict diesel generator building seismic response.

The results of the CLASSI analyses are presented in Figures V-2-3 to V-2-12 for the two soil profiles studied. Soil impedances were developed for all global translational and rocking degrees-of-freedom. This structure was considered to be symmetric and torsional response was not considered in the analysis. Both the real (stiffness) and imaginary (damping) portions of the soil impedances are presented in these figures for a range of soil-structure frequencies varying from 0 to 10 hertz. Figures V-2-3 to V-2-7 present the CLASSI layered site soil impedances developed for the lower bound soil profile while Figures V-2-8 to V-2-12 present the corresponding CLASSI results for the upper bound soil profile. Intermediate soil case site characteristics were developed based on the results of the upper and lower bound layered site analysis.

Both the stiffness and damping terms for the lower bound soil profile Figure V-2-3 to V-2-7 show strong frequency dependence and soil-structure resonance due to layering effects for all degrees-of-freedom. In general, the soil stiffness coefficients exhibit more resonance effects due to soil layering than is shown in the damping coefficients. For the upper bound soil profile, the horizontal translational degrees-of-freedom exhibit resonance due to soil layering in both the stiffness and damping coefficients. Vertical translation and rocking degree-of-freedom primarily show frequency dependent effects with little soil-structure resonance due to layering evident. As discussed in Volume I, it should be noted that because CLASSI incorporates the five percent soil material damping in the layered site analysis, the damping coefficient terms are not zero for the static case (0 hertz) as would be expected if only geometric damping was considered in the analysis.

2.2.2 Effective Elastic Half-Space Shear Moduli

The results of the CLASSI layered site analyses were used to develop effective elastic half-space shear moduli, G_{eff}, for all degrees-of-freedom of the structure (horizontal and vertical translation and rocking). The effective elastic half-space shear moduli were then used to develop soil impedances which accounted for actual foundation geometry and soil layering. The procedure used to develop effective elastic half-space shear moduli from the CLASSI layered site analysis is presented in Volume I. Appendix A of Volume III presents a sample calculation of G_{eff} for the auxiliary building demonstrating the procedure. The procedure used for the diesel generator building is similar.

Table V-2-1 presents the effective soil shear moduli determined from the CLASSI layered site analyses for the lower and upper bound soil profiles. The intermediate soil case G_{eff} was taken as an average of the upper and lower bound soil cases. An effective soil shear modulus value was developed which adequately represented site characteristics for horizontal translational response of the structure for each soil case

studied. Similarly, a shear modulus value was developed which was applicable for rocking degrees-of-freedom of the structure. A separate soil shear modulus value was determined for vertical translation of the diesel generator building. These effective elastic half-space soil shear modulus values account for uncertainty in site characteristics, structure modeling, and strain degradation effects as discussed in Section 1.4.

Comparison of G_{eff} values tabulated in Table V-2-1 with the layered soil profiles presented in Figures V-1-3 and V-1-4 used in the CLASSI layered site analyses demonstrates some general trends. For the lower bound soil profile, the G_{eff} of 500 ksf associated with the horizontal translation of the structure is primarily associated with the soil shear modulus of the fill material above Elevation 603'. The G_{eff} values of 770 ksf for rocking and 1000 ksf for vertical translation show the influence of the stiffer glacial till material below Elevation 603'. Higher G_{eff} would be expected for these degrees-of-freedom which are associated with vertical motion of the structure.

Results for the upper bound soil case are similar. The effective shear modulus, G_{eff}, of 1400 ksf associated with horizontal translation is primarily associated with the soft layer of fill material immediately beneath the structure above Elevation 596'. For vertical response modes such as rocking and vertical translation, the G_{eff} values of 2700 ksf (rocking) and 4600 ksf (vertical translation) both show the influence of the stiff glacial till material below Elevation 596'.

2.2.3 Energy Entrapment Due to Layering

Two types of damping may be defined for the soil. The first type, known as material or hysteretic damping, is due to energy absorption by the soil due to stressing and straining of the material. For the Midland site, this damping has been conservatively estimated to be five percent of critical damping for the SME. Material damping is not significantly affected by layering. The second type of soil damping, known as geometric or radiation damping, involves the wave propagation of energy

through the soil away from the structure. For an elastic half-space, these waves will propagate outwards to infinity. Layered soil profiles, however, tend to trap and reflect some of the energy back up towards the structure. One of the principal reasons for conducting a layered site analysis for the SME was to determine the effect of layering on the geometric damping from the structure. In effect, the geometric damping for the layered profile is reduced to some percentage of the damping which would be determined for an equivalent elastic half-space. This decrease in geometric damping may be determined through the use of a factor defined as

$$F_{Layer} = \frac{C(\text{CLASSI layered site analysis})}{C(\text{theoretical elastic half-space})}$$

where C(CLASSI layered site analysis) is the frequency dependent damping including layering effects determined by the CLASSI layered site analysis. The term C(theoretical elastic half-space) represents the geometric damping which would be calculated for the structure based on the effective elastic half-space shear moduli and idealized foundation shape presented in Table V-2-1 and Figure V-2-2, respectively. This ratio is indicative of the amount of energy entrapped beneath the structure due to layering. The procedure for calculating F_{Layer} is presented in Volume I. A sample calculation of F_{Layer} is presented in Appendix A of Volume III.

Layering factors were determined for each of the soil profiles presented in Figures V-1-3 and V-1-4. Layering factors for the intermediate soil case were conservatively developed from the lower and upper bound soil case results. The layering factors determined for the diesel generator building are presented in Table V-2-2.

These results show that soil layering was significant for the diesel generator building. This structure is founded on top of a layer of fill underlain by glacial till, and significant impedance mismatches

occur at the fill to glacial till interface. For the diesel generator building with exterior foundation dimensions 77.5' by 162.5', soil stresses due to soil-structure interaction will propagate below the bottom of the fill layer. Consequently, some elastic energy radiating outward from the structure is trapped at the fill to glacial till interface and reflects back up toward the structure foundation. This energy entrapment is shown in the layering factors determined for this structure. For a structure with smaller foundation dimensions or less significant impedance mismatches close to the bottom of the foundation, layering factors would approach theoretical elastic half-space damping because of lesser influence of these interfaces.

The layering factors determined for this structure are considered to be conservative. As previously discussed, the soil profiles used in the layered site analyses maximized impedance mismatches at layer interfaces which tended to reduce the soil geometric damping. The actual in-situ soil profile would probably show gradual variation in soil material properties with less significant impedance mismatches occurring and higher geometric soil damping determined for the structure.

2.2.4 Development of Global Soil Stiffnesses and Dashpots

Soil springs modeling the stiffness of the soil beneath the diesel generator building were developed based on the effective soil shear modulus values presented in Table V-2-1 in conjunction with the actual building foundation geometry. Soil stiffnesses were calculated from the frequency dependent elastic half-space equations shown in Table V-2-3. These equations and frequency dependent coefficients are presented in References 11 to 14.

Because the diesel generator building has a spread footing foundation, it is difficult to develop a single set of soil impedances which conservatively predict structure seismic response loads for all soil cases. In order to conservatively bound possible seismic response loads, two sets of soil springs and dashpots were developed for each soil

case which represent reasonable bounds on the maximum and minimum soil stiffnesses and damping expected for the structure. Seismic response loads were developed from an envelope of results determined from dynamic models consistent with these bounding soil impedances. The idealized diesel generator building foundation configurations used to develop these soil impedances are presented in Figure V-2-13.

The first set of soil impedances developed were defined as the upper bound relative soil stiffness case. These soil stiffnesses were developed based on the premise that the structure, entrapped soil, and diesel generators are coupled and are responding in-phase as discussed in Section 2.1. For this case, the foundation configuration shown in Figure V-2-13a was used to develop soil stiffnesses for the structure. This foundation shape is based upon the exterior dimensions of the diesel generator building spread footings. This case maximizes the soil stiffness beneath the structure since both the foundation and entrapped soil are considered to respond integrally with each other.

Using Figure V-2-13a and Table V-2-3 for reference, the soil stiffness terms for the upper bound relative soil stiffness case are defined by:

Horizontal Translation:

$$K_x = K_1 \, 2 \, (1+\nu) \, G_{eff} \, \beta_x \sqrt{BL} \qquad (2\text{-}1)$$

Vertical Translation:

$$K_v = K_3 \, \frac{G_{eff}}{1-\nu} \, \beta_z \sqrt{BL} \qquad (2\text{-}2)$$

Rocking about the B axis (other direction is similar):

$$K_{\psi} = K_2 \frac{G_{eff}}{1-\nu} \beta_{\psi} L^2 B \qquad (2\text{-}3)$$

A second set of soil impedances defined as the lower bound relative soil stiffness case were based on the foundation geometry shown in Figure V-2-13b. These soil stiffnesses were developed consistent with the structure model presented in Section 2.1 which considers the structure, diesel generator, and entrapped soil to be uncoupled. For this case, the horizontal translational soil stiffnesses were developed based on the exterior foundation dimensions of 77.5' by 162.5'. Vertical translation and rocking soil stiffnesses were developed based on the actual foundation footprint. Use of the smaller foundation contact area for these degrees-of-freedom minimizes the soil stiffness beneath the structure. This case represents a reasonable lower bound on the soil stiffnesses determined for the diesel generator building.

The horizontal translational stiffness is given by Equation 2-1 above. The soil stiffness terms for vertical and rocking degrees-of-freedom are defined by:

Vertical Translation:

$$K_v = K_3 \frac{G_{eff}}{1-\nu} \beta_z \sqrt{A_v} \qquad (2\text{-}4)$$

where A_v is the area of the spread footings in contact with the soil (A_v = 6,125 ft^2).

For rocking about the B axis (other direction is similar) define:

$$F = \frac{3W}{L-2W} \tag{2-4}$$

$$K_{\psi_1} = K_2 \frac{G_{eff}}{1-\nu} \beta_{\psi} L^2 B \tag{2-6}$$

$$K_{\psi_2} = K_2 \frac{G_{eff}}{1-\nu} \beta_{\psi} \left[(L^2 B) - (L-2W)^2 (B-2W)\right] \tag{2-7}$$

$$K_{\psi} = F \cdot K_{\psi_1} + (1-F) K_{\psi_2} \tag{2-8}$$

The soil stiffnesses developed the lower and upper bound relative soil stiffness cases for each of the three soil cases studied are presented in Tables V-2-4 and V-2-5.

Dashpots modeling soil geometric and material damping developed using elastic half-space equations are presented in Tables V-2-6 and V-2-7. Material damping of 5 percent of critical damping was assumed for the soil. Soil springs and dashpots were calculated accounting for layering effects as discussed in Volume I. Appendix A of Volume III presents some illustrative calculations of soil impedances for the auxiliary building which demonstrate this procedure.

TABLE V-2-1

DIESEL GENERATOR BUILDING SEISMIC MARGIN EVALUATION

EQUIVALENT ELASTIC HALF-SPACE SHEAR MODULI

Structure Degree-of-Freedom	Dynamic Soil Shear Modulus, G_{eff}		
	Lower Bound Soil Case (KSF)	Intermediate Soil Case (KSF)	Upper Bound Soil Case (KSF)
Horizontal Translation	500	950	1,400
Vertical Translation	1,000	2,800	4,600
Rocking	770	1,700	2,700

TABLE V-2-2

DIESEL GENERATOR BUILDING LAYERING FACTORS

Structure Degree-of-Freedom	$F_{Layer} = \frac{C(\text{CLASSI Layered Site Analysis})}{C(\text{Theoretical Elastic Half-Space})}$		
	Lower Bound Soil Case	Intermediate Soil Case	Upper Bound Soil Case
Horizontal Translation	0.50	0.30	0.20
Vertical Translation	0.50	0.30	0.20
Rocking	0.20	0.10	0.05

TABLE V-2-3

FREQUENCY DEPENDENT ELASTIC HALF-SPACE IMPEDANCE

Direction of Motion	Equivalent Spring Constant For Rectangular Footing	Equivalent Spring Constant For Circular Footing	Equivalent Damping Coefficient
Horizontal	$k_x=k_1 2(1+\nu)G\beta_x\sqrt{BL}$	$k_x=k_1\frac{32(1-\nu)GR}{7-8\nu}$	$c_x=c_1k_x(\text{static})R\sqrt{\rho/G}$
Rocking	$k_\psi=k_2\frac{G}{1-\nu}\beta_\psi B^2L$	$k_\psi=k_2\frac{8GR^3}{3(1-\nu)}$	$c_\psi=c_2k\psi(\text{static})R\sqrt{\rho/G}$
Vertical	$k_z=k_3\frac{G}{1-\nu}\beta_z\sqrt{BL}$	$k_z=k_3\frac{4GR}{1-\nu}$	$c_z=c_3k_z(\text{static})R\sqrt{\rho/G}$
Torsion	———	$k_\theta=k_4\frac{16}{3}GR^3$	$c_t=c_4k_t(\text{static})R\sqrt{\rho/G}$

in which:

ν = Poisson's ratio of foundation medium,

G = shear modulus of foundation medium,

R = radius of the circular base mat,

ρ = density of foundation medium,

B = width of the base mat in the plane of horizontal excitation,

L = length of the base mat perpendicular to the plane of horizontal excitation,

k_1, k_2, k_3, k_4
c_1, c_2, c_3, c_4 = frequency dependent coefficients modifying the static stiffness or damping.

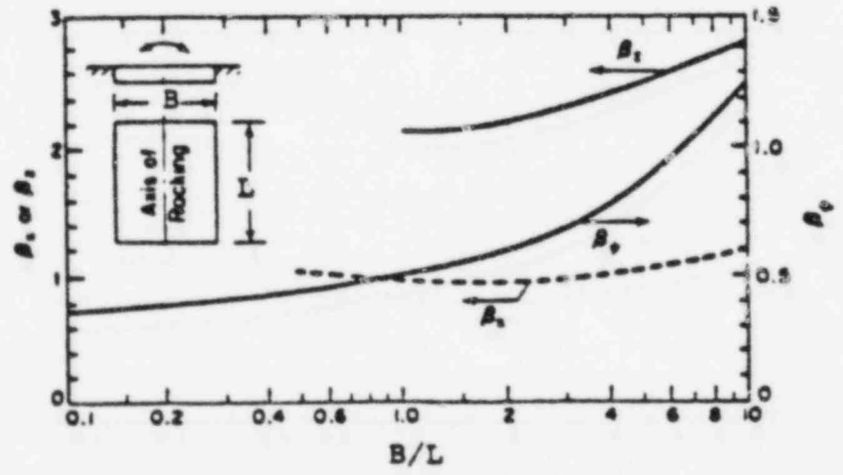

Constants β_x, β_ψ and β_z for Rectangular Bases

TABLE V-2-4

LOWER BOUND RELATIVE SOIL STIFFNESS CASE

Motion	Soil Stiffness		
	Lower Bound Soil	Intermediate Soil	Upper Bound Soil
Translational			
North-South	1.50×10^5	2.80×10^5	4.10×10^5
East-West	1.47×10^5	2.75×10^5	4.02×10^5
Vertical	2.00×10^5	5.37×10^5	8.74×10^5
Rotational			
North-South	2.21×10^8	5.71×10^8	9.21×10^8
East-West	4.81×10^8	1.29×10^9	2.03×10^9

Notes: 1. Units for Translational Soil Springs are K/ft.

2. Units for Rotational Soil Springs are K-ft/rad.

TABLE V-2-5

UPPER BOUND RELATIVE SOIL STIFFNESS CASE

Motion	Soil Stiffness		
	Lower Bound Soil	Intermediate Soil	Upper Bound Soil
Translational			
North-South	1.50×10^5	2.80×10^5	4.10×10^5
East-West	1.47×10^5	2.75×10^5	4.02×10^5
Vertical	2.87×10^5	7.69×10^5	1.25×10^6
Rotational			
North-South	3.94×10^8	9.12×10^8	1.43×10^9
East-West	1.03×10^9	2.44×10^9	3.84×10^9

Notes: 1. Units for Translational Soil Springs are K/ft.

2. Units for Rotational Soil Springs are K-ft/rad.

TABLE V-2-6

LOWER BOUND RELATIVE SOIL STIFFNESS CASE

Motion	Dashpot		
	Lower Bound Soil	Intermediate Soil	Upper Bound Soil
Translation			
North-South	1.07×10^4	8.97×10^4	8.01×10^3
East-West	9.42×10^3	8.18×10^3	7.49×10^3
Vertical	1.40×10^4	1.33×10^4	1.26×10^4
Rotational			
North-South	3.57×10^6	4.18×10^6	5.17×10^6
East-West	1.08×10^7	1.13×10^7	1.26×10^7

Notes: 1. Units for Translational Dashpots are K-sec/ft.

2. Units for Rotational Dashpots are K-sec-ft/rad.

3. Includes 5% Soil Hysteretic Damping.

TABLE V-2-7

UPPER BOUND RELATIVE SOIL STIFFNESS CASE

Motion	Dashpot		
	Lower Bound Soil	Intermediate Soil	Upper Bound Soil
Translation			
North-South	1.07×10^4	8.97×10^4	8.01×10^3
East-West	9.42×10^3	8.18×10^3	7.49×10^3
Vertical	2.76×10^4	2.64×10^4	2.48×10^4
Rotational			
North-South	5.62×10^6	5.94×10^6	6.66×10^6
East-West	2.60×10^7	2.70×10^7	2.94×10^7

Notes: 1. Units for Translational Dashpots are K-sec/ft.

2. Units for Rotational Dashpots are K-sec-ft/rad.

3. Includes 5% Soil Hysteretic Damping.

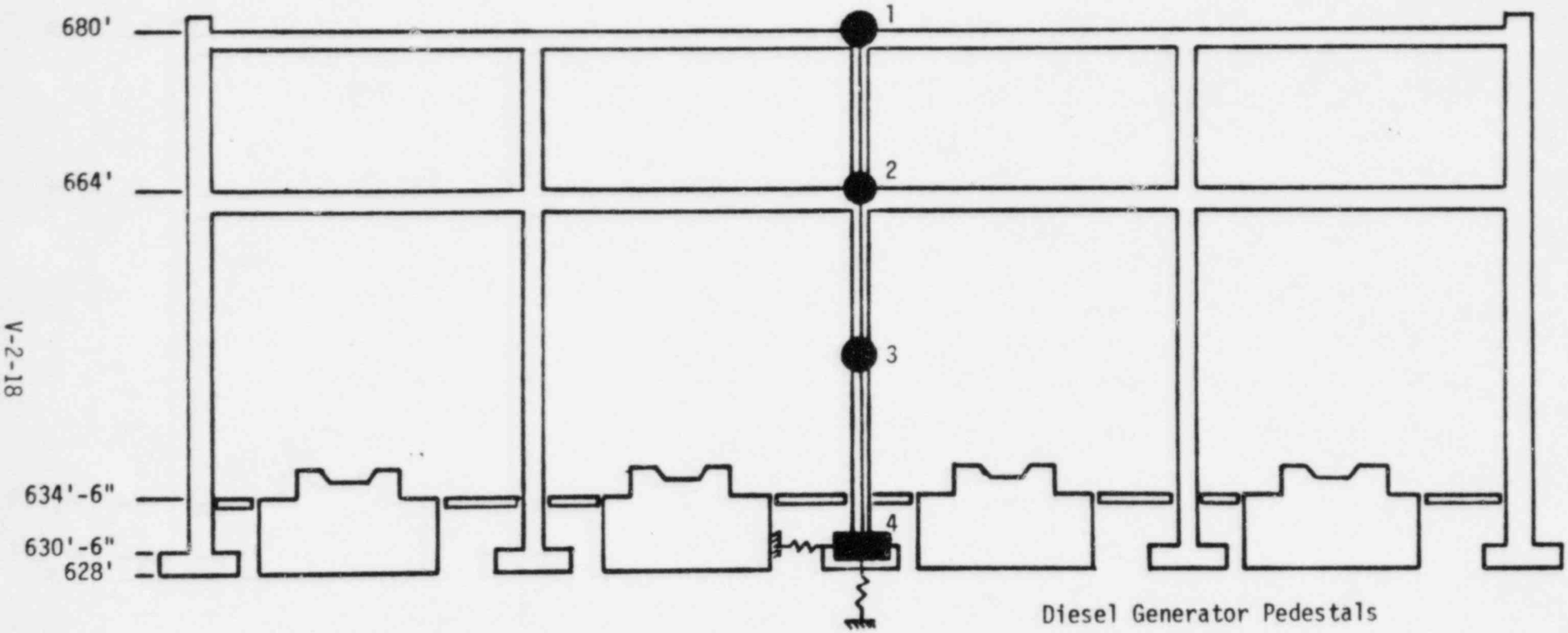

FIGURE V-2-1. DIESEL GENERATOR BUILDING LUMPED MASS MODEL

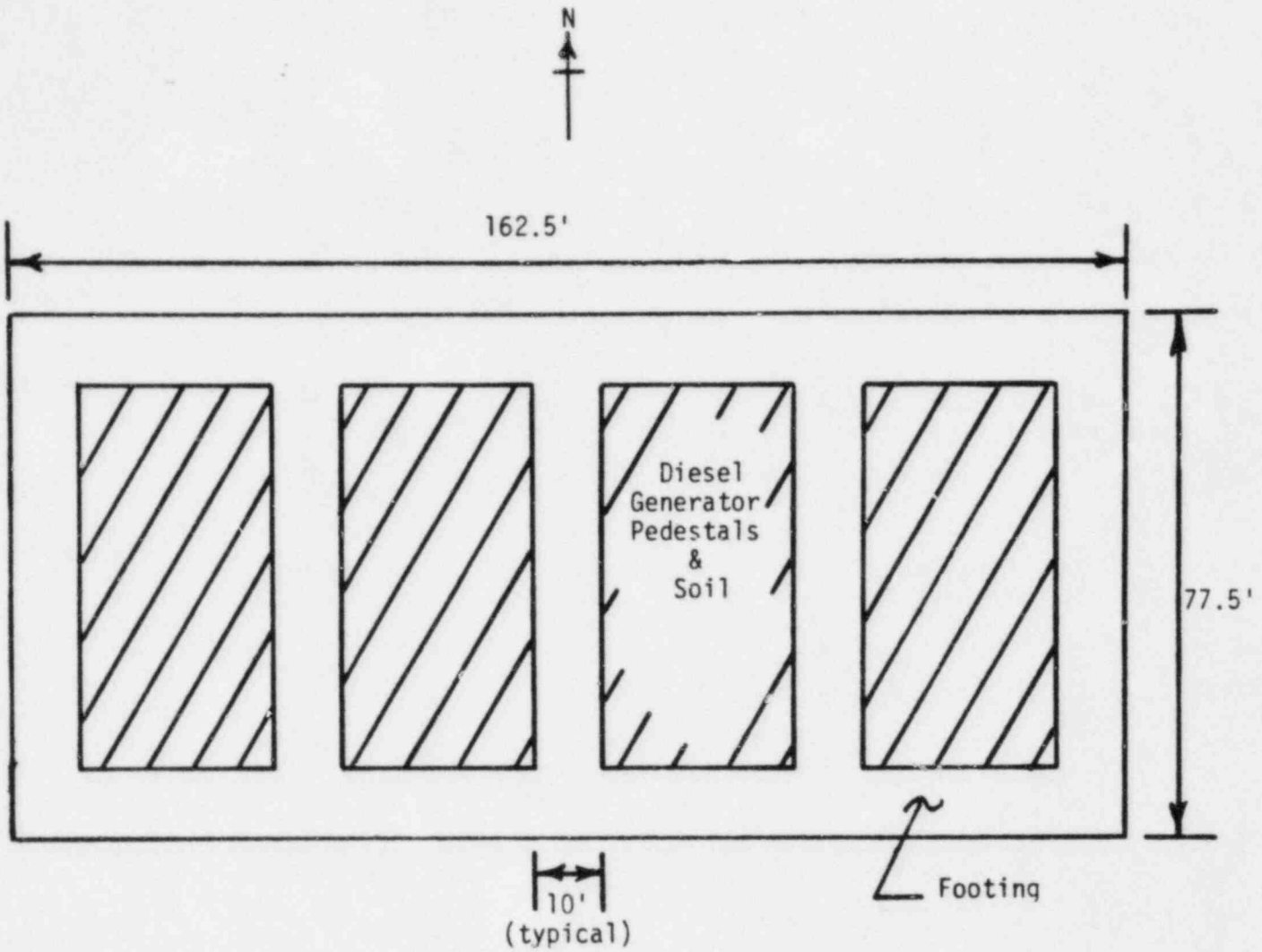

Note: CLASSI layered site analyses are based on exterior foundation dimensions.

FIGURE V-2-2. COMPARISON OF DIESEL GENERATOR BUILDING FOUNDATION TO IDEALIZED FOUNDATION USED IN CLASSI ANALYSES

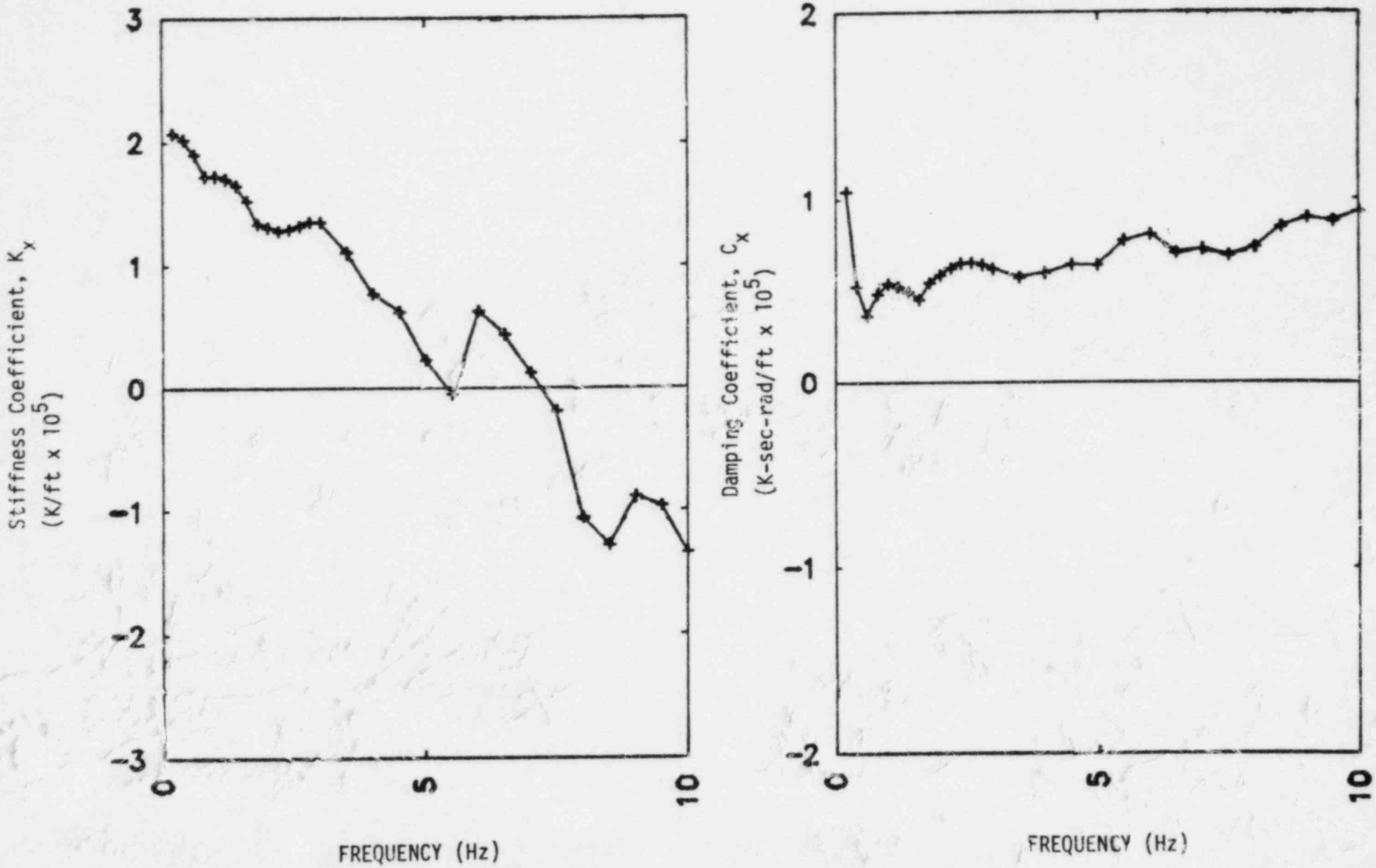

FIGURE V-2-3. EAST-WEST TRANSLATION SOIL IMPEDANCE
LOWER BOUND SOIL CASE

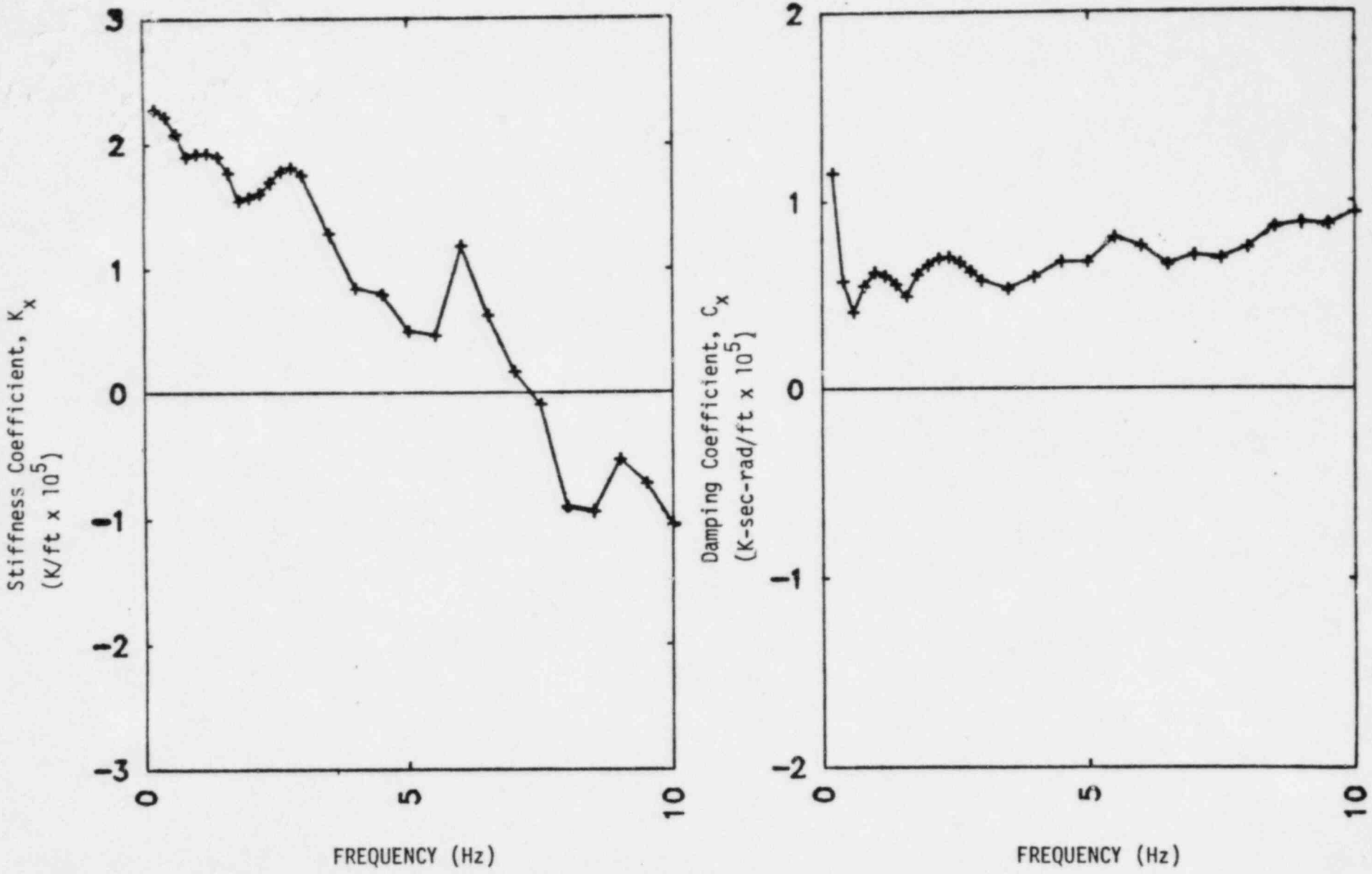

FIGURE V-2-4. NORTH-SOUTH TRANSLATION SOIL IMPEDANCE
LOWER BOUND SOIL CASE

FIGURE V-2-5. VERTICAL TRANSLATION SOIL IMPEDANCE, LOWER BOUND SOIL CASE

FIGURE V-2-6. ROCKING ABOUT THE NORTH-SOUTH AXIS SOIL IMPEDANCE LOWER BOUND SOIL CASE

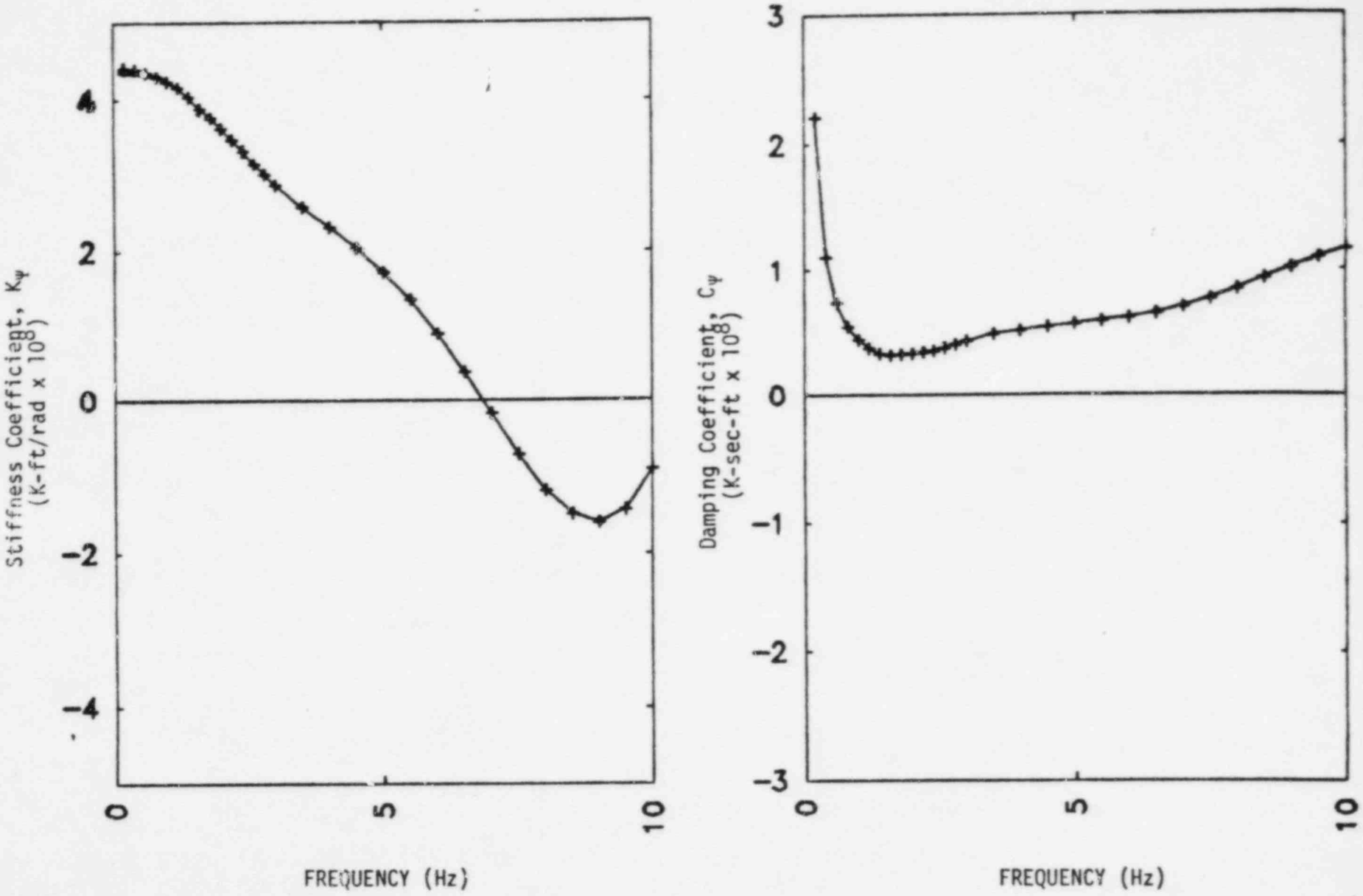

FIGURE V-2-7. ROCKING ABOUT THE EAST-WEST AXIS SOIL IMPEDANCE, LOWER BOUND SOIL CASE

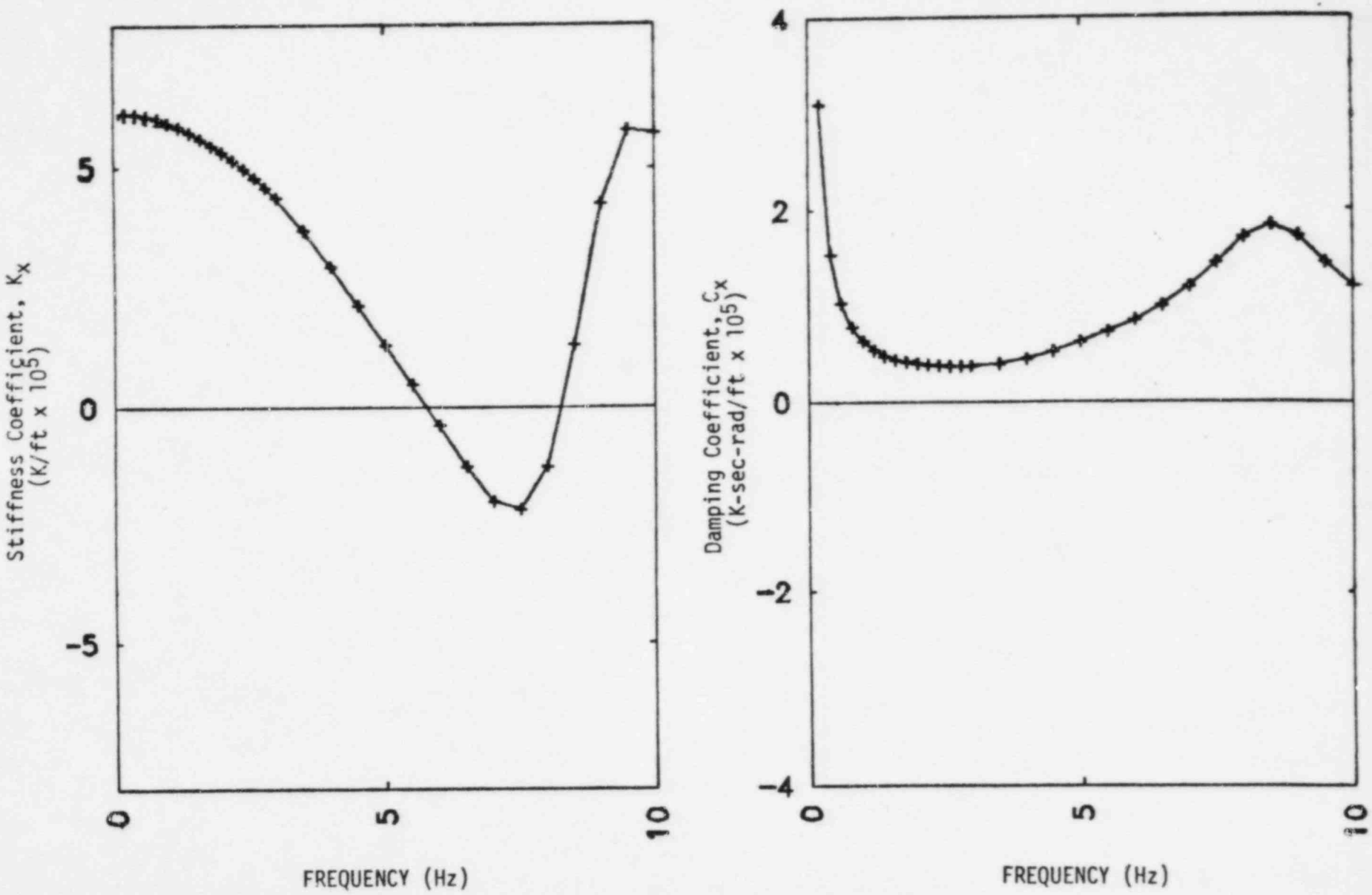

FIGURE V-2-8. EAST-WEST TRANSLATION SOIL IMPEDANCE, UPPER BOUND SOIL CASE

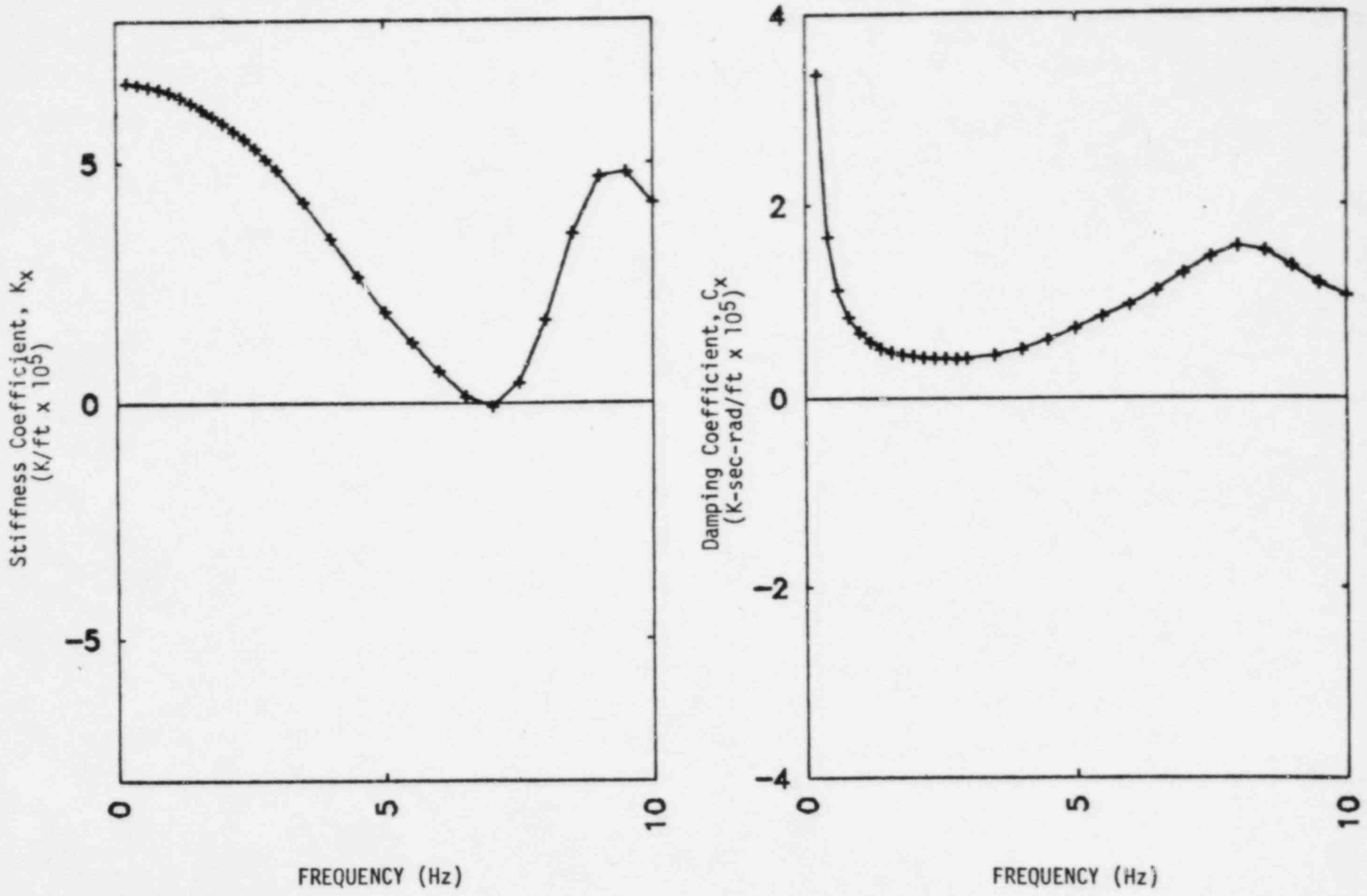

FIGURE V-2-9. NORTH-SOUTH TRANSLATION SOIL IMPEDANCE, UPPER BOUND SOIL CASE

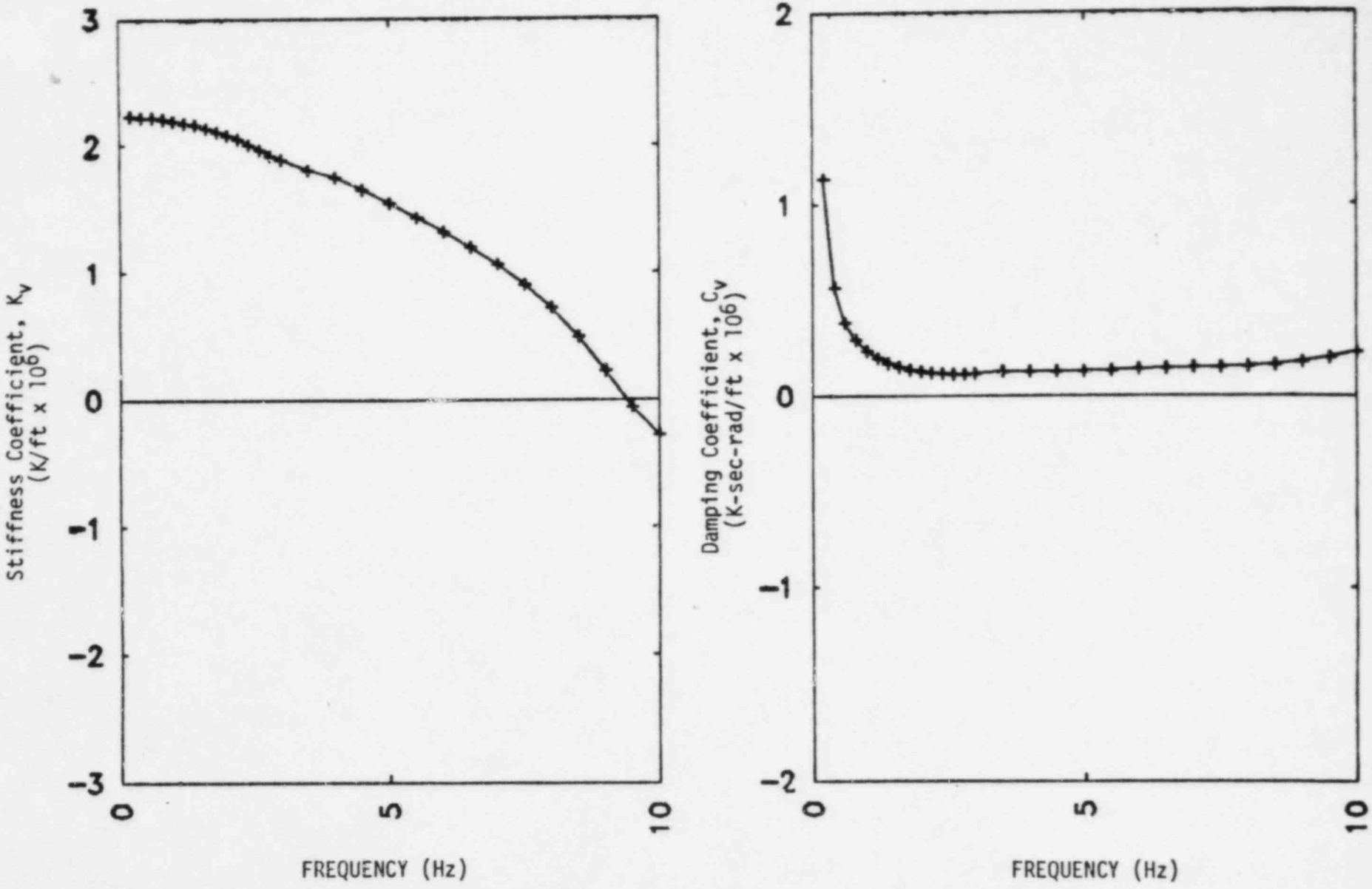

FIGURE V-2-10. VERTICAL TRANSLATION SOIL IMPEDANCE , UPPER BOUND SOIL CASE

FIGURE V-2-11. ROCKING ABOUT THE NORTH-SOUTH AXIS SOIL IMPEDANCE UPPER BOUND SOIL CASE

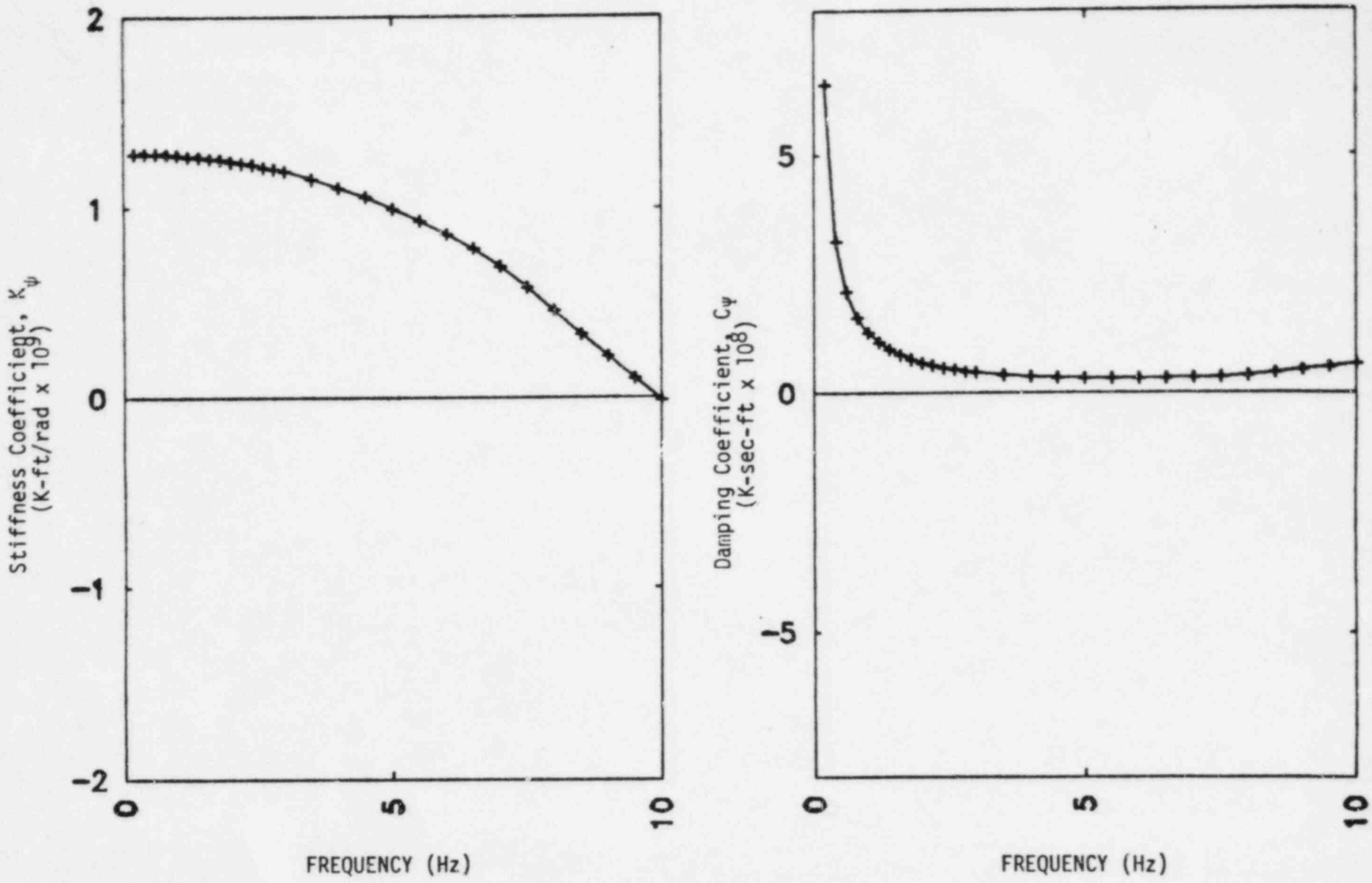

FIGURE V-2-12. ROCKING ABOUT THE EAST-WEST AXIS SOIL IMPEDANCE, UPPER BOUND SOIL CASE

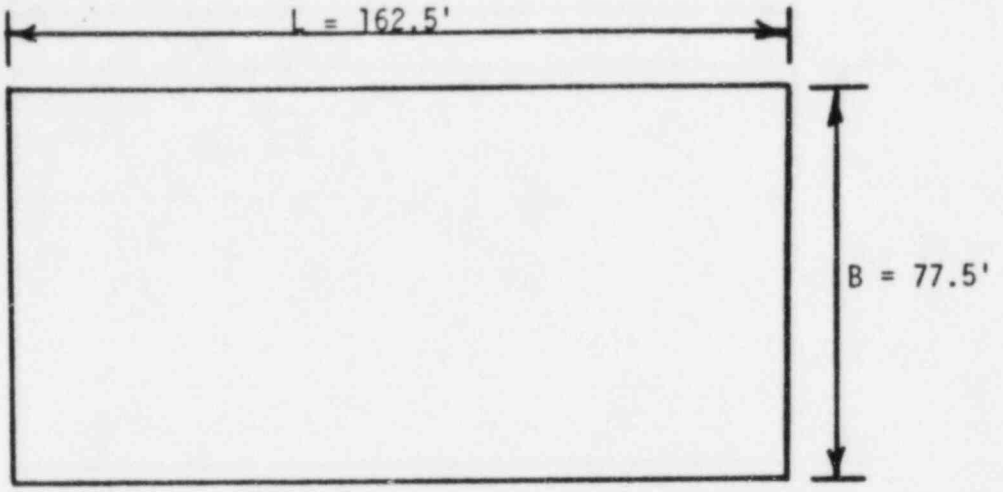

a) Foundation based on Exterior Dimensions of Spread Footings

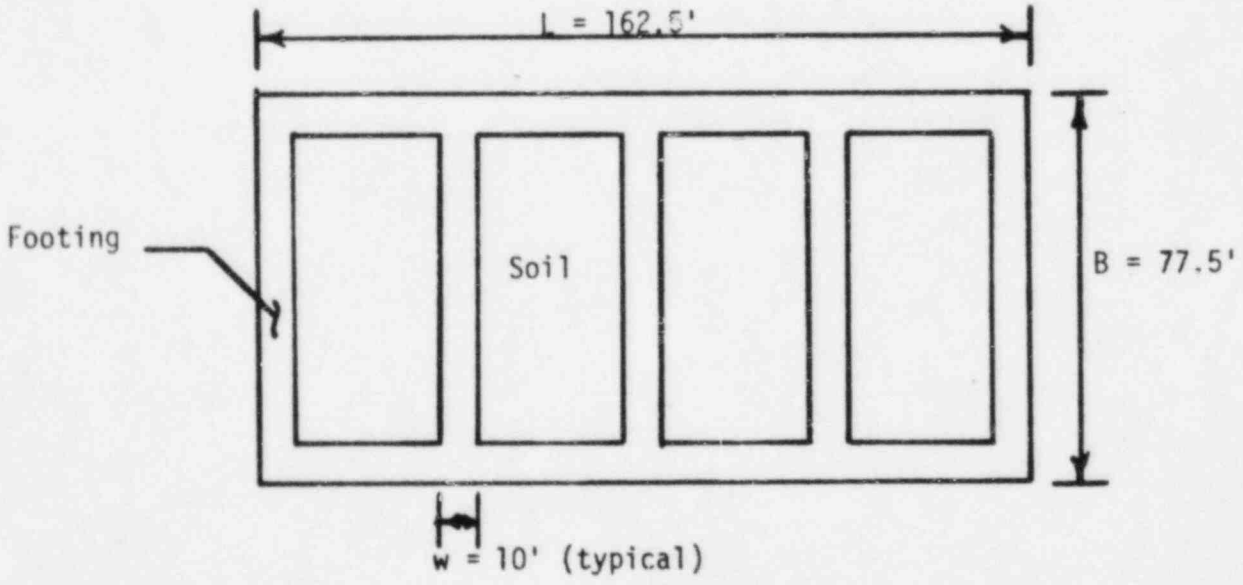

b) Foundation based on Soil Contact Area

FIGURE V-2-13. DIESEL GENERATOR BUILDING FOUNDATION CONFIGURATIONS USED TO DEVELOP BOUNDING SOIL IMPEDANCES

3. SEISMIC RESPONSE

3.1 MODAL CHARACTERISTICS

The diesel generator building natural frequencies, percentage of total structure mass participating in each mode, and mode description are presented in Tables V-3-1 through V-3-2 for the lower bound and upper bound relative soil stiffness cases. Two-dimensional dynamic models oriented in the North-South, East-West, and vertical directions were analyzed for each of the three soil cases in determining diesel generator building dynamic characteristics. Seismic responses in the structure were developed for both the upper and lower bound relative soil stiffness cases described in Section 2.2.4.

Results for the upper bound relative soil stiffness case are presented in Table V-3-1. The fundamental natural frequency for the North-South dynamic model ranges from 1.81 hertz for the lower bound soil case to 3.06 hertz for the upper bound soil case. Between 93 and 96 percent of the total structure mass participates in this soil-structure translational mode. The second structural mode is an out-of-phase soil-structure translational mode. This mode is relatively unimportant in determining structure seismic response with at most 6.6 percent of the structure mass responding in the mode.

Results for the East-West dynamic model are almost identical to those discussed above. Fundamental structure natural frequencies range from 1.92 hertz to 3.20 hertz for the lower bound and upper bound soil cases, respectively. The percentage of total structure mass participating in the soil-structure translational mode is about 98 percent. Higher frequency modes account for only 2 percent of the total mass.

In the vertical direction, diesel generator building dynamic response is fully described by a single soil-structure translational mode. Vertical structure natural frequencies range from 2.82 hertz for the lower bound soil case to 5.82 hertz for the upper bound soil case.

Use of two structure modes in the modal response spectrum analysis for each of the models and soil cases presented above resulted in 100 percent of the structure mass being included.

Table V-3-2 presents the corresponding results for the lower bound relative soil stiffness case. The fundamental natural frequency in the North-South direction varies from 1.90 hertz for the lower bound soil case to 3.44 hertz for the upper bound soil case. The percentage of total structure mass participating in this translational soil-structure mode ranges from 81 to 89 percent. The second mode of the structure is an out-of-phase soil-structure mode. Between 11 and 19 percent of the structure mass responds in this mode.

In the East-West direction, the fundamental natural frequency ranges from 2.03 hertz to 3.67 hertz for the lower bound and upper bound soil cases, respectively. Between 67 and 85 percent of the total structure mass responds in this translational soil-structure mode. Second mode response is associated with out-of-phase soil-structure translation. The percentage of total structure mass participating in this mode ranges from 15 to 33 percent.

In the vertical direction, diesel generator building dynamic response is basically a single soil-structure translational mode. Vertical natural frequencies range from 2.99 hertz for the lower bound soil case to 6.15 hertz for the upper bound soil case.

Table V-3-3 presents a comparison of fundamental structure natural frequencies for the lower bound and upper bound relative soil stiffness cases for each of the excitation directions and soil cases studied. Shifts in fundamental natural frequencies between the two models for identical excitation directions and soil cases were 5 percent or less. The close fundamental frequency comparisons indicated similar seismic response would be expected for the two models. These expectations were confirmed by making comparisons of zero period accelerations in the structure determined from these models. For these comparisons, response

accelerations were determined by directly integrating the coupled equations for both the lower bound and upper bound relative soil stiffness models for all soil cases. Table V-3-4 presents this comparison for the upper bound soil case. Results for the upper bound soil case are presented because seismic response loads are maximized for this soil case. Results for other soil cases are similar.

In both the East-West and North-South excitation directions, zero period accelerations determined in the structure for the upper bound relative soil stiffness case exceed lower bound relative soil stiffness case results by about 10 to 15 percent except at Elevation 680'-0". At this elevation, zero period accelerations for the lower bound relative soil stiffness case exceed the upper bound relative soil stiffness case results by about 7 percent. In the vertical direction, lower bound relative soil stiffness case results are about 10 percent higher than upper bound relative soil stiffness case results except at Elevation 630'-6" where they are 6 percent less. Because seismic loads are directly related to inertial accelerations, these close comparisons of structural accelerations for the two relative soil stiffness cases lead to the conclusion that structural loads could be determined with acceptable accuracy with either model. Therefore, seismic response loads and composite modal damping were determined for the upper bound relative soil stiffness case only. However, in-structure response spectra may be more sensitive to the dynamic model response characteristics, both the upper and lower bound relative soil stiffness cases were used in developing in-structure response spectra for each of the three soil cases. SME in-structure response spectra at each floor were then taken as an overall envelope of three soil cases for both the lower and upper bound relative soil stiffness cases.

3.2 COMPOSITE MODAL DAMPING

As discussed in Section 6 of Volume I of this report, time history and response spectrum analyses were conducted for the SME. Time-history analyses were used to develop the in-structure response

spectra used as input to floor mounted equipment. Response spectrum analyses were used to generate seismic response loads in the diesel generator building.

By using response spectrum analyses to determine seismic response loads, excess conservatism was avoided since the SME ground response spectra are smooth and do not have the peaks and valleys associated with the spectra generated by the synthetic time histories. Use of response spectrum techniques to determine seismic response loads required the development of composite modal damping values for the structure.

The procedure presented in Volume I of this report was used to define composite modal damping for the coupled soil-structure model of the diesel generator building. This method is based on matching the response computed from the coupled equations of motion with the modal response at selected locations. Soil impedances are considered to act at the centroid of the overall foundation in determining structure dynamic characteristics. Structure response transfer functions are developed at a number of locations in the structure for both the rigorous and normal mode solutions. Modal damping values for the normal mode solution are iterated upon until the transfer functions for the two solutions match. By choosing locations which are sensitive to damping, composite modal damping values are determined which generally predict conservative response at all locations.

Composite modal damping values were determined using the program SOILST (Reference 16). The embedded stiffness and dashpots presented in Tables V-2-5 and V-2-7 defined the soil impedances beneath the structure in this analysis. Structural damping of 7 percent of critical damping was used for the reinforced concrete diesel generator building. The fixed-base structure modes and corresponding structural modal damping were input to program SOILST to determine composite modal damping which accounted for both structural damping and soil radiation and material damping.

Composite modal damping values were determined for a number of locations in the structure. Typical floors were chosen in the building that were relatively high in the structure and were judged to have dynamic responses sensitive to modal damping. Composite modal damping values for all modes were chosen based on a conservative fit of the data for all locations studied. Composite modal damping values were determined using the methodology described above for all modes contributing to more than about 10 percent of the total degree-of-freedom response at the structure location studied.

The composite modal damping values used to determine seismic response loads in the diesel generator building for the upper bound relative soil stiffness case are presented in Table V-3-1. Damping for the fundamental horizontal translational soil-structure modes ranges from 15 percent of critical damping for the upper bound soil case to 22 percent of critical damping for the lower bound soil case. Composite modal damping values used for the fundamental vertical mode range from 36 to 60 percent of critical damping. Damping for the second horizontal translational mode ranged from 3.5 to 60 percent of critical damping. Composite modal damping values were not developed for the lower bound relative soil stiffness case as previously discussed.

To ensure that composite modal damping values were conservatively chosen for all structure modes, comparisons of structural response predicted by direct integration time history analysis using concentrated dashpots to model the soil damping were made with the seismic response determined by modal superposition using composite modal damping. Response accelerations at typical locations in the structure were determined from direct integration of the coupled equations of motion. At these same locations, response accelerations were then developed from a modal superposition time history analysis of the flexible base structure model using the modal damping values defined for each soil case by Table V-3-1. The same input time history was used in both time history analyses. Response accelerations from the two analyses were compared to ensure the

accelerations based on the composite modal damping values approximately met or exceeded those determined from the direct integration time-history analyses. Table V-3-5 presents comparisons of zero period accelerations in the structure obtained by these two procedures for the upper bound soil case. The results for the upper bound soil case are presented since seismic response loads throughout the structure are generally controlled by this soil case.

3.3 STRUCTURE SEISMIC RESPONSE

Seismic loads throughout the structure were determined from the upper bound relative soil stiffness case dynamic model of the diesel generator building for each of the three soil cases studied. The overall seismic loads computed for the building were distributed to the individual structural elements as described in Section 3.3.3 of this volume.

The seismic loads in the structure were determined using response spectrum modal analysis techniques. Earthquake excitation was specified as the SME ground response spectra for the top-of-fill ground surface. The development of these spectra is described in Section 2.2 of Volume I of this report. Soil-structure interaction effects were considered for the upper, intermediate, and lower bound soil cases.

The overall seismic loads were developed from the SRSS of the modal responses including consideration of closely spaced modes as discussed in Section 6.4 of Volume I. The structural response loads were determined for each of the three earthquake direction components acting independently. Accidental torsion was accounted for as described in Volume I. For the SMR, the highest load computed for the structural element from any of the three soil cases was used to determine its code margin.

3.3.1 Effects of Soil Conditions on Seismic Loads

Plots of horizontal seismic shear, overturning moments, and axial loads in the structure are presented in Figures V-3-1 through V-3-5 for the three soil cases studied. Seismic response loads were controlled in all cases by the upper bound soil case. The seismic loads were developed based on the upper bound relative soil stiffness case dynamic models from Figure V-2-13(a). Seismic response loads were not obtained for the lower bound relative soil stiffness case for the reasons discussed in Section 3.1.

3.3.2 Comparison of SME and FSAR Loads

One basis for selecting various elements for code margin evaluation for the SMR was the ratio of SME seismic load to the seismic load used for design. In order to determine the relative magnitudes of the SME loads to the corresponding FSAR loads, comparisons of the lateral shear forces, and overturning moments throughout the structure are shown in Figures V-3-6 through V-3-9. Because the structure is considered to be symmetric, dynamic torsional loads were not calculated.

Figures V-3-6 and V-3-7 present comparisons of the lateral shear forces throughout the diesel generator building. SME loads exceed FSAR values by about 5 to 15 percent throughout the structure. The corresponding overturning moments are presented in Figures V-3-8 and V-3-9. SME seismic overturning moments exceed FSAR moments by about 10 percent at all locations.

3.3.3 Element Loads

The dynamic model used for the seismic analysis of the diesel generator building consisted of a single column of vertical beam elements. Each vertical element typically modeled the combined stiffness of the structural members of the load-resisting system at that story. Overall seismic loads acting on the structure were developed for these elements

from the response spectrum analyses. Distribution of the overall loads to the individual structural members was performed using techniques appropriate for the load-resisting system evaluated.

The diesel generator building is composed primarily of concrete shear walls interconnected by concrete floor slabs. For this type of structural system, the floor slabs act as diaphragms transmitting the seismic inertial forces to the load-resisting shear walls. If the diaphragms have sufficient stiffness, the walls spanning a story are constrained to displace together in the lateral directions. The overall seismic lateral loads can then be distributed to the individual walls in proportion to their relative rigidities. This technique is commonly used to develop load distributions for the design of concrete shear wall/floor slab systems.

The rigid diaphragm approximation was judged to be adequate for the determination of lateral seismic loads acting on the shear walls of the diesel generator building. Load distributions to the individual structural elements were developed as described in Section 6.7 of Volume I. In general, the exterior walls as well as the major interior walls separating the individual diesel generator bays were included in the seismic load distributions. As an example, the plan layout of these walls between Elevation 630'-6" and Elevation 664'-0" is shown in Figure V-3-10. Although there are other minor concrete walls located in the diesel generator building, the portion of seismic load resisted by these walls is small and was neglected so that loads acting on the major walls would be conservative. Masonry walls were not considered to be capable of resisting forces due to overall structure seismic response.

Story stiffnesses for the walls identified as being seismic load-resisting were calculated using the approach described in Section 6.7 of Volume I. Out-of-plane wall stiffnesses were not included so that conservative in-plane loads would be produced. In-plane wall story stiffnesses considered the effects of both shear and flexural deformations.

As an approximation, the flexural wall story stiffnesses were based on a condition of rotational fixity imposed at the top and bottom of the stories. The influence of flexural deformations diminishes for walls whose lengths are greater than their story heights and the lateral deflections of these walls are due primarily to shear deformations. The distribution of lateral seismic load, therefore, is not expected to be sensitive to the treatment of wall rotational boundary conditions.

Additional detail was required to determine the lateral story stiffnesses of the south exterior wall. As shown in Figure V-3-11, this wall is perforated by several large openings. At the lower story from Elevation 630'-6" to Elevation 664'-0", the major openings separate the wall into a series of individual piers linked together by horizontal beams. To more accurately account for the effect of these beams, the lateral stiffness of the lower story was based on the results of a MODSAP finite element analysis. The piers and spandrels were discretized into plate elements. Consistent with the development of the lateral stiffnesses of the other walls, a condition of rotational fixity was imposed at the top and bottom of this story. The lateral stiffnesses of the piers of the upper story from Elevation 664'-0" to Elevation 680'-0" were determined in the same manner as the other walls of the diesel generator building.

Seismic in-plane shears and overturning moments for the walls of the diesel generator building were calculated following the methodology for shear wall/floor slab systems described in Section 6.7 of Volume I. Wall element relative rigidities associated with the rigid diaphragm approximation were based on the wall story stiffnesses. Individual wall shears due to overall structure shears and torsional moments were then calculated using equations presented in Reference 18. Load input to these equations consisted of shears and torsional moments predicted by the structure response spectrum analyses. Seismic loads acting on the wall elements evaluated in the SMR are listed in Table V-4-1. As previously noted, the lateral stiffness of the south exterior wall from

Elevation 630'-6" to Elevation 664'-0" was based on the results of a finite element analysis and was used to determine the total seismic load distributed to this wall. This stiffness was compared to the value predicted by modeling the piers as individual walls and neglecting the coupling provided by the beams. Since comparison was close, it was concluded that the piers behaved as independent walls and that the total load distributed to the south exterior wall could in turn be distributed to the piers on the basis of their rigidities relative to each other.

Overall axial loads due to seismic response were available from the results of the response spectrum analyses. These axial loads were distributed to the walls in proportion to their cross-sectional areas. These axial loads have an effect on the capacities of the walls against shear and overturning moment. However, capacities of the walls are not particularly sensitive to small changes in the axial loads due to seismic response.

The concrete floor slab at a given elevation serves as a diaphragm distributing floor inertial forces to the load-resisting shear walls. The slab also redistributes seismic shears from the walls of the story above to the walls of the story below when there is an alteration in the relative wall stiffness distribution from story to story. The diaphragm can be idealized as a beam subjected to load comprised of the seismic floor inertial force and shears from the walls of the story above. Support reaction for the idealized beam consist of the shears for the walls of the story below. Diaphragm in-plane shears and moments at the critical sections were determined based on these applied loads and reactions. For slabs framing into an exterior wall, the diaphragm shear at the wall is equal to the difference in wall shears between the story above and the story below. This treatment accounts for diaphragm loads due to both floor inertial forces and redistribution of lateral seismic loads due to changes in the stiffness distribution of the vertical load-resisting elements. It is conservative since the diaphragm load calculated in this manner includes the inertial load associated with the wall

itself which is not actually transmitted through the diaphragm. Applied seismic loads acting on the diaphragms selected for evaluation in the SMR are listed in Table V-4-2.

The load combination used in the structures capacities evaluation is discussed in Section 7.1 of Volume I. The dead and live load cases account for loads occurring at normal operating conditions. Forces and stresses in the structural members of the diesel generator building due to loads occurring at normal operating conditions were taken from the results of the static analyses supplied by Bechtel (Reference 19). Load cases used in the FSAR static analysis consisting of various combinations of dead, live, and settlement loads were available. The effects of thermal gradients through the walls are discussed in Section 4.4. The code margins for the structural elements were calculated for the worst case obtained from the following combinations:

$$U = D + SME$$
$$U = D + L + SME$$
$$U = D + L + T + SME$$
$$U = D + T + SME$$

where:

D = Dead Loads
L = Live Loads
T = Settlement Loads
SME = Seismic Margin Earthquake Loads

The three-dimensional finite element model used for these static analyses generally consisted of plate elements representing the walls and slabs and beam elements representing the columns and the wall footings. Applied loads accounted for the effects of dead weight, live load, and differential settlement. Results from the static analyses for the plate elements modeling the concrete walls and slabs consisted of membrane normal and shear forces per unit length and out-of-plane bending and

twisting moments per unit length. For the walls and slabs, net in-plane axial forces, shears, and moments were calculated by integrating the reported plate element membrane stresses along the cross-sections being evaluated. In-plane shears and moments due to loads occurring at normal operating conditions for the walls and diaphragms evaluated in this study are also listed in Tables V-4-1 and V-4-2. Out-of-plane moments predicted by the plate elements were taken directly from the analytical results.

TABLE V-3-1

DIESEL GENERATOR BUILDING NATURAL FREQUENCIES, MODAL MASSES, AND MODAL DAMPING

UPPER BOUND RELATIVE SOIL STIFFNESS CASE

Two Dimensional Dynamic Model Evaluated	Mode	Lower Bound Soil			Intermediate Soil			Upper Bound Soil			Mode Description
		Frequency (Hertz)	Modal Mass (%)	Modal Damping (% Critical)	Frequency (Hertz)	Modal Mass (%)	Modal Damping (% Critical)	Frequency (Hertz)	Modal Mass (%)	Modal Damping (% Critical)	
North-South	1	1.81	93.4	28	2.52	95.4	20	3.06	95.8	15	Soil-Structure Translation
	2	4.07	6.6	11	6.01	4.6	11	7.44	4.2	11	Out-of-Phase Soil-Structure Mode
East-West	1	1.92	96.6	34	2.65	97.9	23	3.20	98.2	17	Soil-Structure Translation
	2	3.85	3.4	60	5.85	2.1	3.5	7.30	1.8	3.5	Out-of-Phase Soil-Structure Mode
Vertical	1	2.82	100.	60	4.59	100.	50	5.82	100.	36	Soil-Structure Translation

Note: 1. Modal mass percentage is defined as the percentage of the total structure mass participating in the mode. Modal mass percentages less than 0.1 percent are not shown.

TABLE V-3-2

DIESEL GENERATOR BUILDING NATURAL FREQUENCIES, MODAL MASSES, AND MODAL DAMPING

LOWER BOUND RELATIVE SOIL STIFFNESS CASE

Two Dimensional Dynamic Model Evaluated	Mode	Lower Bound Soil			Intermediate Soil			Upper Bound Soil			Mode Description
		Frequency (Hertz)	Modal Mass (%)	Modal Damping (% Critical)	Frequency (Hertz)	Modal Mass (%)	Modal Damping (% Critical)	Frequency (Hertz)	Modal Mass (%)	Modal Damping (% Critical)	
North-South	1	1.90	81.4	N.A.	2.80	87.6	N.A.	3.44	89.2	N.A.	Soil-Structure Translation
	2	4.44	18.6	N.A.	6.58	12.4	N.A.	8.19	10.8	N.A.	Out-of-Phase Soil-Structure Mode
East-West	1	2.03	66.8	N.A.	3.00	81.1	N.A.	3.67	84.7	N.A.	Soil-Structure Translation
	2	3.38	33.2	N.A.	5.02	18.9	N.A.	6.25	15.3	N.A.	Out-of-Phase Soil-Structure Mode
Vertical	1	2.99	100.	N.A.	4.86	100.	N.A.	6.15	99.7	N.A.	Soil-Structure Translation
	2	–	–	–	–	–	–	18.2	0.3	N.A.	Local Mode

Note: 1. Modal mass percentage is defined as the percentage of the total structure mass participating in the mode. Modal mass percentages less than 0.1 percent are not shown.

2. N.A. - Not applicable for this model.

TABLE V-3-3

COMPARISON OF FUNDAMENTAL DIESEL GENERATOR BUILDING NATURAL FREQUENCIES

Soil Stiffness Case	Lower Bound Soil			Intermediate Soil			Upper Bound Soil		
	N-S Direction	E-W Direction	Vertical Direction	N-S Direction	E-W Direction	Vertical Direction	N-S Direction	E-W Direction	Vertical Direction
Lower Bound Relative Soil Stiffness Case	1.90	2.03	2.99	2.80	3.00	4.86	3.44	3.67	6.15
Upper Bound Relative Soil Stiffness Case	1.81	1.92	2.82	2.52	2.65	4.59	3.06	3.20	5.82

All frequencies are in hertz

TABLE V-3-4

COMPARISON OF IN-STRUCTURE ZERO PERIOD ACCELERATION
DETERMINED BY DIRECT INTEGRATION
UPPER BOUND SOIL CASE

Location	North-South Response Due to North-South Excitation		East-West Response Due to East-West Excitation		Vertical Response Due to Vertical Excitation	
	Lower Bound Relative Soil Stiffness Case	Upper Bound Relative Soil Stiffness Case	Lower Bound Relative Soil Stiffness Case	Upper Bound Relative Soil Stiffness Case	Lower Bound Relative Soil Stiffness Case	Upper Bound Relative Soil Stiffness Case
Elevation 680'-0"	0.313	0.335	0.272	0.282	0.131	0.143
Elevation 664'-0"	0.278	0.277	0.258	0.247	0.130	0.143
Elevation 630'-6"	0.209	0.190	0.228	0.196	0.150	0.141

All accerations are in G units.

TABLE V-3-5

COMPARISON OF IN-STRUCTURE ZERO PERIOD ACCELERATION DETERMINED
BY DIRECT INTEGRATION AND MODAL SUPERPOSITION
UPPER BOUND RELATIVE SOIL STIFFNESS CASE
UPPER BOUND SOIL CASE

Location	North-South Response Due to North-South Excitation		East-West Response Due to East-West Excitation		Vertical Response Due to Vertical Excitation	
	Direct Integration	Modal Superposition	Direct Integration	Modal Superposition	Direct Integration	Modal Superposition
Elevation 680'-0"	0.313	0.308	0.272	0.271	0.131	0.133
Elevation 664'-0"	0.278	0.276	0.258	0.259	0.131	0.133
Elevation 630'-6"	0.209	0.230	0.228	0.241	0.129	0.132

All accelerations are in G units

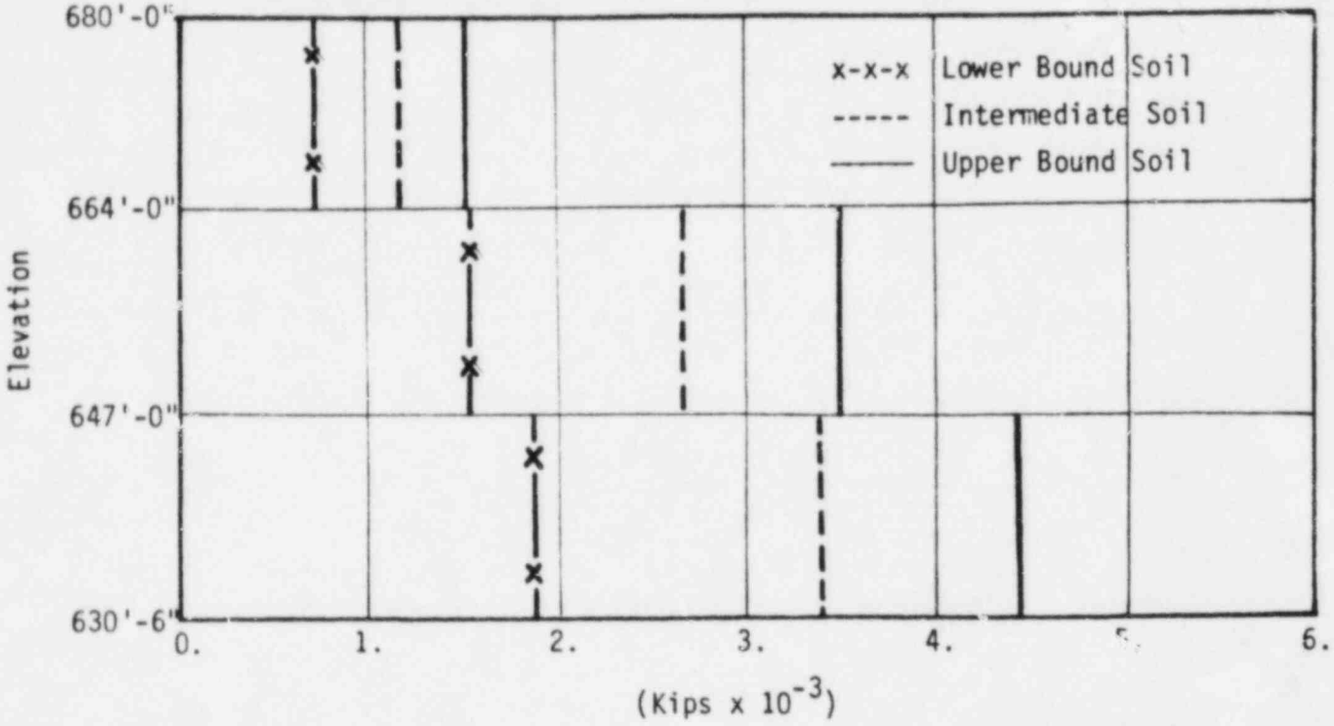

FIGURE V-3-1. DIESEL GENERATOR BUILDING N-S SHEAR

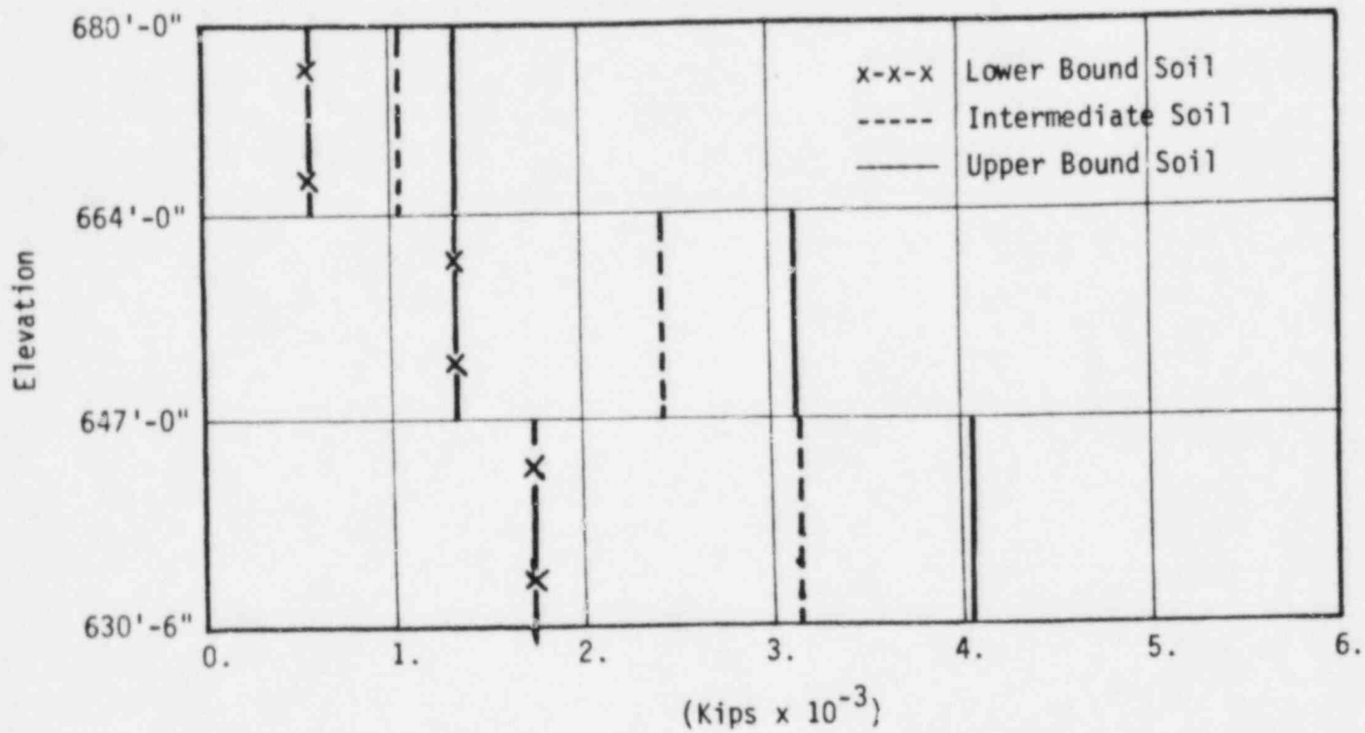

FIGURE V-3-2. DIESEL GENERATOR BUILDING E-W SHEAR

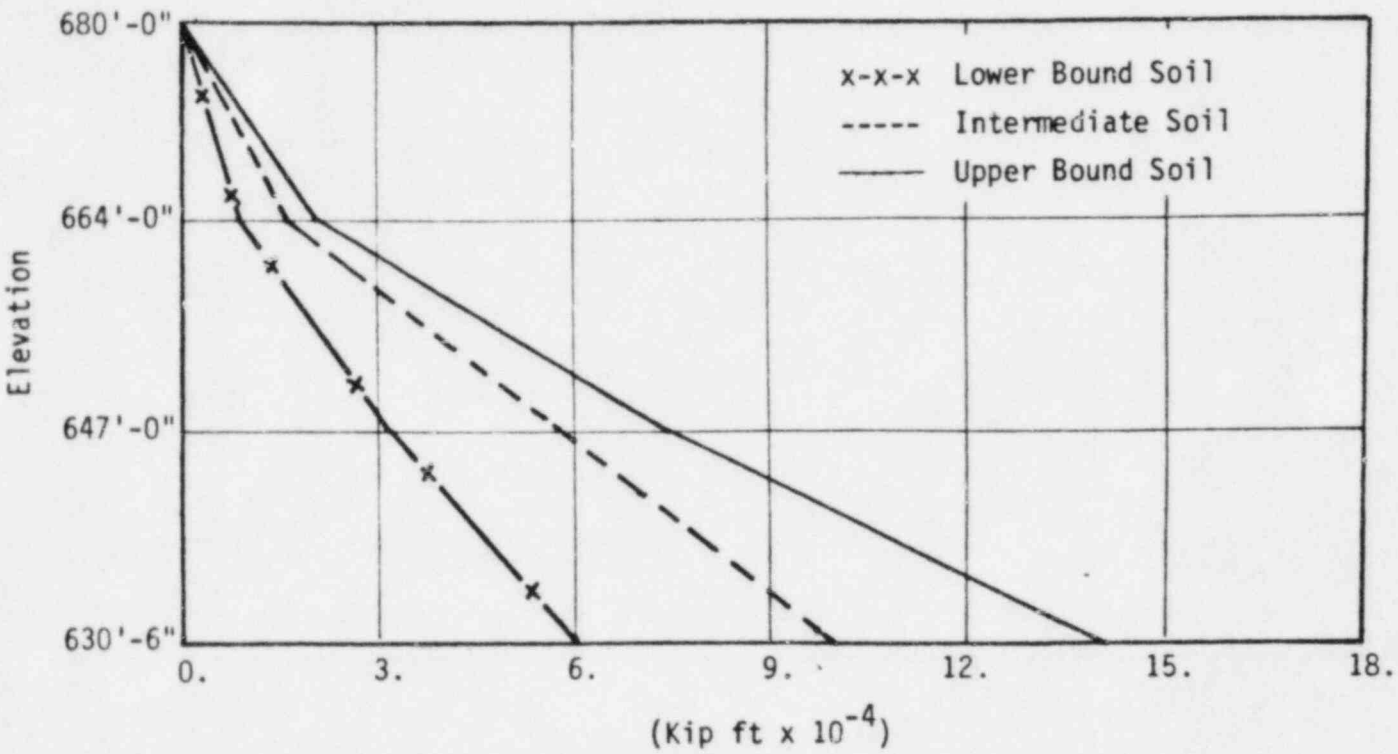

FIGURE V-3-3. DIESEL GENERATOR BUILDING MOMENT ABOUT N-S AXIS

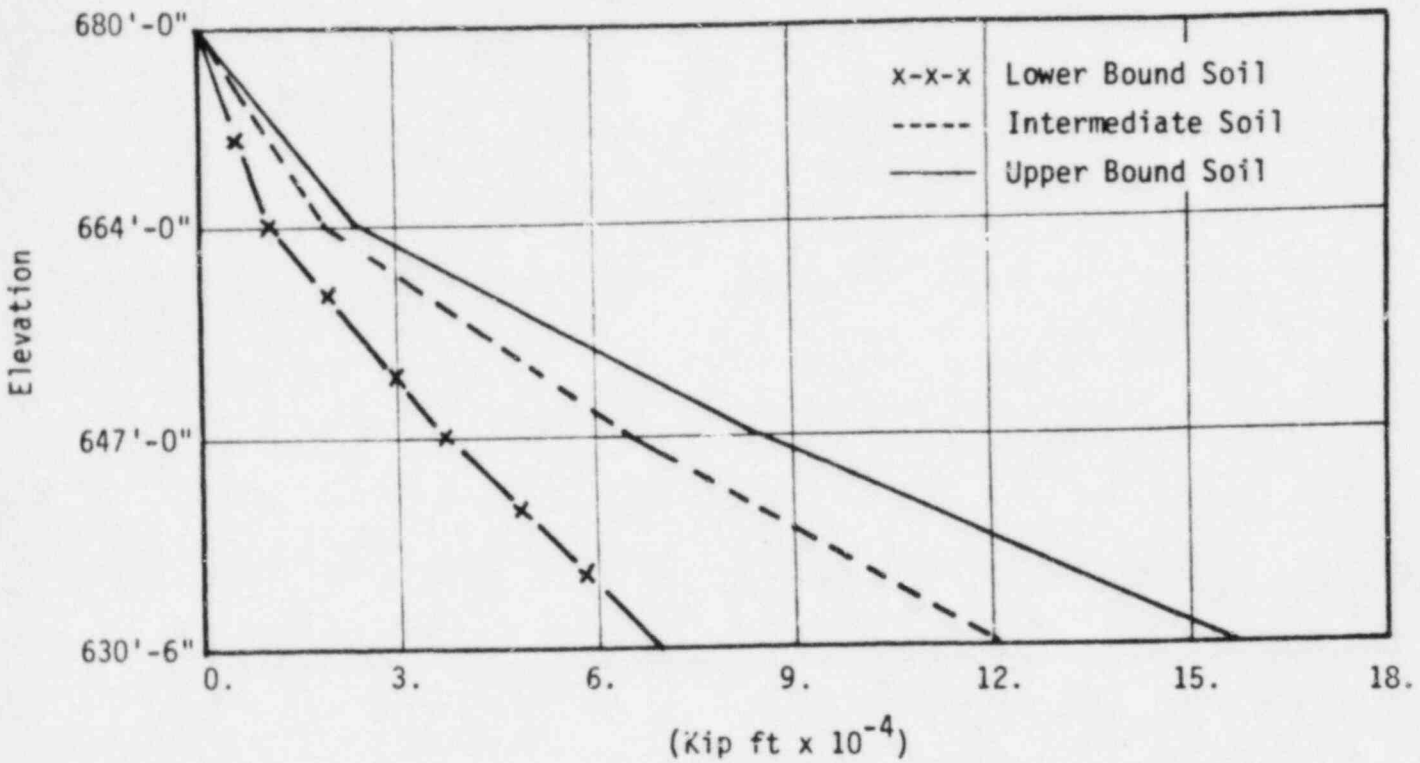

FIGURE V-3-4. DIESEL GENERATOR BUILDING MOMENT ABOUT E-W AXIS

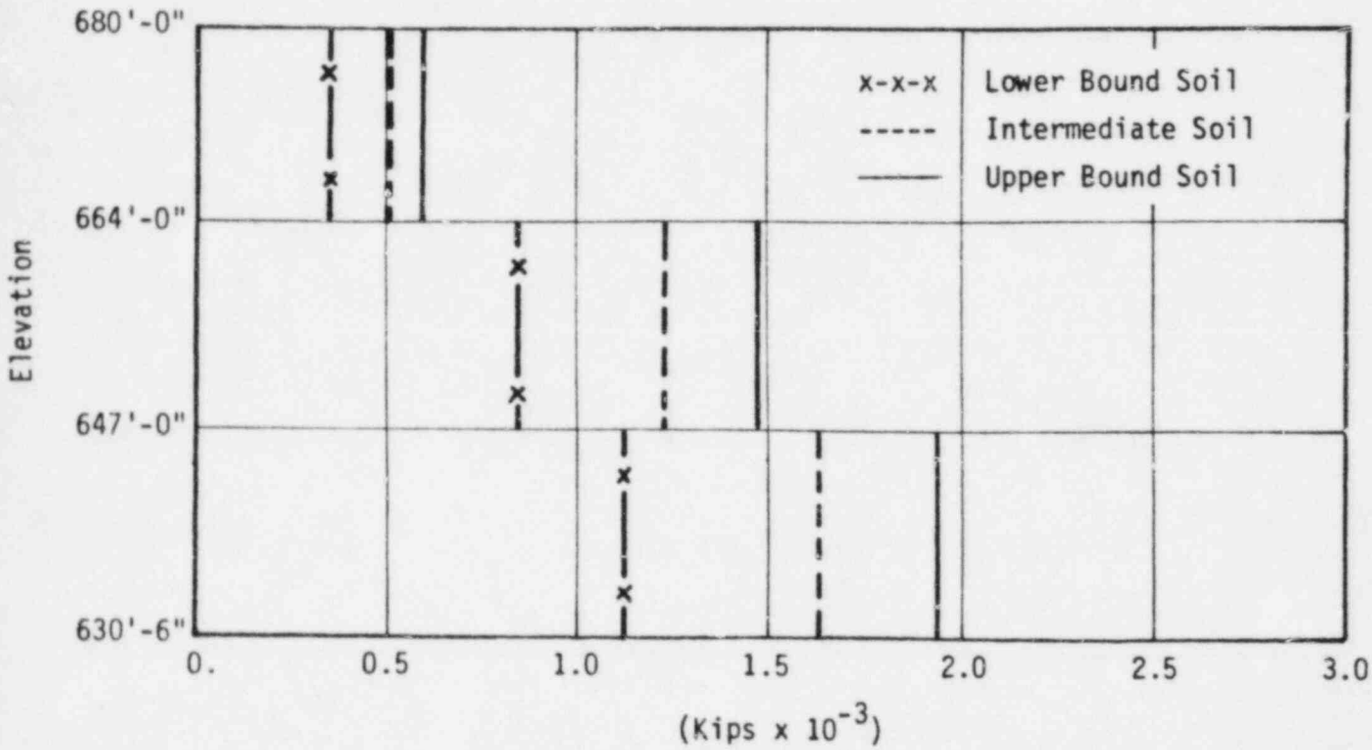

FIGURE V-3-5. DIESEL GENERATOR BUILDING AXIAL FORCE

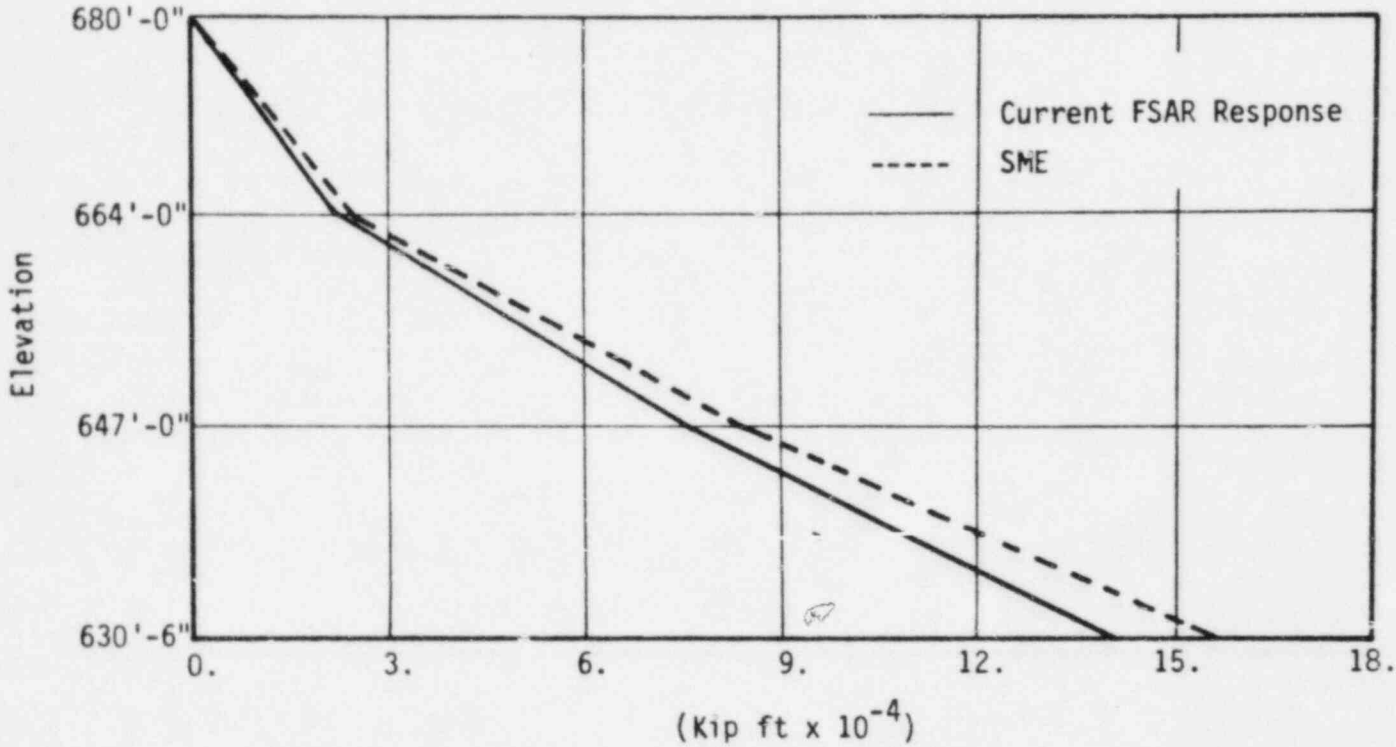

FIGURE V-3-6. DIESEL GENERATOR BUILDING MOMENT ABOUT E-W AXIS COMPARISON

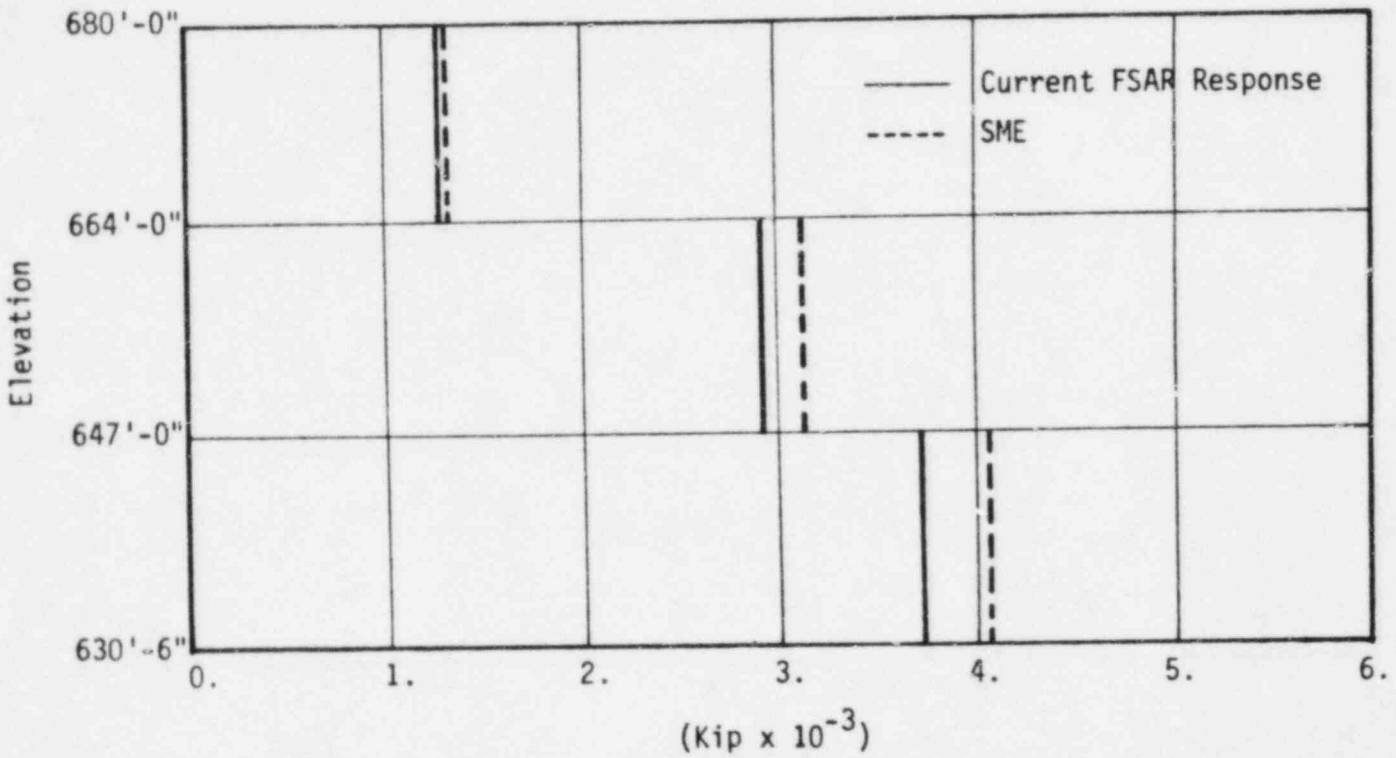

FIGURE V-3-7. DIESEL GENERATOR BUILDING E-W SHEAR COMPARISON

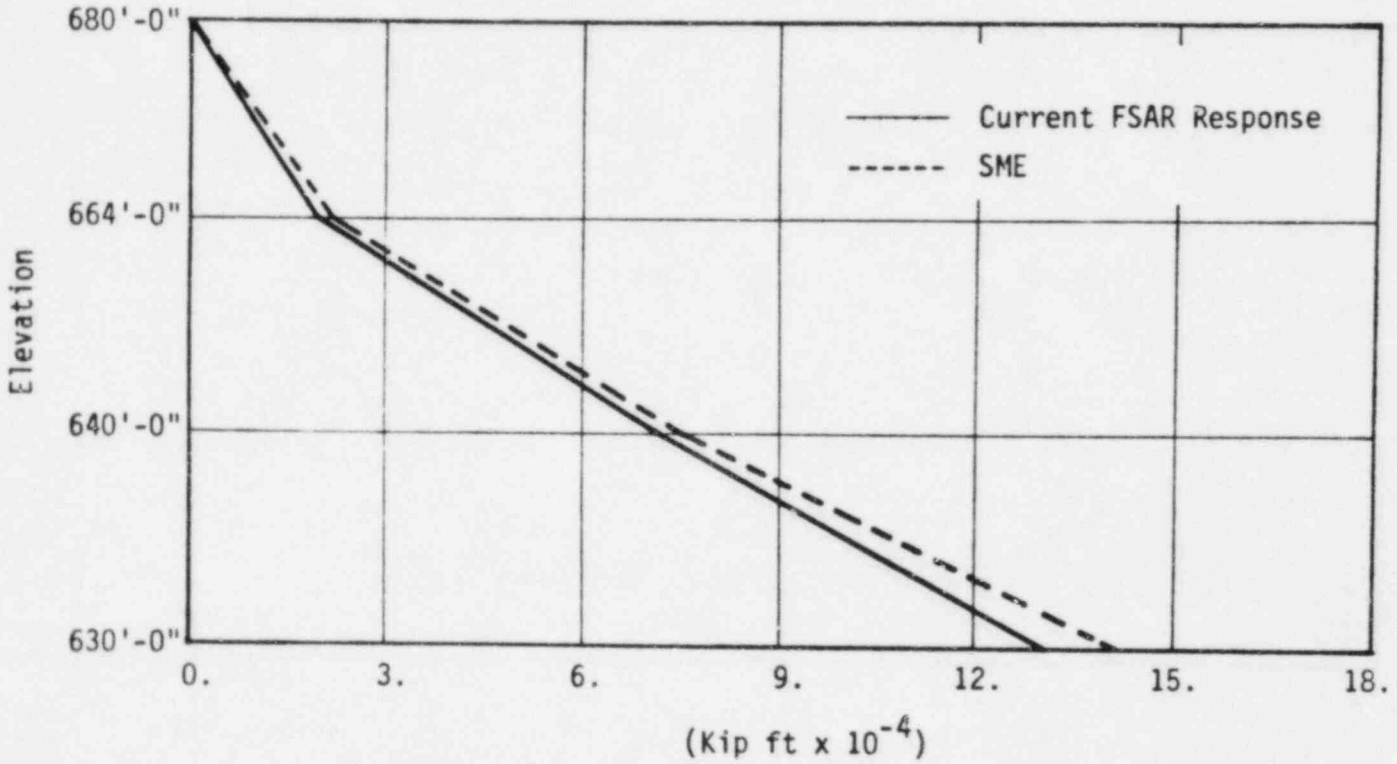

FIGURE V-3-8. DIESEL GENERATOR BUILDING MOMENT ABOUT N-S AXIS COMPARISON

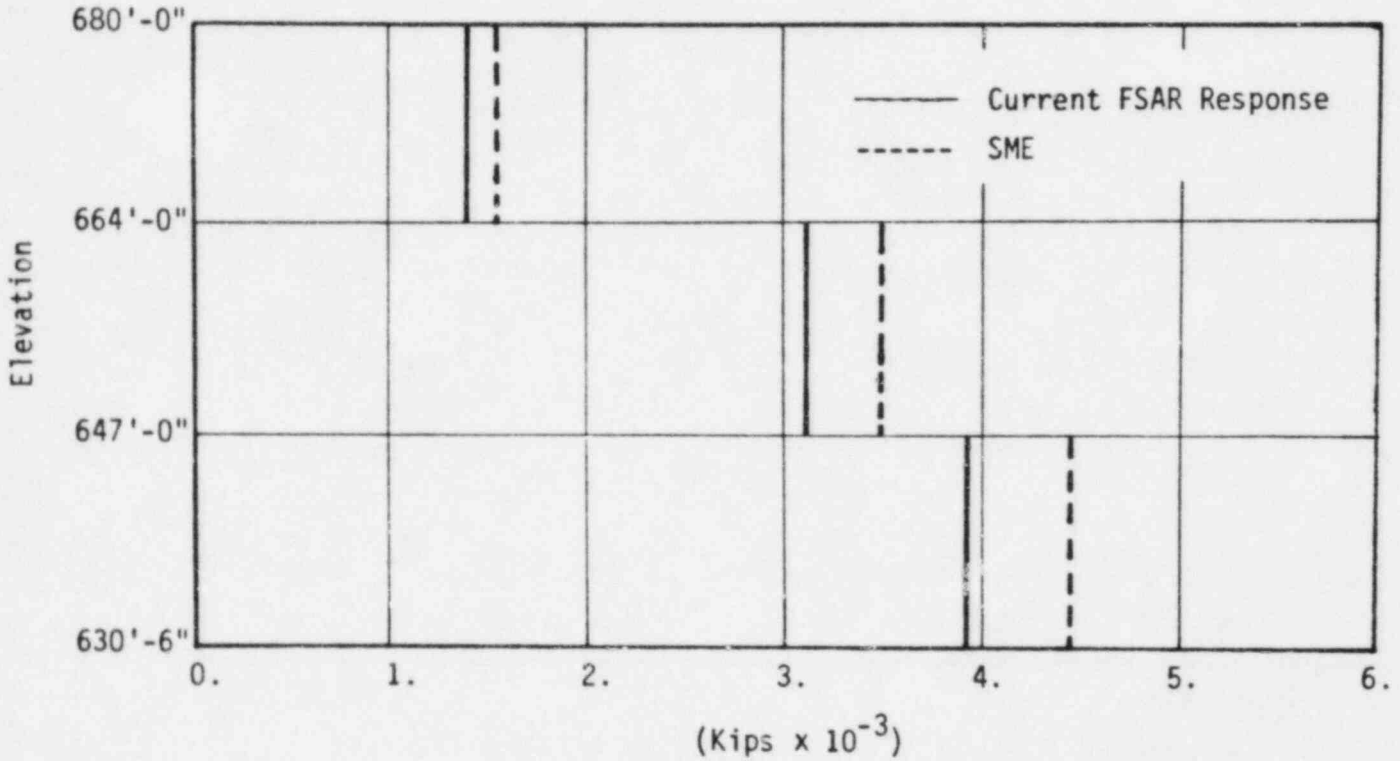

FIGURE V-3-9. DIESEL GENERATOR BUILDING N-S SHEAR COMPARISON

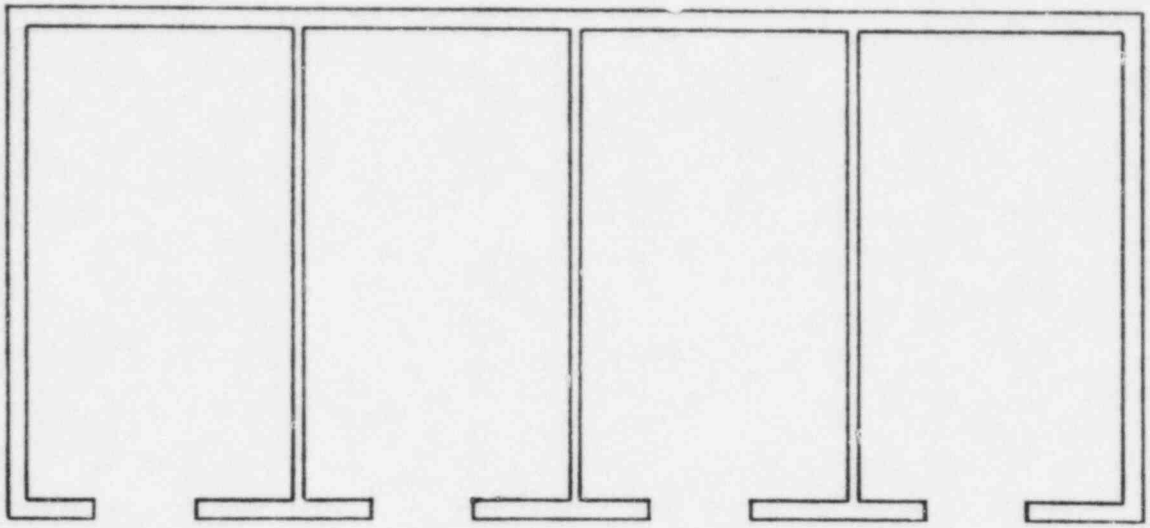

FIGURE V-3-10. IDEALIZED LAYOUT OF WALLS FROM ELEVATION 630'-6" TO ELEVATION 664'-0" INCLUDED IN LOAD DISTRIBUTIONS

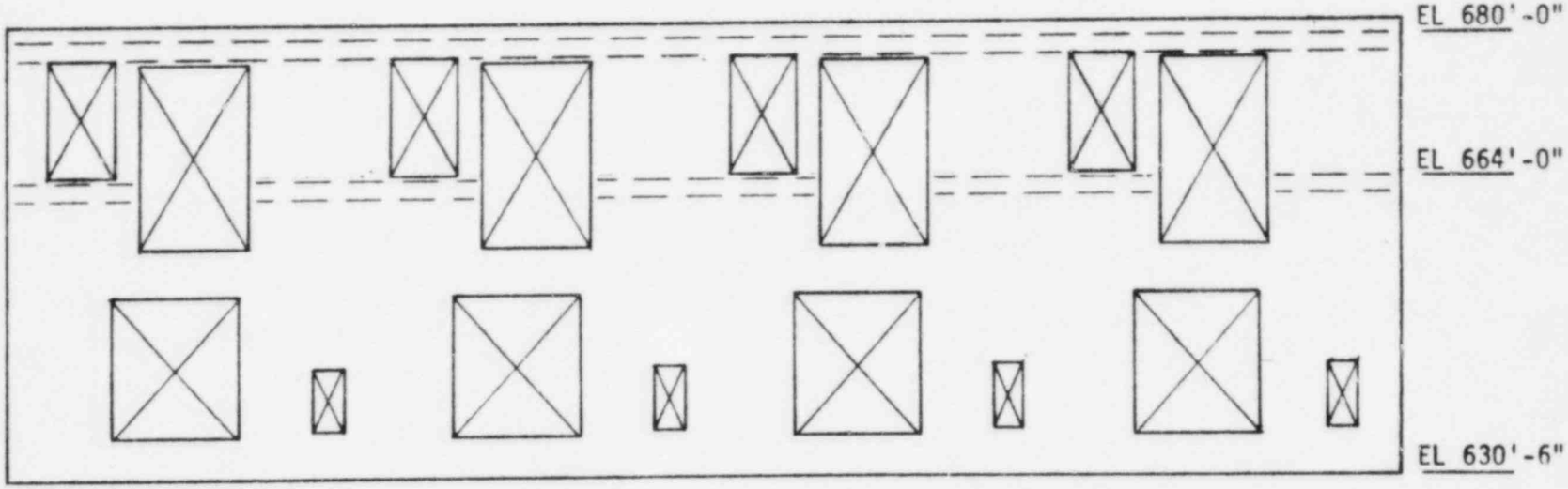

Note: Intersecting walls not shown for clarity

FIGURE V-3-11. ELEVATION OF SOUTH EXTERIOR WALL (LOOKING NORTH)

4. CODE MARGINS

For the structure code margins evaluation, a number of structural elements were selected from locations throughout the diesel generator building to compare their capacities as prescribed by the acceptance criteria against their loads due to the SME combined with normal operating loads. The selected shear wall and floor diaphragms are listed in Tables V-4-1 and V-4-2. Each shear wall and floor diaphragm is assigned an identification number in these tables. The location of the selected elements is then referenced by their identification numbers in Figures V-4-1 to V-4-3.

The structural elements selected for evaluation in this study are those expected to be more highly stressed due to seismic loads relative to other elements within the diesel generator building. General criteria used to identify structural elements to be included in the SME structures capacities evaluation involved several considerations. The layout of the shear walls was reviewed to determine the distribution of walls throughout the structure and the availability of resistance to lateral load. The load distributions were compared to identify walls required to resist a significant portion of the seismic load at each story. The physical conditions of the walls were reviewed to provide an approximate assessment of the relative wall capacities. This included considerations such as wall thickness, reinforcement patterns, and the presence of openings which would tend to reduce the amount of material available for load resistance. Particular attention was given to the major walls since their relative rigidities are typically greater than smaller walls and consequently receive greater loads.

Diaphragm elements were selected for detailed evaluation on a basis similar to that for the shear walls. Review of the shear wall layout through the structure also provided insight into the manner in

which the floor slabs function as diaphragms in providing load paths to the walls. From the load distributions, locations of possible significant diaphragm stress were identified. The physical conditions of the slabs, including slab thickness, reiforcement pattern, and the presence of openings were reviewed to provide an approximate assessment of the relative diaphragm capacities.

Capacities for the structural elements selected for review were developed in accordance with the structural acceptance criteria described in Section 7.2 of Volume I. For the reinforced concrete portions of the diesel generator building, the ultimate strength design provisions of ACI 349-80, "Code Requirements for Nuclear Safety Related Concrete Structures" (Reference 20), were followed. The ultimate strengths were conservatively based on minimum specified concrete crushing strengths. The concrete used in the construction of the diesel generator building was typically specified to have a minimum compressive strength of 4000 psi with the exception of the roof slab which was specified to be 5000 psi concrete. Reinforcing steel used was required to conform to ASTM Designation A615, Grade 60 and has a specified minimum yield stress of 60,000 psi.

4.1 SHEAR WALL CAPACITY

The shear strength provisions for concrete walls are contained in Section 11.10 of ACI 349-80. The total ultimate strength capacity is composed of separate contributions from the concrete and the steel reinforcement. ACI 349-80 provides alternative formulations with different levels of detail required for determining the concrete shear strength. Section 11.10.5 specifies the concrete shear strength as the value corresponding to an average shear stress of $2\sqrt{f'_c}$ (psi) acting on the effective area for walls in compression.

V_c = Nominal concrete shear strength, lb

= $2\sqrt{f'_c}\,hd$ for walls in compression (4-1)

f_c = Concrete compressive strength, psi

h = Wall thickness, in

d = Effective wall depth, in

This strength is subjected to a reduction if the wall is loaded in tension. This definition of the concrete shear strength was typically used to determine the wall capacities. Alternative formulations contained in Section 11.10.6 of ACI 349-80 that could possibly provide an increase in the concrete shear strength above that permitted in Equation 4-1 were not used for the diesel generator building. The wall shear strength contributed by the steel reinforcement was determined following the provisions of Section 11.10.9 of ACI 349-80. The steel shear strength was based on the horizontal reinforcement provided in each wall. The effective wall depth, d, was taken as 0.8 times the wall length as permitted by Section 11.10.4 of ACI 349-80. The wall ultimate shear strength was taken as the sum of the concrete and reinforcing steel shear strengths reduced by a strength reduction factor of 0.85. For walls separated into a series of piers by significant openings, shear capacities were developed for the individual piers. The total seismic shear acting on the wall was distributed to the piers in proportion to their relative rigidities using equations presented in Reference 18. Shears due to loads at normal operating conditions acting on the individual piers were determined as noted in Section 3.3.3 using stresses occurring in the plate elements modeling these piers.

Shear wall resistance to overturning moment is provided by the internal couple consisting of the vertical wall reinforcement stressed in tension and the concrete stressed vertically in compression. An efficient means of developing overturning resistance is by concentrating the necessary vertical reinforcement at the ends of the wall so that the moment arm will be a maximum. As an example, this type of reinforcement was provided

at the ends of the piers of the south wall to replace reinforcement interrupted by the openings. In general however, vertical reinforcement of the diesel generator building walls was uniformly distributed along the lengths of the walls.

As noted in Reference 21, experimental results indicate that the flexural strengths of rectangular shear walls with height-to-length ratios equal to or greater than 1.0 and containing uniformly distributed vertical reinforcement are adequately predicted by the design provisions for reinforcement concrete beams loaded axially and in bending. These provisions are contained in Section 10.2 of ACI 349-80. The flexural strength calculated using these provisions can be expressed by the following equation presented in Reference 21.

$$M'_u = A_s f_y L \left[\left(1 + \frac{N_u}{A_s f_y} \right) \left(\frac{1}{2} - \frac{\beta_1 c}{2L} \right) - \frac{c^2}{L^2} \left(1 + \frac{\beta^2}{3} - \beta_1 \right) \right] \qquad (4\text{-}2)$$

where:

$$\frac{c}{L} = \frac{q + \alpha}{2q + 0.85\beta_1}$$

$$q = \frac{A_s f_y}{L h f'_c}$$

$$\alpha = \frac{N_u}{L h f'_c} \text{ and } \beta = \frac{f_y}{87{,}000}$$

M'_u = Design resisting moment a section, in. lb.

A_s = Total area of vertical reinforcment at section, sq. in.

f_y = Specified yield strenqth of vertical reinforcement, psi

L = Horizontal length of shear wall, in.

c = Distance from extreme compression fiber to neutral axis, in.

d = Distance from extreme compression fiber to resultant of tension force, in.

h = Thickness of shear wall, in.

N_u = Design axial load, positive if compression, lb.

f'_c = Specified compressive strength of concrete, psi

β_1 = 0.85 for strength f'_c up to 4000 psi and reduced continuously at a rate of 0.05 for each 1000 psi of strength in excess of 4000 psi

Reference 21 presented the following approximation to this equation:

$$M'_u = 0.5A_s f_y L \left(1 + \frac{N_u}{A_s f_y}\right)\left(1 - \frac{\beta_1 c}{L}\right) \qquad (4\text{-}3)$$

Upon inspection of Equation 4-3, it is apparent that this approximation is equivalent to obtaining the flexural strength of an underreinforced beam with the uniformly distributed reinforcement lumped at midlength of the wall.

Based on the findings of Reference 21, the design provisions in Section 10.2 of ACI 349-80 were used to determine the resistances to overturning moment for the walls of the diesel generator building. In

accordance with Section 9.3.2 of ACI 349-80, the calculated overturning moment resistances, M_u', were modified by appropriate strength reduction factor ϕ.

$$M_u = \phi M_u'$$

where ϕ = strength reduction factor per Section 9.3.2 of ACI 349-80.

Most of the major walls of the diesel generator building are intersected at their ends by other walls oriented transversely. Due to deformational compatibility at the intersections, these transverse walls will behave similar to flanges of a wide-flanged steel beam. However, only the resistance to overturning moment provided by the web of the wall loaded in-plane was accounted for. This is conservative since the additional overturning resistance provided by the flanges may be significant due to their greater internal moment arms.

Some of the walls evaluated in this study contain small openings for doorways, pipe penetrations, etc. Typical details call for additional vertical reinforcement to be provided at the faces of the openings to make up for the reinforcement interrupted by these openings. The flexural strength of a wall containing small openings was calculated for the wall as a single element rather than as a series of individual piers since the openings are generally small compared to the wall itself and are usually isolated as opposed to occurring in a regular pattern through the wall height. Failure is expected to occur due to gross, overall behavior. The additional reinforcement around the openings is normally sufficient to resist any stress concentrations. An exception to this treatment is the south exterior wall which is separated into a series of individual piers by the large openings occurring in a regular pattern. The selected piers of this wall were evaluated as individual structural elements.

Some of the walls of the diesel generator building are subjected to out-of-plane forces under normal operating conditions including soil settlement. Out-of-plane moments due to normal operating conditions

including soil settlement were available from the results of Bechtel's static analyses performed on their finite element model. The presence of out-of-plane moments about a horizontal axis through the wall is expected to influence the capacity of the wall to resist the in-plane overturning moment due to horizontal seismic response of the building. The procedure used to account for the effects of out-of-plane moments on the wall overturning moment capacities is described in Appendix C of Volume III.

The possibility of failure due to either in-plane shear or overturning moment was considered. Overturning moment was found to govern each of the selected shear walls. The code capacities determined in accordance with ACI 349-80 as well as the loads due to the SME and normal operating conditions are listed in Table V-4-1. The loads were calculated as described in Section 3.3.3. Applied loads due to dead, live, and settlement load cases were combined to create the most adverse loading condition on the walls. That is, if the force due to the live or settlement load cases tended to reduce the effect of the force due to seismic, it was not included for conservatism.

The code margins for the selected shear walls were developed from the calculated loads and capacities and are listed in Table V-4-1. The code margin, CM, is defined as the ratio of the code capacity to the applied load. The applied load is specified by the load combination given in Section 7.1 of Volume I and is taken as the sum of the applied loads due to the seismic and normal operating condition load cases.

CM = Code Margin = $\frac{C}{P}$

C = Element code capacity load

P = Applied load due to the combined normal operating condition seismic load cases = $P_{NOL} + P_{SME}$

P_{NOL} = Applied load due to normal operating condition loads (dead, live, and settlement loads)

P_{SME} = Applied load due to the SME

In general, the walls are subjected to axial loads occurring simultaneously with the shears and overturning moments. The magnitudes of the axial load can have an influence on the shear and overturning capacities. Code margins were determined based on the capacities and loads under consideration (shear or overturning) with the effect of the axial load included in the capacities.

For each of the selected shear walls, a factor F_{SME} is also listed in Table V-4-1. This term is the factor by which the SME ground motion would have to be multiplied to cause loads equal to the code capacities:

$$F_{SME} = \frac{C - P_{NOL}}{P_{SME}}$$

When the effect of axial load was included in the capacity, this equation was modified to account for the influence of the axial load due to seismic response. F_{SME} factors less than the code margins occur when the seismic axial load tends to reduce the capacity against overturning moment. As an example, derivation of the F_{SME} factor for one of the piers forming the south exterior wall from Elevation 630'-6" to Elevation 664'-0" (wall identification number 1) is as follows:

M_{SME} = Overturning moment due to the SME factored by F_{SME}

= $2,760F_{SME}$ k-ft

M_{NOL} = Overturning moment at normal operating conditions

= 1,460 k-ft

$M_{NET} = M_{SME} + M_{NOL}$

= $2,760F_{SME} + 1,460$

M_U = Overturning moment capacity per Equation 4-3 including the effects of the axial load due to the SME factored by F_{SME}

= $-0.731 F_{SM}^2 - 163F_{SME} + 7,850$ k-ft

$M_U = M_{NET}$

$-0.731F_{SME}^2 - 163F_{SME} + 7,850 = 2,760F_{SME} + 1,460$

$-0.731F_{SME}^2 - 2,920F_{SME} + 6,390 = 0$

$F_{SME} = 2.2$

4.2 DIAPHRAGM CAPACITY

Capacities of diaphragms for in-plane shear and moment are not directly addressed by ACI 349-80. However, it is common to design concrete diaphragms by the same provisions as those used for shear walls because of similarities in geometry and loading. Section 11.8 of Reference 23 specifies the same limiting shear stress for shear walls and diaphragms. Consequently, in-plane shear and flexural capacities of the diaphragms selected for evaluation were calculated in the same manner as the corresponding capacities of the shear walls. The slabs must also transmit out-of-plane shears due to vertical forces. Because the in-plane concrete shear strength was determined in accordance with Sections 11.10.2 to 11.10.8 of ACI 349-80, Section 11.10.1 eliminates the need to consider interaction between in-plane and out-of-plane shear.

The diaphragms of the diesel generator building selected for evaluation correspond to locations where slab openings reduce the amount of material available to resist the applied loads. The diaphragm sections evaluated are also on the load paths to the exterior walls. These walls, in addition to being among the major lateral load-resisting walls, resist larger portions of the torsional moments due to their greater distance from the story centers of rigidity. The diaphragm sections selected for evaluation are those expected to be the most highly stressed.

The diaphragms selected for evaluation were found to be governed by shear rather than in-plane moment. As noted in Section 3.3.3, the shears acting on diaphragms adjacent to exterior walls were calculated conservatively. The slab openings separate the diaphragms into piers similar to the piers of a shear wall. Code capacities and applied loads were determined for these piers as individual structural elements. Loads due to the SME and normal operating conditions, code capacities, code margins, CM, and F_{SME} factors are listed in Table V-4-2. The code margins and F_{SME} factors were determined in the same manner as for the shear walls.

4.3 EFFECTS OF REINFORCEMENT BAR CUTTING

The shear wall and diaphragm capacities were based on information available from the structural drawings for the selected elements. The presence of small and large openings indicated on the structural drawings was accounted for in the development of these capacities. Available nonconformance reports noting deviations from the construction specifications were reviewed to verify that there were no gross deviations that would significantly influence the capacity of the selected structural elements. The calculated wall capacities do not include the effect of any minor deviations. The capacities reported in Tables V-4-1 and V-4-2 also do not address the reduction in strength due to reinforcement cutting permitted by Reference 17 since the exact location and number of reinforcement bars cut within this allowance was unavailable. Per Section 2.1 of Appendix E of Reference 17, one bar could be cut each way, each face, with the radial distance to the next cut bar on the same face, in the same direction, no less than five feet. Per Section 2.2 of Appendix E of Reference 17, two bars could be cut each way, each face, with the radial distance to the next cut bar on the same face, in the same direction, no less than 10 feet. Additional limitations are noted in Section 7.2 of Volume I.

To determine the effects of the reinforcement cutting allowance and the non-conformances on the overturning moment capacity of the walls, the wall with the lowest code margin against overturning, which is one of the piers of the south exterior wall from Elevation 630'-6" to Elevation 664'-0", was recalculated. It was assumed that vertical bars at each face were cut every five feet along a horizontal plane. No non-conformances were reported for the wall at this story. Using the effective reinforcement area, the overturning moment was recalculated. A code margin of 1.6 corresponds to this revised capacity compared to 1.8 as originally calculated.

To determine the effect of the reinforcement cutting allowance and non-conformances on the shear capacity of the diaphragms, the diaphragm with the lowest code margin which is adjacent to the west exterior wall at Elevation 664'-0", was recalculated. The effect of reinforcement cutting is expected to be dependent on the crack pattern that leads to failure of the wall. If a crack crosses a horizontal bar where it has been cut or where it does not have sufficient development length from the cut to develop its yield strength, then the effectiveness of that bar may be significantly reduced. As an approximation, a crack was assumed to form at a 45 degree angle from horizontal through the story height of the wall noted above. This angle is approximately consistent with the crack angle assumed in the derivation of the shear strength provided by web reinforcement of concrete beams. For the worst case of horizontal bars cut at both faces every five feet along the assumed crack, the reinforcement area effective in resisting shear was modified and the total diaphragm shear strength recalculated. Using the revised shear strength, a code margin of 1.6 was determined for this diaphragm compared to 2.0 as originally calculated.

The code margins for the walls and the diaphragms were still found to be greater than unity when the reinforcement cutting allowance and non-conformances were considered for the selected examples. It can be concluded that the cutting allowance and the non-conformances do not adversely affect the results of this study for the walls and diaphragms of the diesel generator building.

4.4 EFFECTS OF THERMAL GRADIENTS

Some of the walls and diaphragms whose code margins were evaluated as part of the SMR are subjected to thermal gradients at normal operating conditions. These thermal gradients can introduce additional moments on the structural members due to restraint imposed by their supports against the thermal curvature. Design thermal gradients for the walls and slabs evaluated in the SMR were transmitted by Reference 24. These values were based on the most severe combination of interior operating temperature and effective exterior temperature with the interior temperature being the greater for all cases supplied.

An approach to account for thermal gradients was included in a study described in Appendix C of Volume III to determine the effect of out-of-plane moments on in-plane wall and diaphragm capacities. Based upon the results of this study, it was determined that the effect of out-of-plane moments and thermal gradients on the in-plane moment capacities could be adequately represented by the simplified method described in Appendix C of Volume III.

4.5 SOIL BEARING AND STRUCTURE STABILITY CAPACITY

The factor of safety for net dead, live, and seismic loads reported in the FSAR (Reference 1) is shown as 2.9 based on a net soil ultimate bearing capacity of 14,000 lb/ft^2. As indicated in Figures V-3-6 through V-3-9, SME shears and overturning moments in both the N-S and E-W directions are only slightly greater than the corresponding FSAR loads at the building foundation interface. Using the SME seismic loads and a peak net dead plus live load bearing stress of 3600 lb/ft^2 listed in the FSAR, a margin of 2.5 against ultimate soil bearing capacity failure is indicated. This margin of 2.5 is considered to be more than adequate in preventing failure of the soil beneath the diesel generator building foundation. Since the SME base shears and overturning moments are only slightly greater than the corresponding FSAR loads, factors of safety for structure stability against sliding and overturning are expected to be approximately equal to corresponding FSAR values.

TABLE V-4-1

CODE MARGINS AND F_{SME} FACTORS FOR SHEAR WALLS

Wall	Wall ID No.(1)	M_{SME} (k-ft)	M_{NOL} (k-ft)	M_{NET} (k-ft)	M_u (k-ft)	CM	F_{SME}
South Wall, EL 630'-6" to EL 664'-0"	1	2,760	1,460	4,220	7,660	1.8	2.2
South Wall, EL 630'-6" to EL 664'-0"	2	13,800	378	14,200	34,800	2.5	2.4
East Exterior Wall, EL 630'-6" to EL 664'-0"	3	48,400	5,550	54,000	203,000	3.8	3.8
West Interior Wall, EL 630'-6" to EL 664'-0"	4	26,800	8,050	34,900	148,000	4.2	4.9
South Wall, EL 664'-0" to EL 680'-0"	5	1,450	262	1,710	10,400	6.1	6.6

Note: (1) See Figures V-4-1 to V-4-3 for locations of walls corresponding to wall identification numbers

M_{SME} = Overturning moment due to SME

M_{NOL} = Overturning moment due to normal operating loads

M_{NET} = $M_{SME} + M_{NOL}$

M_u = Code ultimate overturning moment capacity

CM = Code margin

TABLE V-4-2

CODE MARGINS AND F_{SME} FACTORS FOR DIAPHRAGMS

Diaphragm	Diaphragm ID No.(1)	V_{SME} (k)	V_{NOL} (k)	V_{NET} (k)	V_u (k)	CM	F_{SME}
Adjacent to west exterior wall, EL 664'-0"	1	794	60	854	1,700	2.0	2.1
Adjacent to north wall, EL 664'-0"	2	169	31	200	497	2.5	2.8
Adjacent to west exterior wall, EL 680'-0"	3	88	25	113	469	4.2	5.0

Notes: (1) - See Figures V-4-1 to V-4-3 for locations of diaphragms corresponding to diaphragm identification numbers

(2) - Each diaphragm consists of a series of sections separated by openings. Load and capacity are reported for the controlling section only

V_{SME} = Shear due to SME

V_{NOL} = Shear due to normal operating loads

V_{NET} = $V_{SME} + V_{NOL}$

V_u = Code ultimate shear strength capacity

CM = Code margin

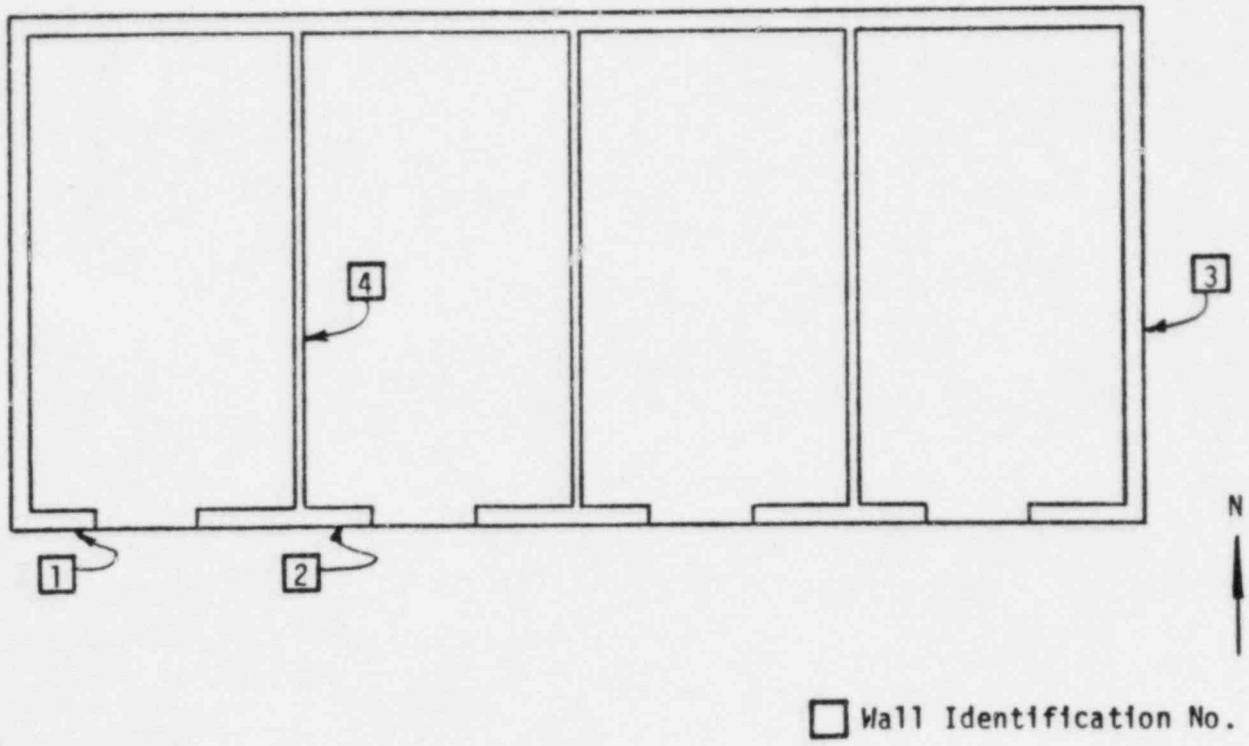

FIGURE V-4-1. DIESEL GENERATOR BUILDING PLAN, ELEVATION 630'-6"

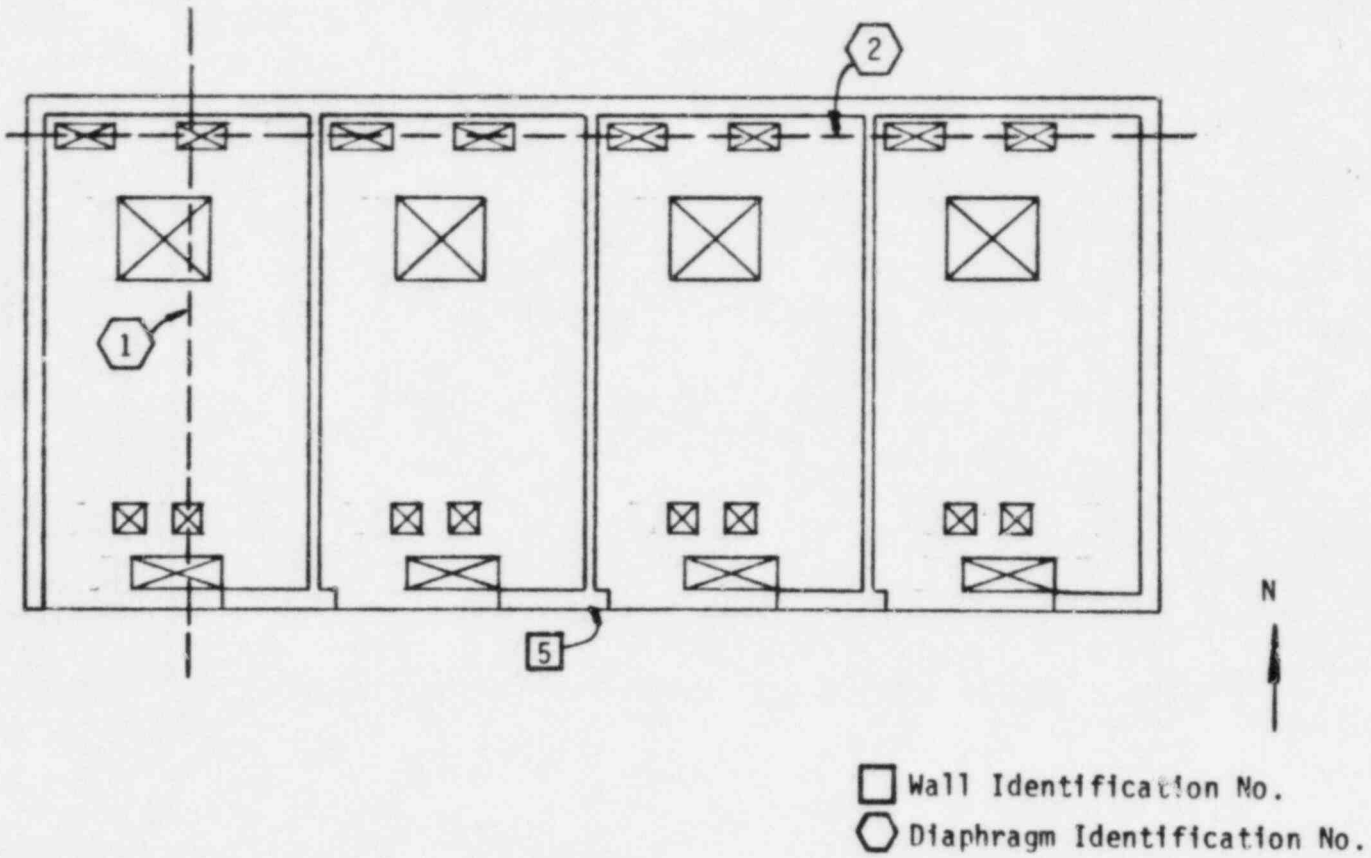

FIGURE V-4-2. DIESEL GENERATOR BUILDING PLAN, ELEVATION 664'-0"

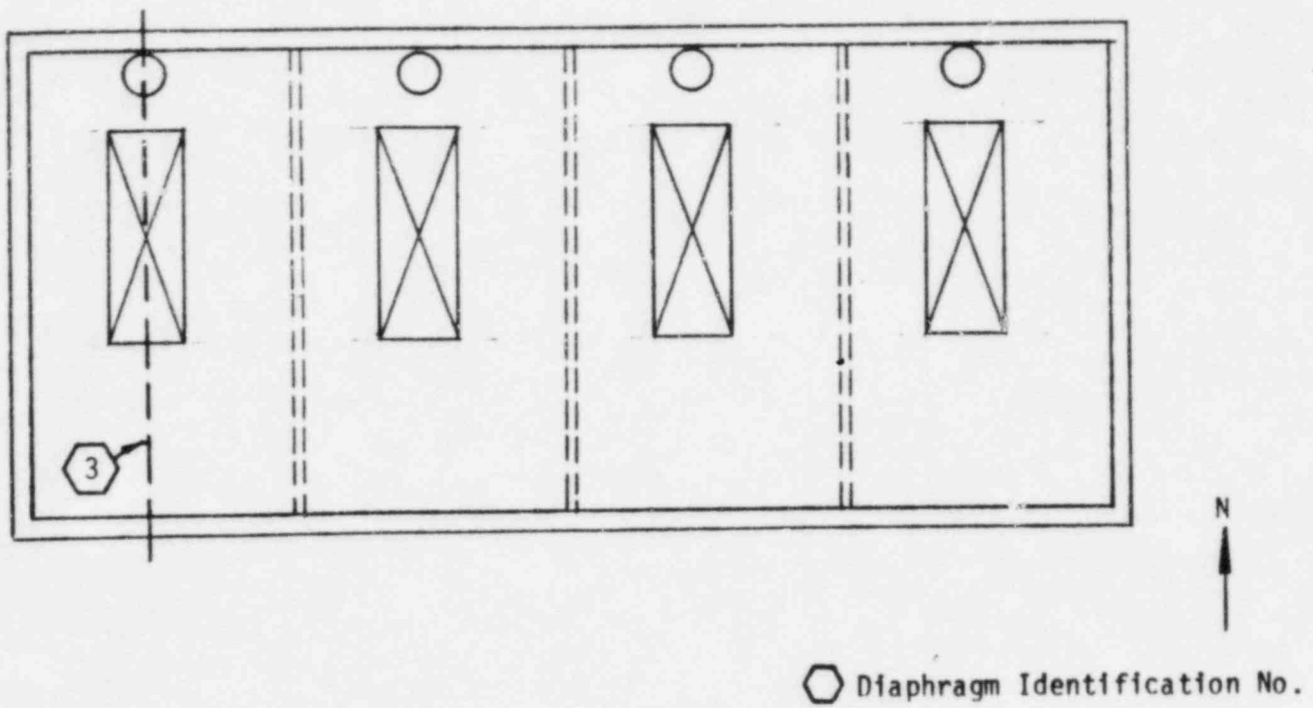

FIGURE V-4-3. DIESEL GENERATOR BUILDING PLAN, ELEVATION 680'-0"

5. INPUT TO EQUIPMENT

Seismic input to equipment for the SMR was specified by in-structure response spectra. These spectra were generated by time history analysis using the coupled equations of motion of the structure as discussed in Section 8 of Volume I of this report. The time history input used was an artificial earthquake whose response spectra essentially envelop the SME ground response spectra at the top-of-fill location. The development of the artificial earthquake is discussed in Section 2 of Volume I.

In-structure response spectra were developed for all locations of critical equipment within the diesel generator building. Spectra were generated for the lower bound, intermediate, and upper bound soil conditions. These spectra were smoothed and the peaks broadened $\pm$ 10 percent as discussed in Section 8 of Volume I. Final spectra were developed from an envelope of the three soil conditions and as an overall envelope of the in-structure response spectra determined for both the lower bound and upper bound relative soil stiffness case dynamic models. The in-structure response spectra developed for the diesel generator building included a 5 percent increase in spectral acceleration at all frequencies to account for accidental torsion. Enveloped in-structure response spectra for the North-South (N-S), East-West (E-W), and vertical directions for equipment damping ratios of 2, 3, 4, and 7 percent of citical are shown in Appendix A of this report. These spectra are applicable to all equipment items mounted on the structure.

The vertical spectra as shown are applicable for piping and equipment located adjacent to major walls or on rigid slabs. For flexible floor slabs within the diesel generator building, vertical input to equipment for the SMR was determined by means of Vertical Amplification Factors (VAFs). These factors were developed from analyses of selected flexible floor slabs throughout the structure as described in Appendix A of Volume I.

Because of the independence of the diesel generator pedestals from the building foundation, additional in-structure response spectra were developed for use with the diesel generators and attached equipment. These spectra were determined based on the dynamic characteristics of the individual diesel generators and foundation pedestals. The development and use of these spectra is presented in Volume VII of this report.

6. SUMMARY

As part of the Seismic Margin Review (SMR) conducted for Midland, the ability of the diesel generator building to withstand seismic excitation was investigated. The evaluation was conducted using new seismic response loads developed for the SME together with normal operating design loads. The seismic loads were developed using a site specific earthquake for Midland as well as new soil-structure interaction parameters which reflect the site layering characteristics. Margins against code allowable values were calculated for selected elements throughout the structure.

The seismic excitation of the structure was specified in terms of site specific response spectra developed for the top-of-fill location. These spectra have a peak ground acceleration of approximately 0.15g. The vertical component was specified as 2/3 of horizontal.

Two soil profiles representing soft site and stiff site soil conditions were used in the analysis. Layered site analyses were used to develop the soil impedance functions for the structure using an equivalent rectangular foundation plan. Effective shear moduli (G_{eff}) were calculated based on elastic half-space formulae by maintaining the same stiffness values as those obtained for the layered site analyses. The G_{eff} values were then used to develop global stiffnesses and dashpots for the lower and upper bound soil cases. Intermediate soil case soil impedances were an approximate average of these two cases. Damping values were conservatively limited to a fraction of theoretical elastic half-space values to account for energy entrapment due to soil layering beneath the building. Soil layering factors for horizontal and vertical translation ranged from 20 percent of theoretical values for the upper bound soil case to 50 percent of theoretical for the lower bound soil case. Rocking layer factors varied from 5 to 20 percent of theoretical for these soil cases.

Vertical beam element, two-dimensional lumped-mass dynamic models in the North-South, East-West, and vertical directions were used for the SMR. One structure model was the same model used for the seismic design. As part of the SMR, the model was reviewed for the general methodology used in its development and for adequacy to characterize the seismic response of the structure. A separate model was developed which assumed the diesel generators, their pedestals, and entrapped soil were decoupled for the rocking and vertical degrees-of-freedom.

Composite modal damping ratios were computed for the combined soil-structure model by matching structure response determined by directly integrating the coupled equations of motion to the dynamic response calculated by modal analysis techniques at several locations in the structure. Structural damping based on seven percent of critical was used throughout the structure.

Structural loads were determined using response spectrum modal analysis. Modal responses were combined on an SRSS basis except for closely spaced modes which were combined by the absolute sum. The responses to three directions of input motion were calculated independently.

In general, the upper bound soil condition resulted in maximum structural loads. The code margin evaluation was based on the maximum load condition in all instances. When compared with seismic design loads, the maximum SME loads were found to be slightly higher in all instances. Overall seismic loads determined by the structure response spectrum analyses were distributed to the resisting structural elements by methods appropriate to the load-resisting system being evaluated.

Overall seismic loads determined by the response spectrum analyses were distributed to the resisting structural elements by the rigid diaphragm approximation. This method is appropriate for the concrete shear wall and diaphragm system of the diesel generator building.

Seismic shears and overturning moments were distributed to the individual walls in proportion to their relative rigidities. Seismic loads acting on the diaphragms were determined using information available from the load distributions to the individual walls. The shear walls and diaphragms were evaluated for seismic loads combined with loads due to normal operating conditions predicted by Bechtel's static analyses.

Capacities for the shear walls were developed in accordance with the ultimate strength design provisions contained in ACI 349-80. Shear walls were checked for their ability to resist in-plane shears and overturning moments. Code margins and F_{SME} factors were determined for the selected walls based on comparisons of the loads due to seismic and normal operating conditions and the code ultimate strength capacities. The selected walls were found to be governed by overturning moment. The lowest code margin calculated was found to be 1.8. The SME would have to be increased by at least a factor of 2.2 before the code margin for any wall would be exceeded. To account for the effects of the reinforcement cutting allowance and available non-conformance reports indicating deviations from the construction specifications, the governing wall was reevaluated assuming the worst case possible due to these field conditions. A code margin of 1.6 was calculated for this wall.

Diaphragm capacities were determined using ACI 349-80 criteria developed for shear walls. The diaphragms evaluated were found to be governed by shear. The lowest code margin for the diaphragms was found to be 2.0. For any diaphragm to reach code capacity, the SME would have to be increased by a factor of 2.1. Accounting for the worst case effects of the reinforcement cutting allowance led to a code margin of 1.6 for the governing diaphragm.

Code margins for the selected structural elements were all conservatively based on minimum specified material strengths and maximum seismic load cases. Reductions in loads to account for inelastic energy dissipation were not used for the diesel generator building. All code margins were determined to be greater than unity. Before code capacity is reached for any diesel generator building element investigated, the SME would have to be increased by 2.1. It can, therefore, be concluded that the diesel generator building has more than sufficient structural capacity to resist the SME based on code criteria and significantly higher capacity before failure is expected.

In-structure response spectra were generated for the diesel generator building SMR by time-history analyses using the coupled equations of motion. Envelopes of spectra for the three soil cases and upper and lower bound relative soil stiffness conditions were generated for the two horizontal and the vertical directions. Horizontal in-structure response spectra were increased five percent at all frequencies to account for accidental torsion. Vertical amplification factors to account for the vertical response of flexible floor slabs were developed for use in the evaluation of piping and equipment located near the centers of the flexible slabs. The effects of out-of-plane moments and thermal gradients on in-plane wall and diaphragm capacities were considered.

REFERENCES

1. Final Safety Analysis Report (FSAR), Midland Plant - Units 1 and 2, Consumers Power Company.

2. TID-7024, Nuclear Reactors and Earthquakes, Lockheed Aircraft Corporation and Holmes and Narver, Inc., August 1963.

3. Site Specific Response Spectra, Midland Plant - Units 1 and 2, Part I, Response Spectra - Safe Shutdown Earthquake, Original Ground Surface, Weston Geophysical Corp., prepared for Consumers Power Company, February 1981.

4. Site Specific Response Spectra, Midland Plant - Units 1 and 2, Part II, Response spectra - Applicable for the Top of Fill Material at the Plant Site, Weston Geophysical Corp., prepared for Consumers Power Company, April 1981.

5. Draft, Site Specific Response Spectra, Midland Plant - Units 1 and 2, Part III, Seismic Hazard analysis, Weston Geophysical Corp. prepared for Consumers Power Company, Revision 1, May 1982.

6. This reference has been deleted.

7. "Soil Dynamic Modulus Study, Midland, Units 1 and 2, Consumers Power Company", Dames & Moore Job No. 05697-039-07, Dames & Moore, Park Ridge, Illinois, February, 1982.

8. Letter corespondence dated February 23, 1982 from E. M. Hughes (Bechtel) to R. P. Kennedy (SMA) Subject: "Seismic Model Properties for the Reactor Building and Midland Units 1 and 2."

9. Wong, H. L. and J. E. Luco, "Soil-Structure Interaction: A Linear Continuum Mechanics Approach (CLASSI), Report, CE, Department of Civil Engineering, University of Southern California, Los Angeles, California, 1980.

10. This reference has been deleted.

11. Richart, F. E., Hall, Jr. R. and R. A. Woods, Vibrations of Soils and Foundations, Prentice-Hall, Inc., New Jersey, 1970.

12. Kausel, E., and R. Ushijima, "Vertical and Torsional Stiffness of Cylindrical Footings", Massachusetts Institute of Technology, Research Report R79-6, February, 1979.

REFERENCES (Continued)

13. Veletsos, A. S., and Y. T. Wei, "Lateral and Rocking Vibration of Footings", Journal of the Soil Mechanics and Foundations Division, Proceedings of ASCE, EM5, pp 1381-1395, October, 1971.

14. Luco, J. E., and R. A. Westmann, "Dynamic Response of Circular Footings", Journal of the Engineering Mechanics Division, Proceedings of ASCE, EM5, pp 1381-1395, October, 1971.

15. Letter correspondence dated November 25, 1981 from L. H. Curtis (Bechtel) to R. P. Kennedy (SMA), Subject: "Soil Spring Summary for Diesel Generator Building", November 25, 1981.

16. Johnson, J. J., "SOILST - A Computer Program for Soil-Structure Interaction Analyses", General Atomic Company, GA-A15067, April 1979.

17. Bechtel Associates Professional Corporation, "Technical Specifications for Forming, Placing, Finishing and Curing of Concrete for the Consumers Power Company Midland Plant - Midland, Michigan", Spec. 7220-C-231Q, Revision 21, September 28, 1981.

18. Derecho, A. T., et. al., "Analysis and Design of Small Reinforced Concrete Buildings for Earthquake Forces", Portland Cement Association, 1974.

19. Letter correspondence from E. M. Hughes (Bechtel) to R. P. Kennedy (SMA), January 4, 1983, Subject: Midland Plant Units 1 and 2, Consumers Power Company, Bechtel Job 7220, Seismic Margin Review.

20. ACI 349-80, "Code Requirements for Nuclear Safety Related Concrete Structures", American Concrete Institute, 1980.

21. Cardenas, A. E., et. al., "Design Provisions for Shear Walls", ACI Journal, March, 1973.

22. This reference has been deleted.

23. "Tentative Provisions for the Development of Seismic Regulations for Buildings", National Bureau of Standards Special Publication 510, Applied Technology Council.

24. Letter correspondence from N. W. Swanberg (Bechtel) to D. A. Wesley (SMA), April 6, 1983, Subject: Design Thermal Gradients.

APPENDIX V-A

DIESEL GENERATOR BUILDING
IN-STRUCTURE RESPONSE SPECTRA

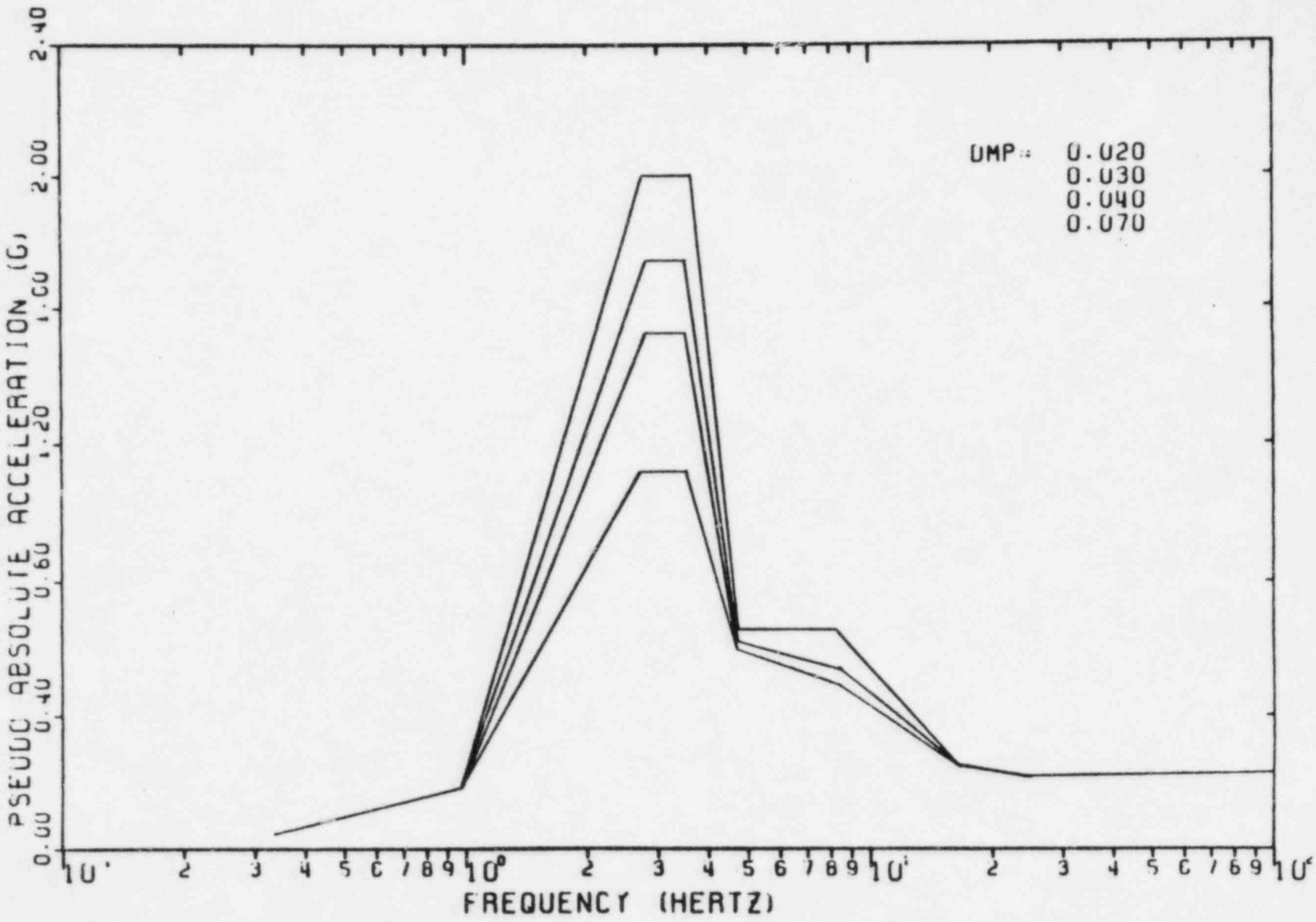

FIGURE V-A-1. TWO MODEL ENVELOPE, SRSS COMBINED RESPONSE SPECTRA, DIESEL GENERATOR BUILDING, ELEVATION 634'-6", NORTH-SOUTH DIRECTION

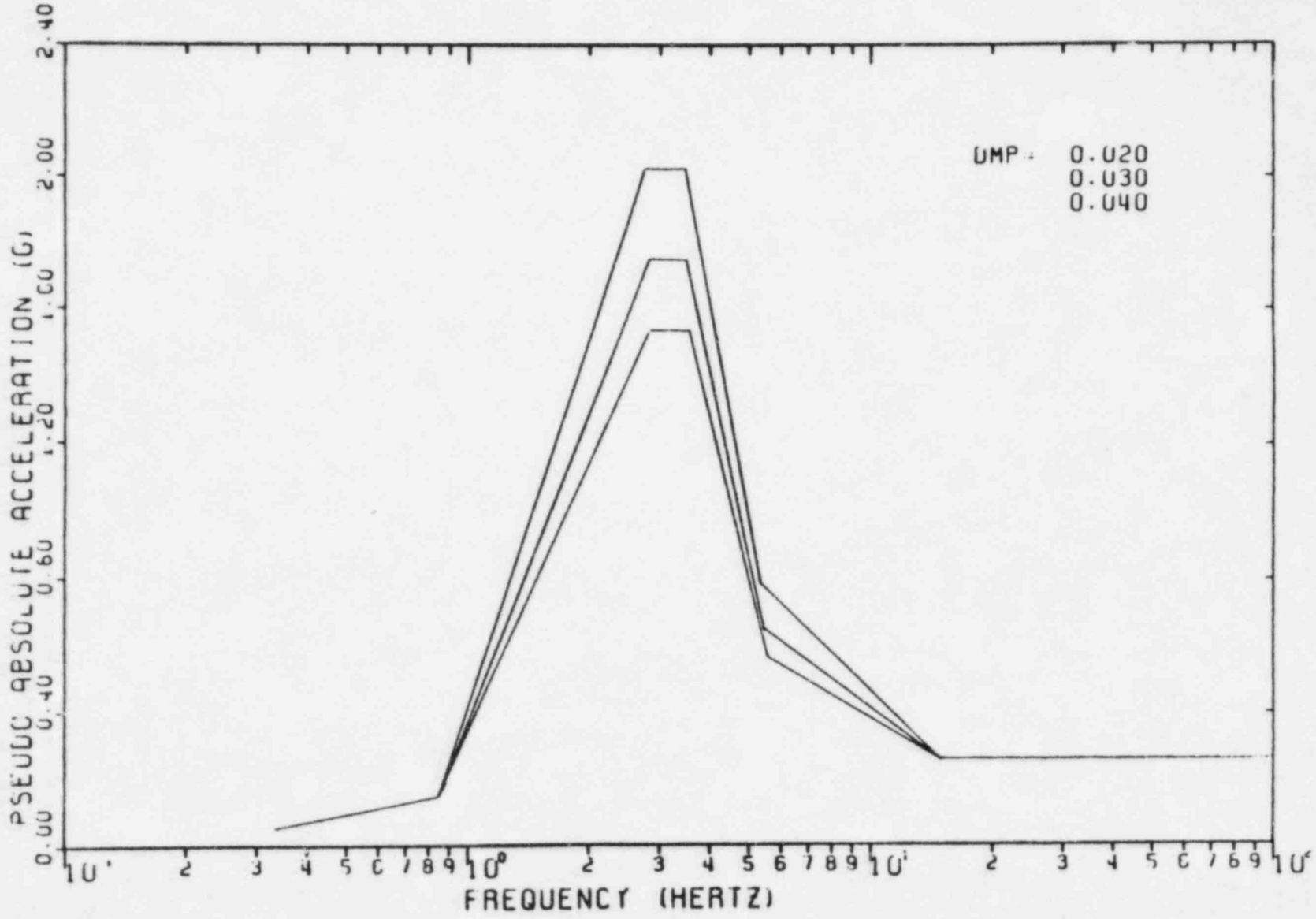

FIGURE V-A-2. TWO MODEL ENVELOPE, SRSS COMBINED RESPONSE SPECTRA, DIESEL GENERATOR BUILDING, ELEVATION 634'-6", EAST-WEST DIRECTION

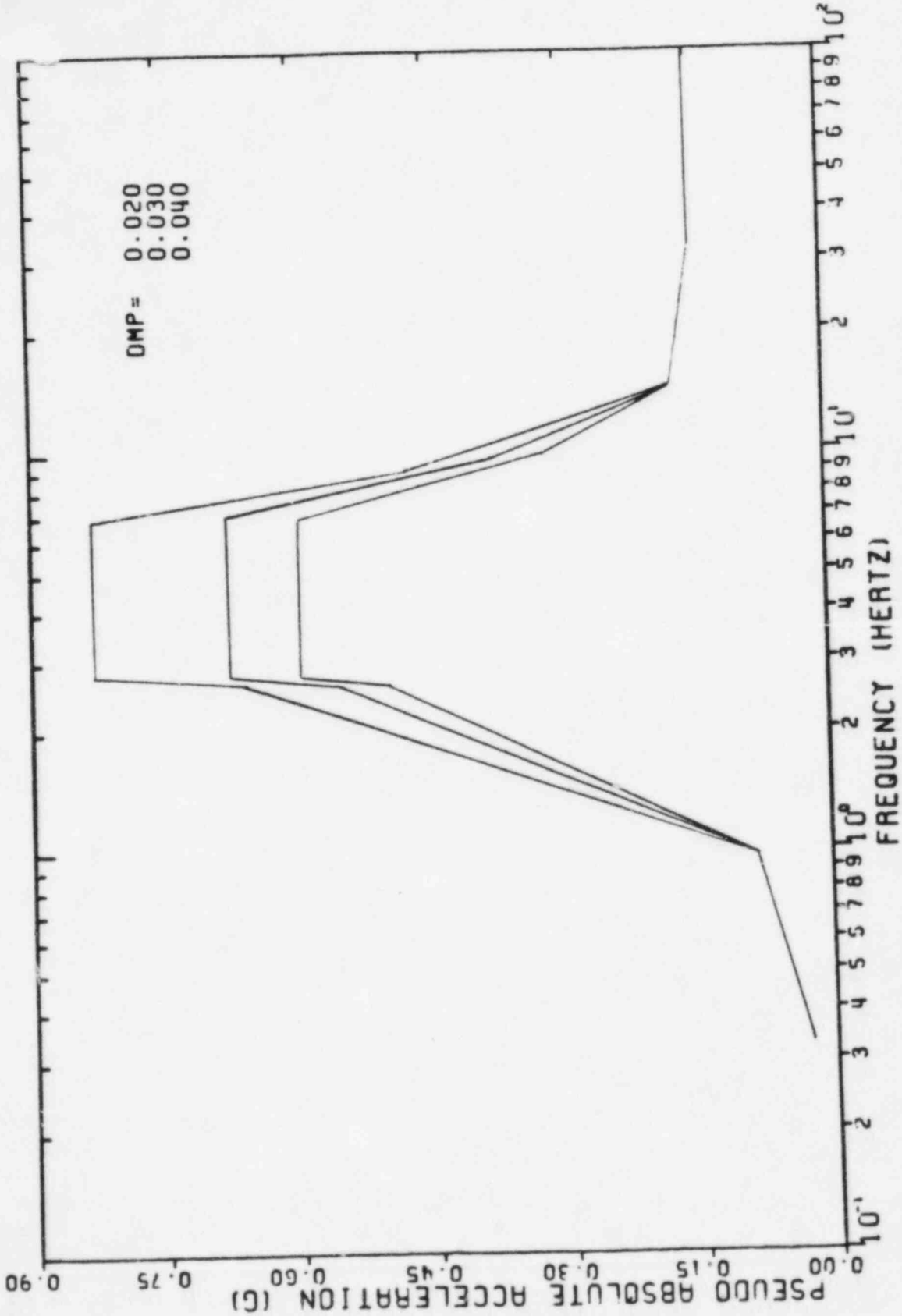

FIGURE V-A-3. TWO MODEL ENVELOPE, SRSS COMBINED RESPONSE SPECTRA, DIESEL GENERATOR BUILDING, ELEVATION 634'-6", VERTICAL DIRECTION

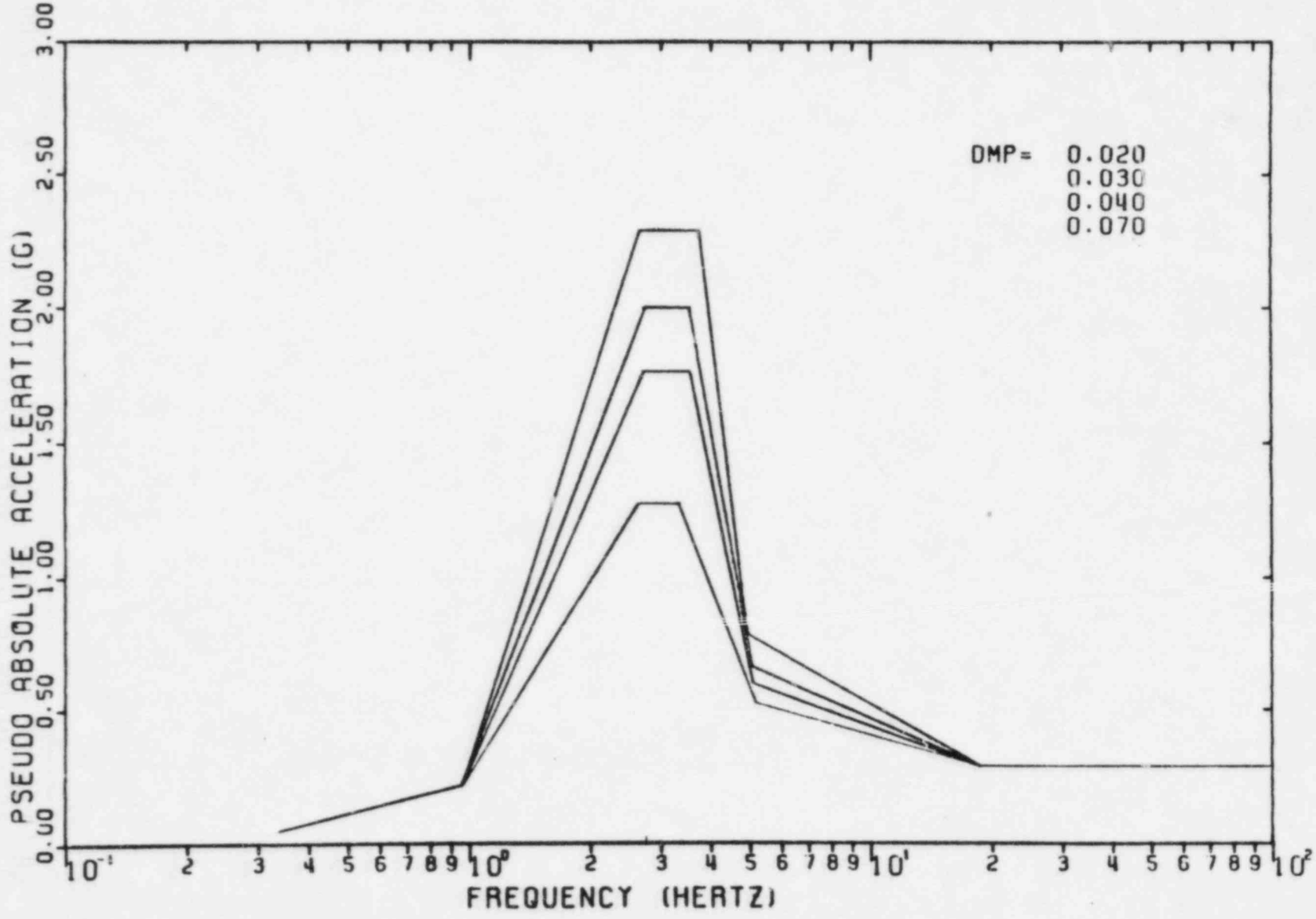

FIGURE V-A-4. TWO MODEL ENVELOPE, SRSS COMBINED RESPONSE SPECTRA, DIESEL GENERATOR BUILDING, ELEVATION 647'-0", NORTH-SOUTH DIRECTION

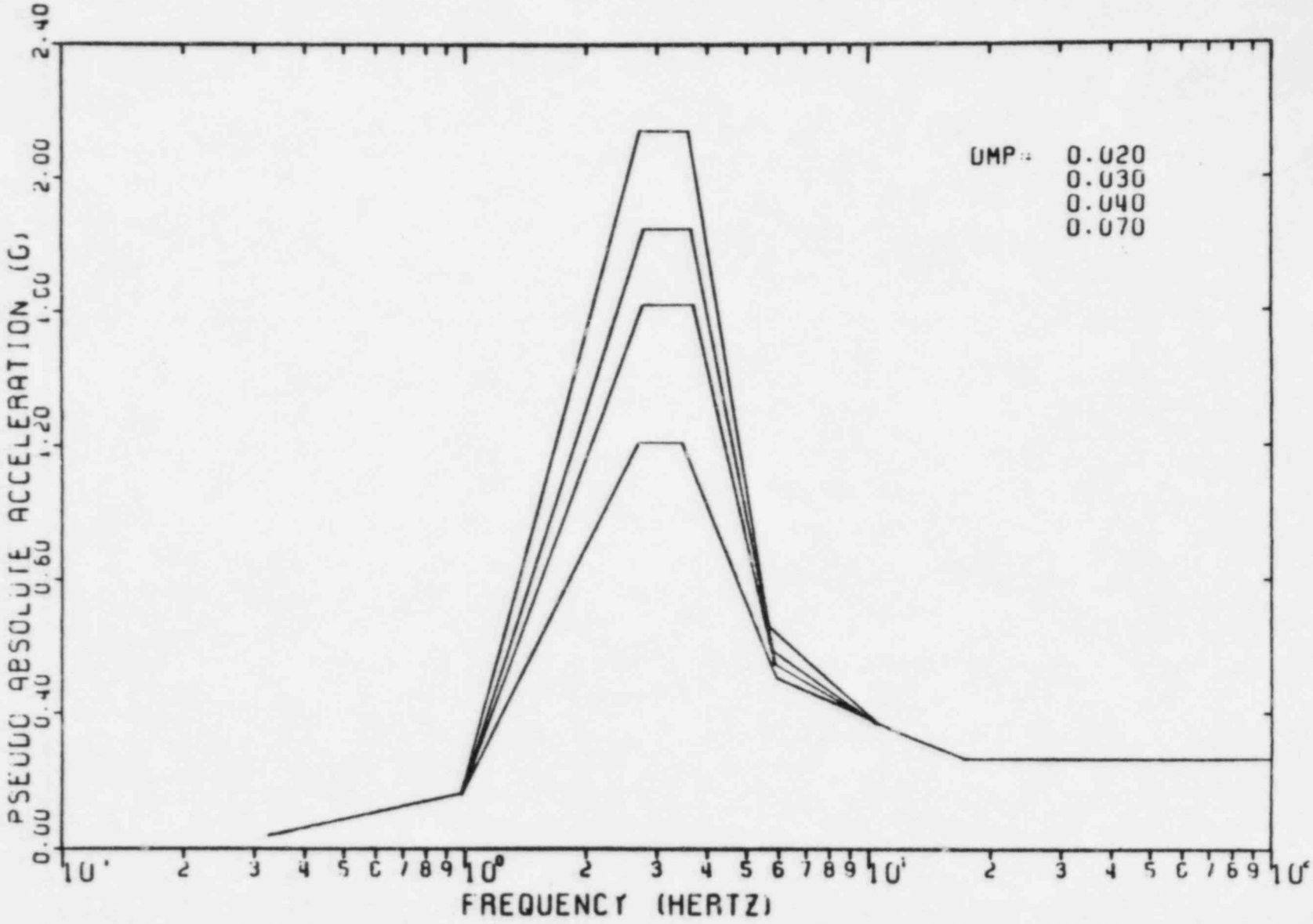

FIGURE V-A-5. TWO MODEL ENVELOPE, SRSS COMBINED RESPONSE SPECTRA, DIESEL GENERATOR BUILDING, ELEVATION 647'-0", EAST-WEST DIRECTION

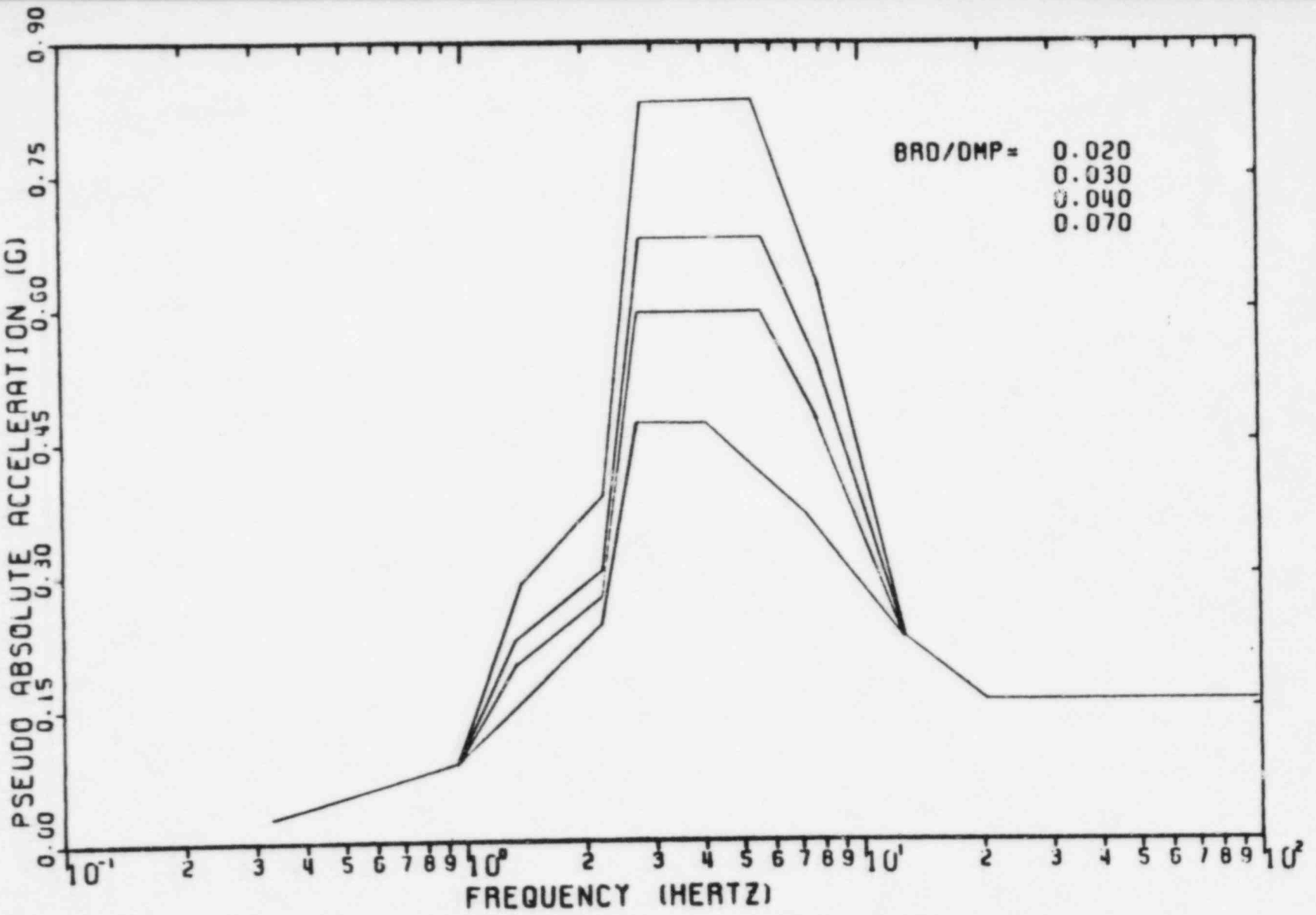

FIGURE V-A-6. TWO MODEL ENVELOPE, SRSS COMBINED RESPONSE SPECTRA, DIESEL GENERATOR BUILDING, ELEVATION 647'-0", VERTICAL DIRECTION

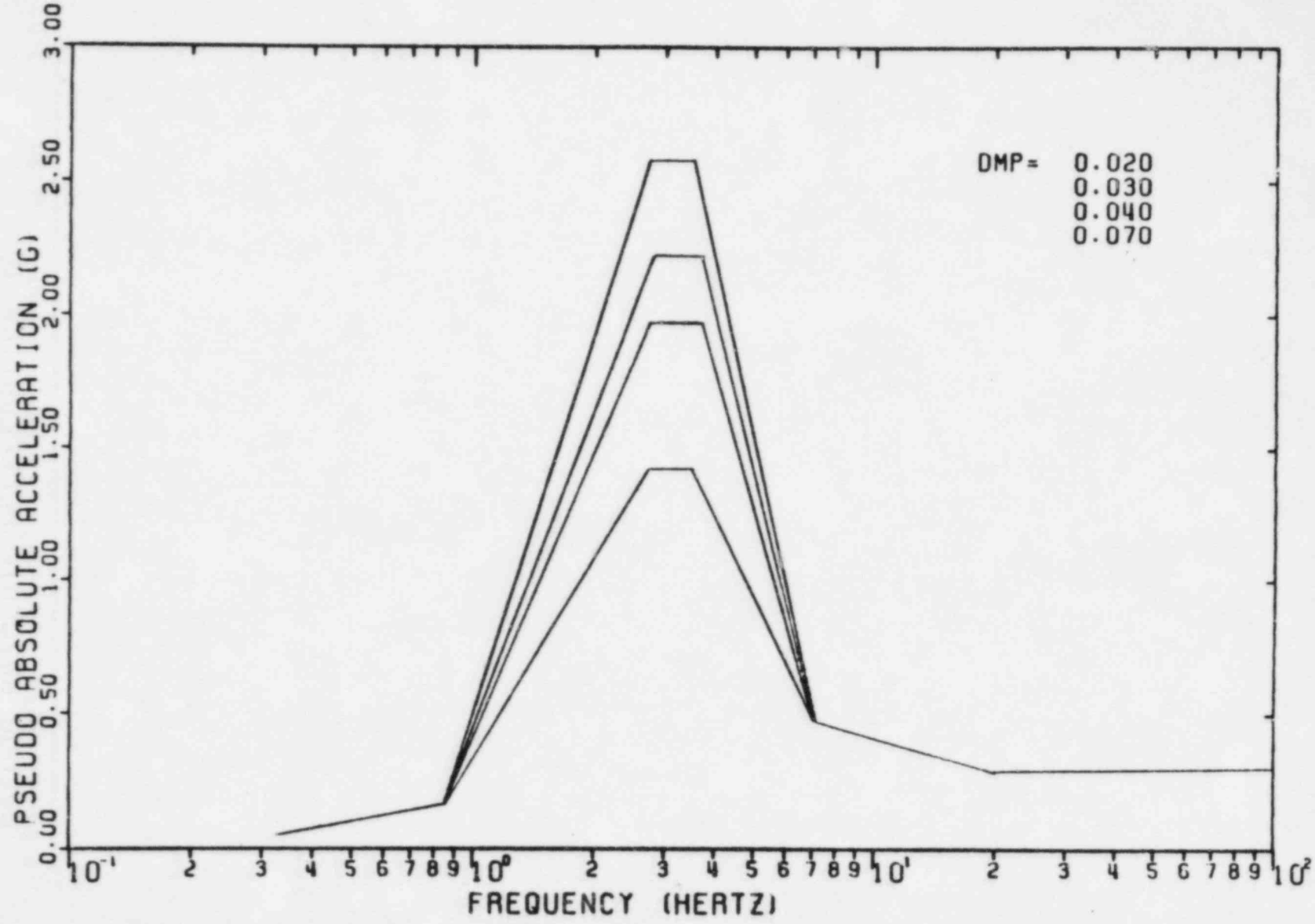

FIGURE V-A-7. TWO MODEL ENVELOPE, SRSS COMBINED RESPONSE SPECTRA
DIESEL GENERATOR BUILDING, ELEVATION 664'-0", NORTH-SOUTH DIRECTION

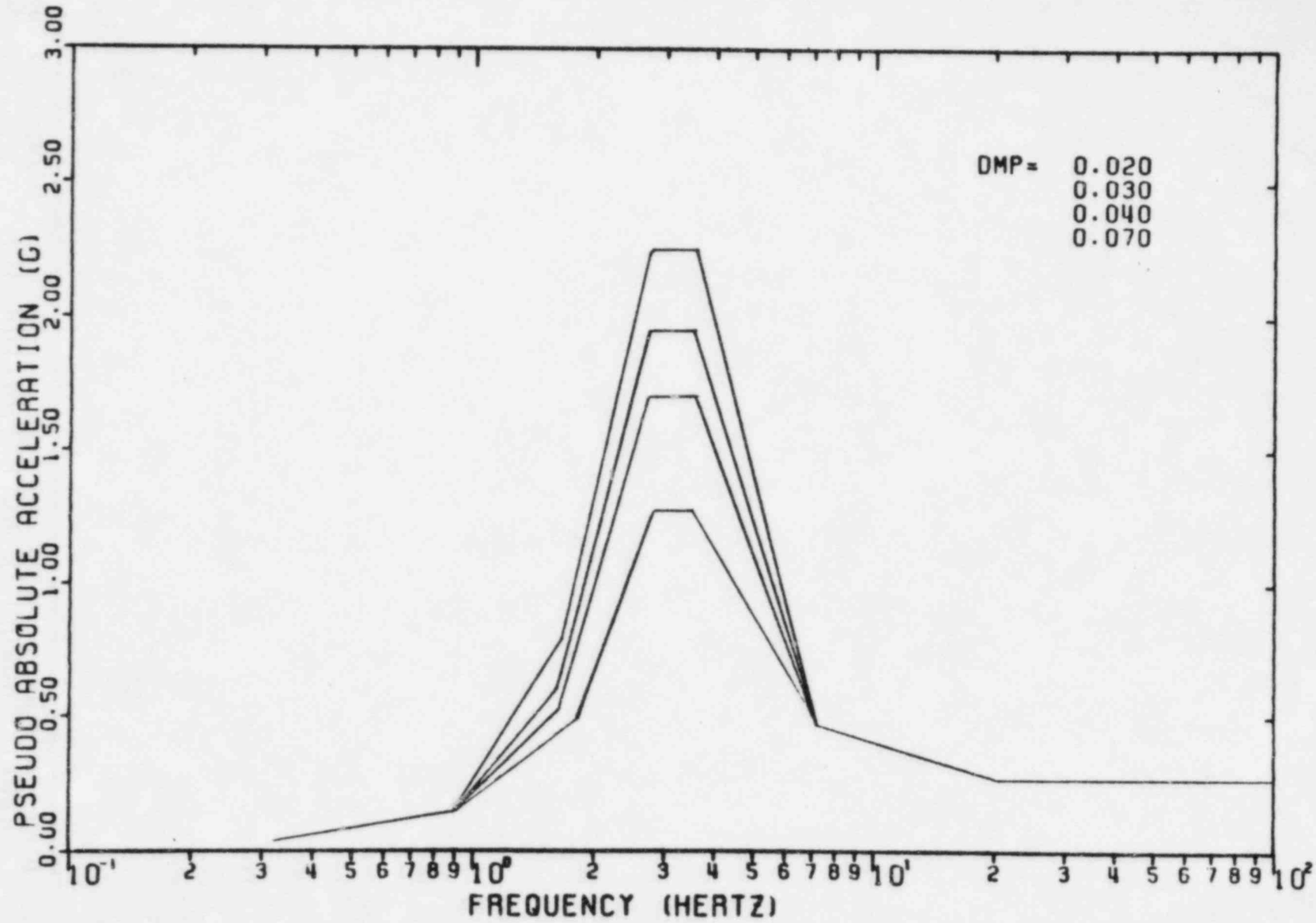

FIGURE V-A-8. TWO MODEL ENVELOPE, SRSS COMBINED RESPONSE SPECTRA, DIESEL GENERATOR BUILDING, ELEVATION 664'-0", EAST-WEST DIRECTION

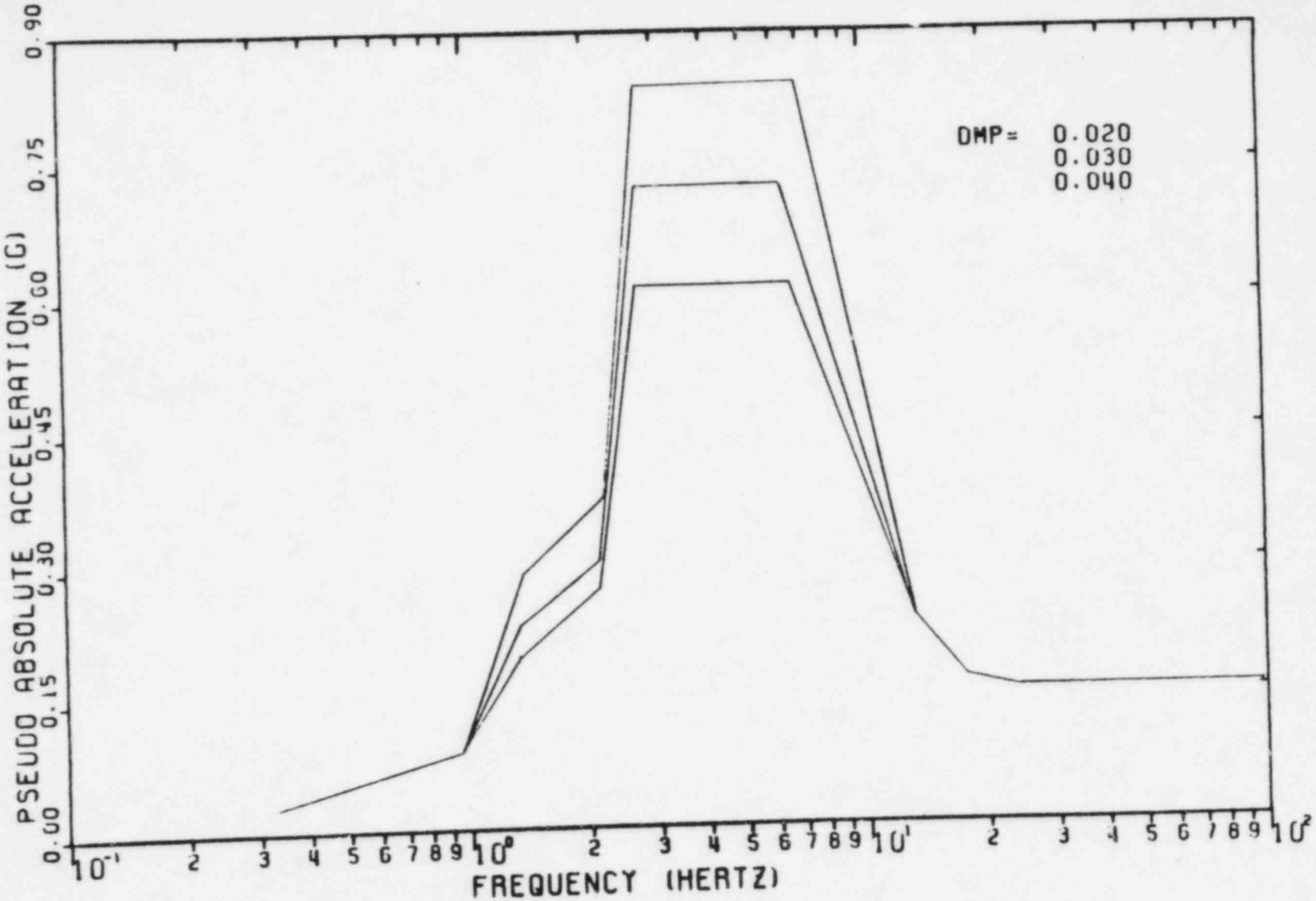

FIGURE V-A-9. TWO MODEL ENVELOPE SRSS COMBINED RESPONSE SPECTRA, DIESEL GENERATOR BUILDING, ELEVATION 664'-0", VERTICAL DIRECTION

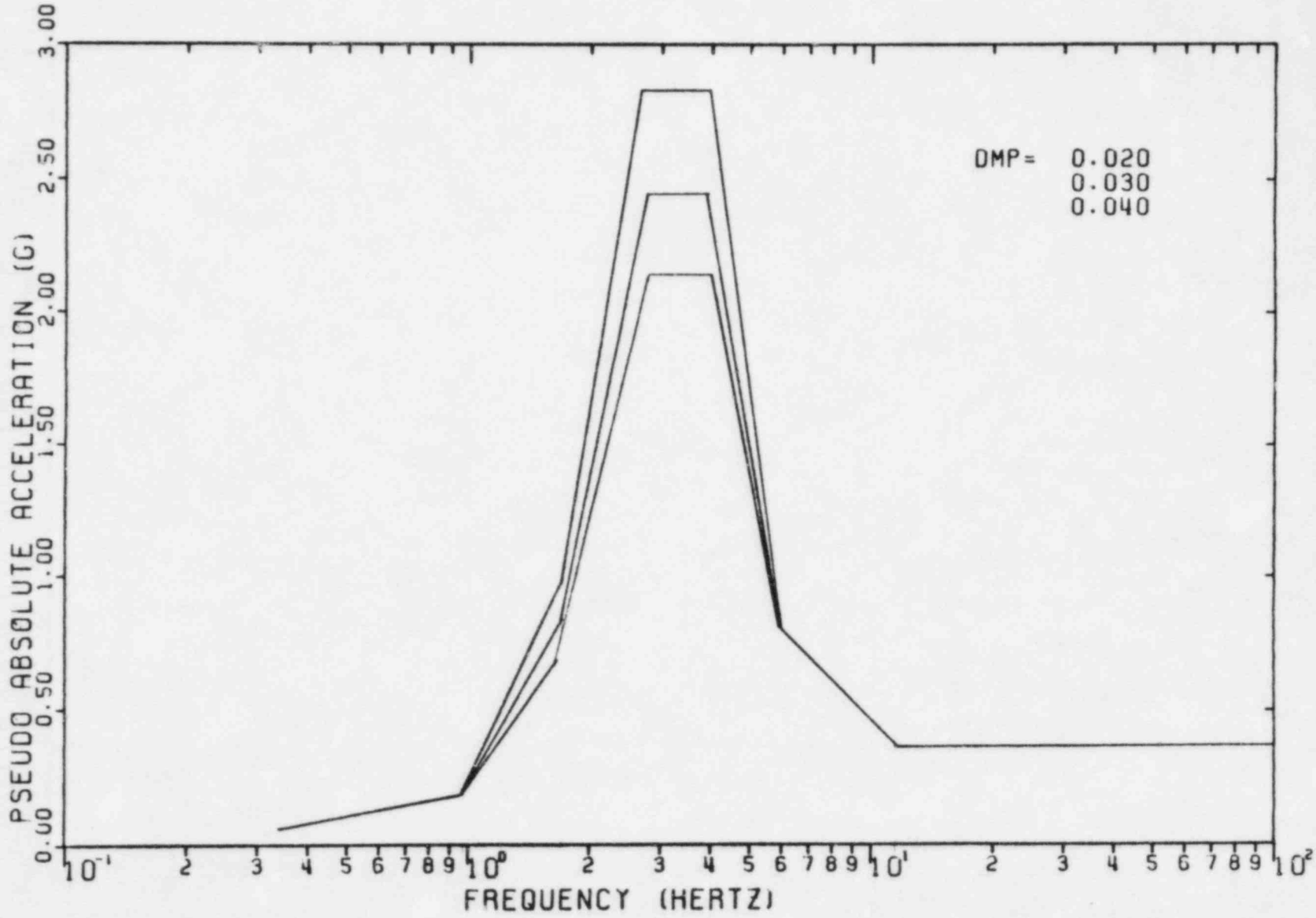

FIGURE V-A-10. TWO MODEL ENVELOPE, SRSS COMBINED RESPONSE SPECTRA, DIESEL GENERATOR BUILDING, ELEVATION 680-0", NORTH-SOUTH DIRECTION

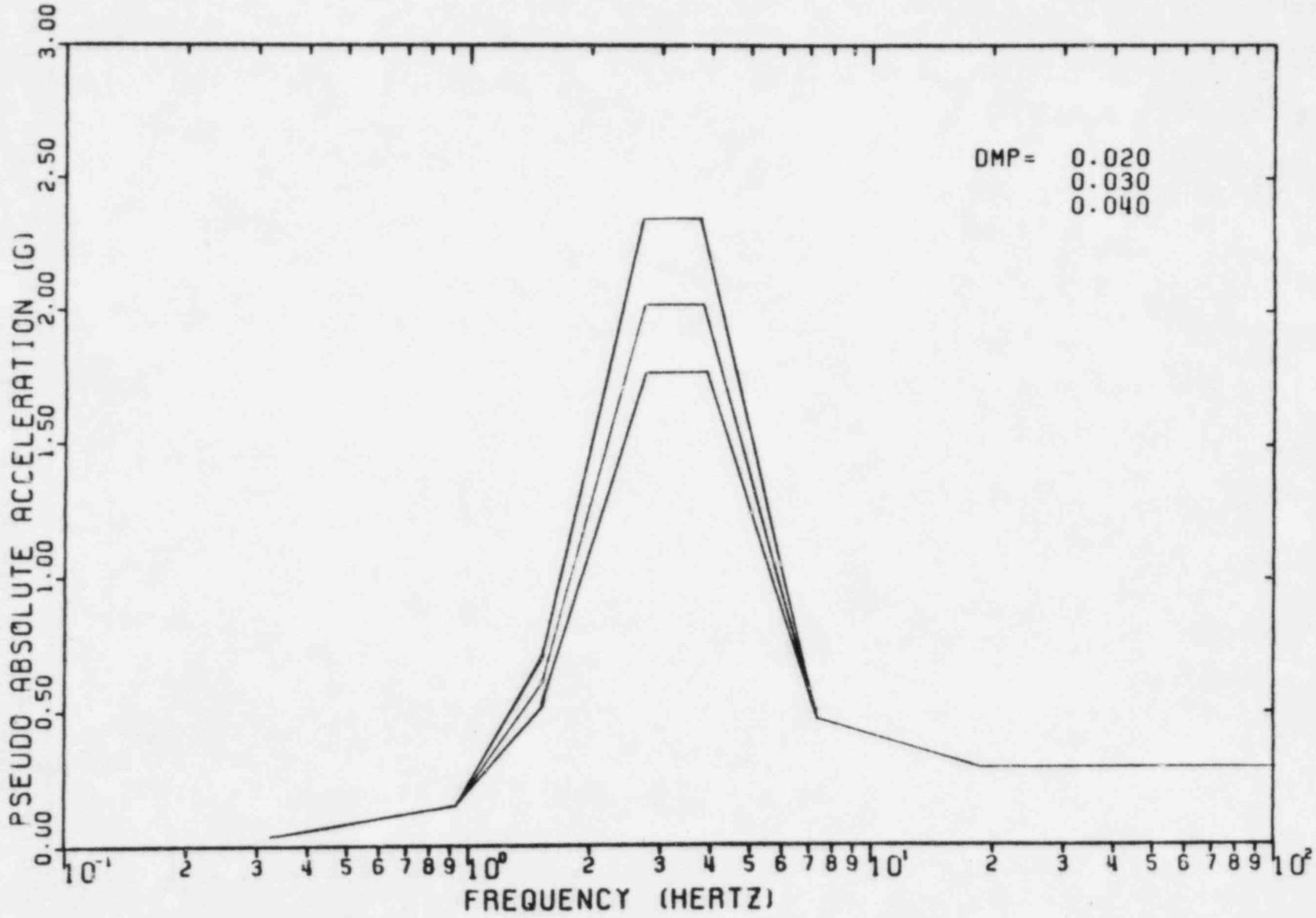

FIGURE V-A-11. TWO MODEL ENVELOPE, SRSS COMBINED RESPONSE SPECTRA, DIESEL GENERATOR BUILDING, ELEVATION 680'0", EAST-WEST DIRECTION

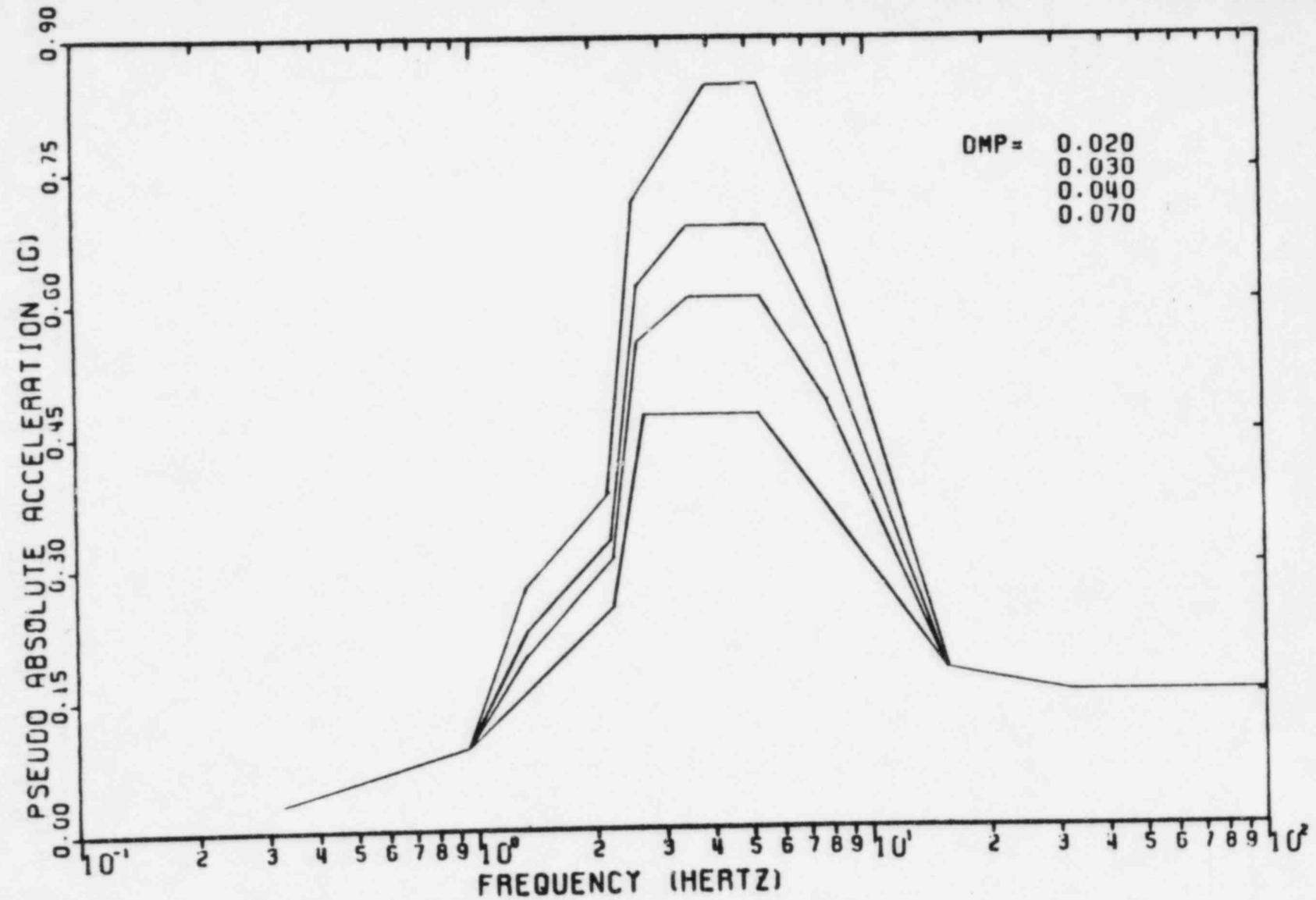

FIGURE V-A-12. TWO MODEL ENVELOPE, SRSS COMBINED RESPONSE SPECTRA, DIESEL GENERATOR BUILDING, ELEVATION 680'-0", VERTICAL DIRECTION

SMA 13701.05R003(VOLUME V)

SEISMIC MARGIN REVIEW

VOLUME V

DIESEL GENERATOR BUILDING

prepared for

CONSUMERS POWER COMPANY
Jackson, Michigan

July, 1983

STRUCTURAL MECHANICS ASSOCIATES
A Calif. Corp.
5160 Birch Street, Newport Beach, Calif. 92660 (714) 833-7552